I. ELECTRON SPIN RESONANCE LINE SHAPE OF A POLYCRYSTALLINE RADICAL

II. PARAMAGNETIC EXCITONS IN MOLECULAR CRYSTALS

Thesis by

Himan Sternlicht

In Partial Fulfillment of the Requirements

For the Degree of

Doctor of Philosophy

California Institute of Technology

Pasadena, California

1963

ACKNOWLEDGEMENTS

I would like to express my indebtedness to Professor Harden M. McConnell, who was my Scientific Adviser during my four years at the California Institute of Technology. His encouragement and stimulation have been of immeasurable value to me.

I wish also to thank Professor George W. Robinson and Professor Robert M. Mazo, and the many other faculty members who have aided me in my work.

My graduate studies were made possible by the National Science Foundation, the Eastman Kodak Company, and the E. I. du Pont de Nemours Company. I gratefully acknowledge their financial support.

ABSTRACT

PART I:

Electron spin resonance spectra of polycrystalline radicals are complicated by the anisotropic dipolar magnetic interactions between the unpaired electron and the nuclear spins. Although general expressions in the form of multiple integrals can be derived for the polycrystalline line shapes, their complicated nature makes closed form evaluations very difficult to do except in certain limiting cases.

We derive a theorem which enables us to calculate the polycrystalline line shape of an arbitrary polynuclear radical when the external magnetic field is larger than the internal dipolar fields. Our results are applied to polyconjugated hydrocarbon radicals. We find that we can explain a fact heretofore not well understood: namely, the polycrystalline spectra of such radicals can be remarkably similar to those obtained from the liquid state, despite the fact that significant anisotropic dipolar interactions are present in the solid state but not in the liquid.

PART II:

The possibility of using electron spin resonance to study paramagnetic excited electronic states of aromatic crystals is explored. Two limiting cases are considered: On the one hand, the excitation

energy moves from molecule to molecule by a diffusion process; on the other, the triplet excitation is described by a Frenkel wave exciton. In either case intermolecular propagation of the triplet excitation is assumed to proceed through virtual triplet ionization states.

A. The theory of the spin resonance of triplet wave excitons is developed in some detail. It is shown that large Davydov splittings between the exciton bands require that there be only a weak dependence of the ESR spectra on the $\hat{k}$ vector of the exciton wave, except when $\hat{k}$ is near regions of band degeneracies. Band degeneracies arise from time-reversal symmetry in benzene, naphthalene, and coronene crystals and occur on boundary planes of the first Brillouin zone. A spin Hamiltonian is calculated for these three aromatic crystals for most $\hat{k}$ vectors which are far removed from regions of band degeneracy. Two-line spectra (with no hyperfine structure), representing an average over the molecular sites in the unit cell, are obtained. Scattering of the exciton wave by lattice perturbations can be a mechanism for spin lattice relaxation.

B. The ESR line shape is correlated with the characteristic time, τ, for a diffusing triplet exciton to undergo a random walk between the nontranslatory neighbors of a two site unit cell. A general expression for the line shape is derived by time dependent perturbation treatment. This expression is valid for (1) sufficiently large transfer rates τ^{-1}; (2) for all transfer rates provided that significant differences between the spin Hamiltonians of the nontranslatory neighbors only occur to first and second order. Wave and diffusional triplet exciton spectra are compared.

TABLE OF CONTENTS

		Page
I	THE ELECTRON SPIN RESONANCE LINE SHAPE OF A POLYCRYSTALLINE RADICAL	1
	Introduction	1
	The Polycrystalline Line Shape Formula	7
	I_H a Good Quantum Number	14
	A General Polynuclear Radical	18
	Spectra of Polyconjugated Hydrocarbon Radicals	23
	Conclusion	25
	References	27
II	PARAMAGNETIC EXCITONS IN MOLECULAR CRYSTALS.	29
	Introduction	29
	A. Wave Excitons	40
	An Effective Hamiltonian	40
	Exciton Band Degeneracies	43
	Resonance Spectra	57
	The $\Delta \leftrightarrow \Gamma$ Scattering Process	65
	Conclusion	73
	Addendum	76
	B. Diffusing Excitons	77
	Introduction	77
	Density Matrix Method: Calculation Procedure	79
	Density Matrix Method: Model	85
	Case I: $H_o = 0$	85
	Case II: Intermediate Field. $g_e \lvert\beta\rvert H_o = 3D$	90
	The "Frequency Modulation" Method	93
	Zero Field Case	99
	Intermediate Field. $g_e \lvert\beta\rvert H_o = 3D$	102
	General Case	107
	Comparison of Wave and Diffusional Exciton Spectra	109
	References	113
	APPENDIX	116
	a. The Simplified Spin-Spin Operator	116
	b. Time-Reversal Degeneracies	119
	c. Accidental Degeneracies	121
	d. Diffusing Excitons: Intermediate Field Case $(g_e \lvert\beta\rvert H_o = 3D)$	125
	PROPOSITIONS	127

PART I*

ELECTRON SPIN RESONANCE LINE SHAPE OF A POLYCRYSTALLINE RADICAL

INTRODUCTION

The electron spin resonance (ESR) spectra of an oriented radical are generally more complex than the solution spectra of the same radical. The rapid tumbling of the radical when in a liquid of low viscosity results in isotropic, sharp line spectra. Furthermore, the nuclear hyperfine structure present can be interpreted in terms of the isotropic Fermi contact interaction between the unpaired electron spin distribution and the nuclei with nonzero spin (2). When the radical is oriented, as in a crystal lattice, the ESR spectra are complicated by the additional presence of (electron spin)-(nuclear spin) dipolar interaction terms (3-6), which average out to zero in the liquid case. The selection rules are somewhat altered; in addition, the resonance spectra, while still fairly sharp, are now anisotropic--the orientation of the internal dipolar magnetic fields relative to the externally applied magnetic field must be taken into account. A detailed study of the anisotropic spectra can provide much information concerning the molecular

---

*Most of the contents of Part I have appeared in an earlier paper by the author (1).

structure of the radical, and for this reason considerable experimental and theoretical attention has been given to oriented radicals.

Often it is not convenient or possible to prepare single crystals containing oriented radicals. Under such circumstances work must be done on polycrystalline (or amorphous) samples, despite the fact that the resonance lines are now dipolar broadened, and that much of the hyperfine structure may be obscured. Clearly, it is desirable to know what information can be extracted from polycrystalline samples.

If the unpaired electron interacts magnetically with only one nucleus of spin $\frac{1}{2}$,* the spin Hamiltonian of the radical can be written (3) as

$$= h\nu_e \underset{\sim}{S} \cdot \underset{\sim}{H} - h\nu_n \underset{\sim}{I} \cdot \underset{\sim}{H} + \hat{\underset{\sim}{S}} \cdot \underline{T} \cdot \hat{\underset{\sim}{I}} \,. \tag{1}$$

ν_e and ν_n are the electron and nuclear spin Zeeman frequencies, respectively, where

$$\begin{aligned} \nu_e &= h^{-1} g_e |\beta| H \,; \\ \nu_n &= h^{-1} g_n \beta_n H \,. \end{aligned} \tag{2}$$

H is the magnitude of the externally applied magnetic field, $\hat{H}$; $|\beta|$ is the absolute value of the electronic Bohr magneton; β_n is the nuclear Bohr magneton; g_e is the electronic g factor; and g_n is the nuclear

---

*For simplicity, we only consider spin 1/2 nuclei in this section. The treatment can be readily extended to include higher spins.

g factor. S_H and I_H are the respective spin components (in units of $\hbar$) of the electron and nucleus along $\hat{H}$. $\hat{\underline{S}} \cdot \underline{T} \cdot \hat{\underline{I}}$ is the hyperfine interaction term. $\underline{T}$ is a symmetric dyadic and includes the combined (electron spin)-(nuclear spin) Fermi contact interaction, and the (electron spin)-(nuclear spin) dipolar interaction. It is assumed that the (electron orbit)-(nuclear spin) and (electron orbit)-(electron spin) magnetic interactions are negligible. (This is generally true for organic radicals.)

$\underline{T}$ can be derived in the following manner as shown by McConnell and Strathdee (6). Let $\hbar \hat{\underline{S}} \rho(x,y,z)$ denote the vector density of electron spin angular momentum at a point x,y,z in the radical. The spin density function can be expressed in terms of a density matrix, $\rho_{\lambda\mu}$:

$$\rho(x,y,z) = \sum_{\lambda\mu} \rho_{\lambda\mu} \phi_\mu^* \phi_\lambda \quad . \tag{3}$$

ϕ_μ, ϕ_λ can be taken as the one-electron atomic orbitals from which the exact many electron molecular wave function ψ can be constructed. $\underline{T}$ can be expressed as:

$$\underline{T} = h a \underline{U} - g_e g_n |\beta| \beta_n \sum_{\lambda,\mu} \rho_{\lambda\mu} \langle \phi_\mu | \underline{D} | \phi_\lambda \rangle , \tag{4a}$$

where

$$\underline{D} = (r')^{-3} [\, \underline{U} - 3(r')^{-2} \hat{r}' \hat{r}' \,] . \tag{4b}$$

$\underline{U}$ is the unit dyadic and $\hat{r}'$ is the vector from the nucleus to the position

of the electron; h a $\underline{U}$ denotes the Fermi contact interaction contribution.

$\underline{T}$ can be written in diagonal form for a suitably chosen set of cartesian axes, x, y, z:

$$\underline{T} = hA\hat{k}\hat{k} + hB\hat{i}\hat{i} + hC\hat{j}\hat{j} . \qquad (5a)$$

i, j, k are unit vectors in the direction of the positive x, y, z axes, respectively, and will coincide with magnetic symmetry axes. The hyperfine interaction term becomes

$$\hat{S} \cdot \underline{T} \cdot \hat{I} = \mathcal{H}_{hf} = hA S_z I_z + hB S_x I_x + hC S_y I_y . \qquad (5b)$$

Experiments are most commonly done at X-band, where H is approximately 3,500 gauss; ν_e, approximately 9,500 Mc. S_H and I_H will be good quantum numbers provided $|A|, |B|, |C| \ll \nu_e, \nu_n$. If we assume that S_H is a good quantum number and do not commit ourselves as to the magnitude of ν_n relative to $|A|, |B|, |C|$, * the spin Hamiltonian (eq. 1) becomes (3):

$$\underline{\mathcal{H}} = h\nu_e S_H - h\nu I_u . \qquad (6)$$

---

* In the case of "simple" π-electron hydrocarbon radicals like malonic acid, where most of the electron spin density is confined on a single carbon atom, experiments have shown that $30 \text{ Mc} < |A|, |B|, |C| < 100$ Mc (2-4). At X-band the Zeeman frequency, ν_p, of the proton spin is approximately 15 Mc.; consequently only S_H is a good quantum number. (A π-electron radical is defined as "a paramagnetic molecule containing a number of co-planar atoms such that the spin paramagnetism is largely distributed in atomic orbitals having a node in the molecular plane" (6).)

I_u is the nuclear spin component along the unit vector $\hat{u}$. Both ν and $\hat{u}$ depend on S_H as shown:

$$\nu\hat{u} = \nu_\eta \hat{e}_H - S_H[\hat{k}\, A\cos\theta + \hat{i}\, B \sin\theta\cos\phi + \hat{j}\, C \sin\theta \sin\phi\,] \,. \quad (7)$$

$\hat{e}_H$ is a unit vector in the direction of the externally applied field $\hat{H}$; $\cos\theta$, $\sin\theta\cos\phi$, $\sin\theta\sin\phi$ denote the direction cosines of the external field relative to the z, x, y axes respectively. Equations 6 and 7 express the fact that the nuclear spin is quantized along the direction of the total magnetic field at the nucleus--the total magnetic field being the sum of the external field and the dipolar field. If we let $\nu'\hat{u}'$, $\nu''\hat{u}''$ designate the vector $\nu\hat{u}$ when $S_H = 1/2$ and $-1/2$, respectively, we obtain the following four transition frequencies from the oriented radical:

$$\begin{aligned} \nu_1 &= +1/2\,(\nu' - \nu'') \\ \nu_2 &= -1/2\,(\nu' - \nu'') \end{aligned} \quad (8a)$$

$$\begin{aligned} \nu_3 &= +1/2\,(\nu' + \nu'') \\ \nu_4 &= -1/2\,(\nu' + \nu'') \,. \end{aligned} \quad (8b)$$

(The origin of all transition frequencies are taken at ν_e in this paper.)

ν', ν'' are functions of the orientation of the radical with respect to the external field, H:

$$\nu' = \left[\left(\nu_n - \frac{1}{2}A\right)^2 \cos^2\theta + \left(\nu_n - \frac{1}{2}B\right)^2 \sin^2\theta \cos^2\phi + \left(\nu_n - \frac{1}{2}C\right)^2 \sin^2\theta \sin^2\phi \right]^{1/2}$$

$$\nu'' = \left[\left(\nu_n + \frac{1}{2}A\right)^2 \cos^2\theta + \left(\nu_n + \frac{1}{2}B\right)^2 \sin^2\theta \cos^2\phi + \left(\nu_n + \frac{1}{2}C\right)^2 \sin^2\theta \sin^2\phi \right]^{1/2} . \quad (9)$$

The magnitude of the external field is contained in ν_n. $R_\lambda(\theta,\phi)$, the relative intensity (or transition probability) of the resonance line of the λ transition, is given by (3):

$$R_1(\theta,\phi) = R_2(\theta,\phi) = \cos^2 \zeta/2 = 1/2\,(1 + \hat{u}' \cdot \hat{u}'')$$

$$R_3(\theta,\phi) = R_3(\theta,\phi) = \sin^2 \zeta/2 = 1/2\,(1 - \hat{u}' \cdot \hat{u}'') , \quad (10)$$

where

$$u' \cdot u' = (1/4\nu'\nu'')\,(2\nu_n)^2 - [A^2\cos^2\theta + B^2\sin^2\theta\cos^2\phi + C^2\sin^2\theta\sin^2\phi] . \quad (11)$$

The resonance spectrum consists of a symmetrical quartet centered on ν_e. The outer doublet with splitting $\nu' + \nu''$ has relative intensity $\sin^2 \zeta/2$; the inner doublet with splitting $\nu' - \nu''$ has relative intensity $\cos^2 \zeta/2$. When A^2, B^2, $C^2 > (2\nu_n)^2$, the outer lines are more intense; when A^2, B^2, $C^2 < (2\nu_n)^2$, the inner lines will always be more intense. (Experimental work on the "simple" hydrocarbon π-electron radicals (3-5) has shown that at X-band the outer lines are five to ten times more intense than the inner lines. When the external field is $\geq$ 12,000 gauss, the inner lines are generally more intense, and also insensitive to the magnitude of the field.)

THE POLYCRYSTALLINE LINE SHAPE FORMULA

The extension of the above discussion to polycrystalline samples is as follows: We regard the polycrystalline sample as an ensemble of minute crystallites each having one radical. The probability, $g_\lambda(\bar{\nu})\, d\nu$, that a particular transition,* ν_λ, will occur between $\bar{\nu}$ and $\bar{\nu} + d\nu$ is then proportional to

$$\sum_K R_\lambda(\theta_{K_i}, \phi_{K_i}) \sin\theta_K \, d\theta_K d\phi_K .$$

The above represents a statistical averaging of the random orientation of the crystallites. Only those increments of solid angle, $\sin\theta_K d\theta_K d\phi_K$, are added up such that θ_K, ϕ_K corresponds to a ν_λ between $\bar{\nu}$ and $\bar{\nu} + d\nu$. Since the transition probability is a function of θ, ϕ, each increment of solid angle must be multiplied by $R_\lambda(\theta_K, \phi_K)$. It is more convenient to express $g_\lambda(\bar{\nu})\, d\bar{\nu}$ in the following manner:

$$g_\lambda(\bar{\nu})\, d\nu \propto \left\{ \int_0^{2\pi} d\phi \int_{-1}^{1} \delta\left[\bar{\nu} - \nu_\lambda(\theta,\phi)\right] R_\lambda(\theta,\phi)\, d\cos\theta \right\} d\nu . \qquad (12)$$

($\propto$ is the proportionality symbol.)

$\delta(\bar{\nu} - \nu_\lambda)$ is a delta function; $\delta(\bar{\nu} - \nu_\lambda)\, d\nu$ assures that only those values of θ and ϕ are considered such that their substitution into $\nu_\lambda(\theta, \phi)$ gives a transition between $\bar{\nu}$ and $\bar{\nu} + d\nu$. Equation 12 can also be written as:

---

* We shall attach a Greek letter subscript to ν when ν refers to a transition frequency; Roman letter subscripts will be used when ν refers to a nuclear Zeeman frequency.

$$g_\lambda(\bar{\nu}) \propto \frac{1}{2\pi}\int_{-\infty}^{\infty} \exp\left\{i\omega[\bar{\nu}-\nu_\lambda(\theta,\phi)]\right\} d\omega \int_{-1}^{1} I_\lambda(\theta,\phi)\, d\cos\theta \int_{0}^{2\pi} d\phi \,. \tag{13}$$

The polycrystalline line shape, $g(\bar{\nu})$, is clearly proportional to the sum of the $g_\lambda(\bar{\nu})$ terms:

$$g(\bar{\nu}) = N/2\pi \sum_{\lambda=1}^{4} \int_{-\infty}^{\infty} \exp\left\{i\omega\,[\bar{\nu}-\nu_\lambda(\theta,\phi)]\right\} d\omega \int_{-1}^{1} R_\lambda(\theta,\phi)\, d\cos\theta \int_{0}^{2\pi} d\phi. \tag{14}$$

N is a normalization factor so that

$$\int g(\bar{\nu})\, d\bar{\nu} = 1 \,.$$

We easily see from equations 8 and 9 that $g(\bar{\nu})$ is symmetric about $\bar{\nu} = \nu_e$. $g(\bar{\nu})$ is also a function of H because of the H dependence of ν_λ and $R_\lambda(\theta,\phi)$.

We have only taken the dipolar broadening into account. Relaxation, field inhomogeneities, saturation, spin exchange effects, for example, can also alter the line shape. The actual line shape can be represented more appropriately by

$$g_{actual} = \int f(\nu - \bar{\nu}) g(\bar{\nu})\, d\bar{\nu} \,, \tag{15}$$

where $f(\nu - \bar{\nu})$ is a function taking into account all line broadening factors other than the anisotropic interaction above. Usually $f(\nu - \bar{\nu})$ can be taken

as a normalized gaussian:

$$f(v-\bar{v}) = \gamma^{-1}(2/\pi)^{1/2} \exp[-2(v-\bar{v})^2/\gamma^2] \quad . \tag{16}$$

γ is the width between the points of maximum and minimum slope. $g_{actual}(v)$ is given by

$$g_{actual}(v) = (1/8\pi\gamma)(2/\pi)^{1/2} \int_0^{2\pi} d\phi \int_{-1}^{1} d\cos\theta \times \left[\cos^2(\zeta/2)\{\exp[-2(v-v_1)^2/\gamma^2] + \exp[-2(v-v_2)^2/\gamma^2]\} + \sin^2(\zeta/2)\{\exp[-2(v-v_3)^2/\gamma^2] + \exp[-2(v-v_4)^2/\gamma^2]\} \right] . \tag{17}$$

A closed form evaluation of equations 14 or 17 in terms of v_n, A, B, C appears to be very difficult to do, and we have succeeded in doing it only for a number of limiting cases. (If necessary, an evaluation of equations 14 or 17 can be done on an electronic computer (7).)

The above discussion can be extended in a straightforward manner to the cases where (1) more than one nucleus interacts with the unpaired electron; (2) the nuclear spins, I, are greater than $\frac{1}{2}$. Although multiple integral expressions for the polycrystalline line shape are readily derived, closed form evaluations of the integrals again are difficult to do.

We shall primarily concern ourselves in this thesis with solving equation 14 and its $I > \frac{1}{2}$ analogue, when I_H is a good quantum number ($I_H = I, I-1, \ldots -I+1, -I$). The following theorem will be shown to be true:

Theorem I

A transition frequency, ν_{I_H}, having the form

$$\nu_{I_H} = I_H \hat{e}_H \cdot (A \hat{k}\hat{k} + B \hat{i}\hat{i} + C \hat{j}\hat{j}) \cdot \hat{e}_H$$

gives rise to a polycrystalline resonance peak at I_H times the middle value of A, B, C (e.g., $I_H C$ if $A < C < B$). The width of the resonance line $g_{I_H}(\bar{\nu})$ is I_H times the magnitude of the difference between the largest and smallest of the A, B, C terms.

This theorem will enable us to construct the polycrystalline line shape of polynuclear radicals.

I_H is a good quantum number if: (a) the external magnetic field is sufficiently large; (b) the electron spin density at any one atom of the radical is small, as would occur in polyconjugated radicals, for example; or (c) the hyperfine interaction is reduced by some dynamic process, such as a short electron spin relaxation time, or by electron exchange as in solid DPPH and TPPAP (8). (Condition (c) can best be exploited by nuclear magnetic resonance (8).)*

*McConnell and Chesnut (9) have shown that a sufficiently short electron spin relaxation time, or significant electron exchange effects cause the hyperfine interaction (eqs. 5b and 6) to become

$$\mathcal{H}_{hf} = \langle S_H \rangle \hat{e}_H \cdot \underline{T} \cdot \hat{\underline{i}} \ ,$$

where $\langle S_H \rangle$ is the average value of the electron spin component in the external field direction:

$$\langle S_H \rangle = g_e |\beta| \ H \ / 4KT \ . \quad \left\{ \begin{array}{l} T \text{ is the temperature;} \\ K \text{ is the Boltzmann factor.} \end{array} \right\}$$

In the case of hydrocarbon π-electron radicals, the modified hyperfine term can cause shifts in the proton resonance spectra of the order of 40 gauss. The hyperfine term is clearly a small perturbation, and I_H is a good quantum number at X-band; consequently, Theorem I can be used for proton resonance lines.

There are a number of "simple" hydrocarbon radicals like malonic acid whose hyperfine interaction dyadics are very accurately approximated by the CH fragment model (3). The I_H component of the single interacting proton is not a good quantum number at X-band. However, at J-band ($\sim 12,000$ gauss) the dominant contribution to the spectrum comes from the inner transitions, v_1, v_2, which now are relatively field insensitive (see above). This implies that for purposes of determining the dominant features of the polycrystalline spectrum when $H \geq 12,000$ gauss, we can take I_H to be a good quantum number and apply our theorem. (Lefebvre(7) has recently evaluated equation 17 at both X-and J-band frequencies for a CH radical fragment by using an IBM 704 computer. He finds that when $H \geq 12,000$ gauss, the most intense peaks do indeed conform to the above theorem.)

The more realistic assumption that the nuclear Zeeman term is negligible at X-band for radicals like malonic acid still leads to serious mathematical difficulties. The nuclear spin is quantized along the internal magnetic field at the nucleus; the outer doublet, v_3 and v_4, corresponding to $M_I = 1/2, -1/2$, respectively, dominate (M_I is the spin component along the internal field produced by the electron). The resonance frequencies of the oriented radical, relative to the origin, $v = \nu_e$, are now given by:

$$v_{M_I} \sim (A^2\cos^2\theta + B^2\sin^2\theta\cos^2\phi + C^2\sin^2\theta\sin^2\phi)^{1/2} M_I \qquad (18)$$

We can readily determine the polycrystalline line shapes if (1) the dipolar interaction shows axial symmetry (B = C); if (2) the anisotropy is small so that A^2, B^2, C^2 are approximately equal. If B = C, equation 18 becomes:

$$\nu_{M_I} = [B^2 + (A^2 - B^2)\cos^2\theta]^{1/2} M_I \tag{19}$$

The corresponding line shapes, $g_{M_I}(\bar{\nu})$, are given by

$$g_{M_I}(\bar{\nu})d\nu \propto \sin\theta\, d\theta; \quad g_{M_I}(\bar{\nu}) \propto \left|\frac{d\cos\theta}{d\nu}\right| ;$$

$$g_{M_I}(\bar{\nu}) \propto \frac{1}{\left|A^2-B^2\right|^{1/2}} \left|\frac{(\nu/M_I)}{(\nu/M_I)^2-B^2}\right|^{1/2} \tag{20}$$

The resonance peak occurs at $\bar{\nu} = B\ M_I$; the width of the resonance is $\left|(B - A)\, M_I\right|$. (Equation 20 is also valid when $I > \frac{1}{2}$; now $M_I = I, I-1, \ldots, -I+1, -I$.)

When the anisotropy is small, make the following substitutions:

$$\bar{a} = 1/3\,(A^2 + B^2 + C^2) ;$$
$$\bar{b} = 1/6\,(B^2 + C^2 - A^2) ; \tag{21}$$
$$\bar{\ell} = 1/2\,(C^2 - B^2) .$$

Equation 18 becomes:

$$\nu_{M_I} = [\bar{a} + \bar{b}\,(1 - 3\cos^2\theta) + \bar{\ell}\cos^2\phi(\cos^2\theta - 1)]^{1/2} M_I ; \tag{22}$$
$$\sim (\bar{a})^{1/2}\,[1 + \bar{b}/2\bar{a}\,(1 - 3\cos^2\theta) + \bar{\ell}/2a\cos 2\phi(\cos^2\theta - 1)]M_I .$$

We have used the fact that $|b/a|$, $|\ell/a| \ll 1$ for sufficiently small

anisotropies. If one now uses the evaluation procedure given in the next section (see equations 22 ' ff.), one can show that the polycrystalline spectrum resulting from equation 22 conforms to Theorem I.

Although we have not been able to rigorously evaluate the polycrystalline line shape expressions for arbitrary A^2, B^2, C^2, the above cases (1) and (2) strongly suggest that Theorem I may also be valid when the hyperfine term dominates the Zeeman term. (M_I now replaces I_H.)*

---

*Blinder (10) has also considered the case of an axially symmetric interaction having a negligible nuclear Zeeman term. In addition, he asserts in a footnote that when the axial symmetry is removed ($B \neq C$), the resonance peaks occur at $(B^2 + C^2)^{1/2} M_I$. (The reader is cautioned not to confuse our notation with Blinder's notation.) This result clearly cannot be right since it is not invariant to a relabelling of the principal axes of the hyperfine dyadic. Lefebvre (7) has carried out a computer evaluation of equation 17 for a $\dot{C}H$ fragment when $H \sim 850$ gauss. S_H is still a good quantum number, but the nuclear Zeeman term is now negligible. The observed resonance peaks conform very well to Theorem I. (Actually somewhat better results are obtained if one adds the small Zeeman term, $\nu_p M_I$, to the peak positions given by Theorem I.)

I_H A GOOD QUANTUM NUMBER

We now proceed to examine the consequences of assuming I_H to be a good quantum number. The following substitutions:

$$S_{\hat{z}} = S_H \cos\theta; \quad I_{\hat{z}} = I_H \cos\theta; \qquad a = \frac{1}{3}(A + B + C);$$

$$S_x = S_H \sin\theta \cos\phi; \quad I_x = I_H \sin\theta \cos\phi;$$

$$b = \frac{1}{6}(B + C - 2A); \qquad (21)'$$

$$S_y = S_H \sin\theta \sin\phi; \quad I_y = I_H \sin\theta \sin\phi;$$

$$\ell = \frac{1}{2}(C - B)$$

permit equation 5b to be written as

$$h\nu_{I_H}^{\prime} S_H = hS_H I_H [a + b(1 - 3\cos^2\theta) + \ell \cos 2\phi(\cos^2\theta - 1)] \quad (22)'$$

The isotropic term, a, in equations 21' and 22' arises from the Fermi contact interaction. We easily see from equation 22' that the spectrum will be symmetric about $\bar{\nu} = \nu_e$; consequently, once $g_{I_H}(\bar{\nu})$ is known, $g_{-I_H}(\bar{\nu})$ is also known. If $I_H = \frac{1}{2}$, $g_{1/2}(\bar{\nu})$ is given by:

$$g_{1/2}(\bar{\nu}) = \frac{1}{2\pi}\int_{-\infty}^{\infty} \exp\left(i\omega\left\{\bar{\nu} - 1/2[a + b(1 - 3\cos^2\theta) + \ell \cos 2\phi(\cos^2\theta - 1)]\right\}\right) d\omega$$

$$\times \int_{-1}^{1} d\cos\theta \int_{0}^{2\pi} d\phi \,. \qquad (23)$$

The evaluation of equation 23 proceeds as follows:

$$\int_0^{2\pi} \exp\left\{i\left[-\frac{\omega}{2}\ell(\cos^2\theta - 1)\cos 2\phi\right\}\right] d\phi = 2\pi J_0\left[\frac{\omega}{2}\ell(\cos^2\theta - 1)\right], \quad (24)$$

where J_0 is a Bessel function of zero order. Equation 23 now becomes

$$g_{1/2}(\bar{v}) = \int_{-1}^{1} \left\{ \int_{-\infty}^{\infty} \exp\left(i\omega\left\{ \bar{v} - \frac{1}{2}[a+b(1-3\cos^2\theta)]\right\}\right) \right. \tag{25}$$

$$\left. \times J_0\left[\frac{\omega \ell}{2}(\cos^2\theta - 1)\right] \right\} d\omega \, d\cos\theta .$$

Set

$$M = (\ell/2)(\cos^2\theta - 1), \quad p = \bar{v} - \frac{1}{2}[a + b(1 - 3\cos^2\theta)] .$$

The expression within the large brackets of equation 25 is one of Weber's discontinuous integrals (11), and evaluates either to zero if $M^2 < p^2$, or to $2/(M^2 - p^2)^{1/2}$, if $M^2 > p^2$. Equation 25 reduces to the following elliptic integral:

$$g_{1/2}(\bar{v}) = 4\int_R \frac{dx}{\left[M^2 - p^2\right]^{1/2}} = 4\int_R \frac{dx}{\left\{(\ell^2/4)(x^2-1)^2 - \left[\bar{v} - \frac{1}{2}(a+b) + \frac{3}{2}bx^2\right]^2\right\}^{1/2}} . \tag{26}$$

$x = \cos\theta$. R denotes the range of values of x between 0 and 1 such that $M^2 > p^2$. Setting $M^2 = p^2$, we obtain the boundary points, x_+ and x_- :

$$x_+ = \left| \frac{\bar{v} - (a+b-\ell)/2}{(\ell - 3b)/2} \right|^{1/2} = \left| \frac{\bar{v} - B/2}{A/2 - B/2} \right|^{1/2} ; \tag{27}$$

$$x_- = \left| \frac{-\bar{v} + (a+b+\ell)/2}{(\ell + 3b)/2} \right|^{1/2} = \left| \frac{\bar{v} - C/2}{A/2 - C/2} \right|^{1/2} .$$

The integrand of equation 26 becomes infinite at x_+ and x_-; nevertheless, the integral behaves properly except when $\bar{v} = B/2, A/2, C/2$. If $A < B < C$ and $A/2 \leq \bar{v} < B/2$,* R is given by $x_+ \leq x \leq x_-$; if $B/2 < \bar{v} \leq C/2$, R is given by $0 \leq x \leq x_-$. The integral, equation 26, can be shown to diverge at $\bar{v} = B/2$. The integral would also diverge at $\bar{v} = A/2, C/2$ if the ranges of integration were not zero. (When $\bar{v} = A/2$, $x_- = x_+ = 1$; when $\bar{v} = C/2$, $x_- = x_+ = 0$.) $g_{1/2}(A/2)$ and $g_{1/2}(B/2)$, although finite, must be obtained by a limiting process. The peak, therefore, occurs at $B/2$ when $A < B < C$.

If we assume that $B < C < A$, we obtain the following ranges of integration:

$$\begin{aligned} &0 \leq x \leq x_+ \quad \text{when} \quad B/2 \leq \bar{v} < C/2 ; \\ &x_- \leq x \leq x_+ \quad \text{when} \quad C/2 < \bar{v} \leq A/2 . \end{aligned} \tag{28}$$

The peak now occurs at $C/2$, $g_{1/2}(A/2)$, $g_{1/2}(B/2)$ must be obtained by a limiting process.

If $C \ll A \ll B$, the following ranges of integration are obtained:

$$\begin{aligned} &0 \leq x \leq x_- \quad \text{when} \quad C/2 \leq \bar{v} < A/2; \\ &0 \leq x \leq x_+ \quad \text{when} \quad A/2 < \bar{v} \leq B/2 . \end{aligned} \tag{29}$$

The peak now occurs at $\bar{v} = A/2$; $g_{1/2}(C/2)$ and $g_{1/2}(B/2)$ must be obtained by a limiting process.

Other inequalities can be examined. The result is always the same: the maximum peak of $g_{1/2}(\bar{v})$ always occurs at the middle value

*$A < B < C$ implies that $\frac{A}{2} \leq \bar{v} \leq \frac{C}{2}$.

of A/2, B/2, C/2. The width of the $g_{1/2}(\bar{\nu})$ resonance is given by 1/2 times the magnitude of the difference between the largest and smallest of the A, B, C terms. We have thus proven Theorem I when $I_H = \pm 1/2$. (The extension of the proof to $I_H > 1/2$ is trivial.)

We note further, if two of the three terms A, B, C are equal, as occurs when the interaction has cylindrical symmetry, the line shape contribution of $g_{1/2}(\bar{\nu})$ is the same as that arising from the interaction of two-point dipoles.* If A = B = C, there is only the Fermi contact term, and $g_{1/2}(\bar{\nu})$ gives a delta function at A/2.

---

*When B is equal to C, ℓ is equal to 0; equation 22 reduces to the sum of a Fermi term, $h a S_H I_H$, and a term $h S_H I_H b(1 - 3\cos^2\theta)$, which looks like the interaction of two-point dipoles. The Fermi term clearly gives no line broadening; the dipolar term gives the well-known line shape $G(\bar{\nu}) \propto \left|\cos\theta\right|^{-1}_{\nu=\bar{\nu}}$ (E. R. Andrew, "Nuclear Magnetic Resonance," p. 155 ff., Cambridge Press). Our equation 26 also gives the same result:

When ℓ is equal to 0, M is equal to 0; consequently, $g_{1/2}(\bar{\nu})$ is zero whenever $p > 0$. When $p = 0$, the integrand is 1/0, and is infinite. This defines a delta function, $\delta(p) = \delta[\bar{\nu} - 1/2(a + b) + 3/2\, bx^2]$.

$$\therefore g_{1/2}(\bar{\nu}) \propto \int \delta(p)\, dx \propto \left|x\right|^{-1}_{\nu=\bar{\nu}} = \left|\cos\theta\right|^{-1}_{\nu=\bar{\nu}}.$$

A GENERAL POLYNUCLEAR RADICAL

We now examine the polycrystalline spectrum of a radical consisting of n nuclei interacting with an unpaired electron. We again assume that the spins of all n nuclei are quantized along the external field direction. The experimental spectrum is symmetrical about $v = \nu_e$, and is a linear superposition of the "allowed" resonances, $g_\lambda(v)$. (The number of "allowed" resonances if all nuclei had I = 1/2 spin, for example, would be 2^n.) If n is large, the resonances superimpose to form "composite" resonances; the number of dominant composite resonances that need be considered in practice are generally smaller than the number of "allowed" transition.

We assert that any "allowed" resonance, $g_\lambda(v)$, can be calculated from a single $\underline{T}$ dyadic $\underline{T}_\lambda$. The proof is as follows: The spin Hamiltonian for the polynuclear problem is:

$$\underset{\sim}{\mathcal{H}} = h\nu_e \underset{\sim}{S}_H - h \sum_{m=1}^{n} v_m I_{H_m} - \underset{\sim}{S}_H \sum_{m=1}^{n} \hat{e}_H \cdot \underline{T}_m \cdot \hat{e}_H \underset{\sim}{I}_{H_m} . \tag{30}$$

The transition frequencies of the oriented radical are:

$$v_\lambda = \left[\sum_m I_{H_m} (A \cos^2\theta + B \sin^2\theta \cos^2\phi + C \sin^2\theta \sin^2\phi)_m\right]_\lambda \tag{31}$$

The subscript, λ, denotes a particular assignment of nuclear spin components, I_{H_m}, to the n nuclei. The direction cosines in equation 31 are taken relative to the principal vectors of the corresponding $\underline{T}_m$ dyadics.

Choose a convenient axes system $\hat{k}'$, $\hat{i}'$, $\hat{j}'$, and express the direction cosines (eq. 31) in terms of the direction cosines, x_1', x_2', x_3', relative to $\hat{k}'$, $\hat{i}'$, $\hat{j}'$, respectively. ($x_1' = \cos\theta_1$; $x_2' = \sin\theta_1\cos\phi_1$; $x_3' = \sin\theta_1\sin\phi_1$). Equation 31 now has the general quadratic form:

$$v_\lambda = \sum_{s,t=1}^{3} A'_{st}(\lambda)\, x'_s\, x'_t \qquad (32)$$

$A'(\lambda)$ denotes a symmetric matrix whose elements are functions of the geometry of the molecule, the magnitudes of the nuclear interactions with the electron, and the particular choice of axes, $\hat{k}'$, $\hat{i}'$, $\hat{j}'$. We now diagonalize the A' matrix and obtain the principal values $\bar{A}_\lambda, \bar{B}_\lambda, \bar{C}_\lambda$ relative to the principal vectors, $\hat{k}_\lambda, \hat{i}_\lambda, \hat{j}_\lambda$. Our diagonalized matrix defines the $\underline{T}_\lambda$ dyadic, $\underline{T}_\lambda = \left\{ \bar{A}\,\hat{k}\,\hat{k} + \bar{B}\,\hat{i}\,\hat{i} + \bar{C}\,\hat{j}\,\hat{j} \right\}_\lambda$. Equation 31 can be written as

$$v_\lambda = 1/2\ \hat{e}_H \cdot \underline{T}_\lambda \cdot \hat{e}_H \quad . \qquad (33)$$

The results are independent of our initial choice of axes. Theorem I tells us that the resonance peak of $g_\lambda(v)$ will occur at 1/2 times the middle value of $\left\{\bar{A}, \bar{B}, \bar{C}\right\}_\lambda$, and that the width of the resonance will be given by 1/2 times the difference between the maximum and minimum values of the set $\left\{\bar{A}, \bar{B}, \bar{C}\right\}_\lambda$. We can calculate the line shape from the elliptic integral, equation 26 ($a_\lambda, b_\lambda, \ell_\lambda$ replaces a, b, ℓ).

As an illustration we consider the special case of π-electron radicals. We choose an axes system, $\hat{k}$, $\hat{i}'$, $\hat{j}'$, fixed in the radical

system. The $\hat{k}$ axis is taken perpendicular to the molecular plane; all nuclei have a principal vector parallel to $\hat{k}$. We substitute

$$\begin{pmatrix} \cos\theta \\ \sin\theta\cos\phi \\ \sin\theta\sin\phi \end{pmatrix}_m = \begin{pmatrix} 1 & 0 & 0 \\ 0 & \cos\xi_m & \sin\xi_m \\ 0 & -\sin\xi_m & \cos\xi_m \end{pmatrix} \begin{pmatrix} \cos\theta \\ \sin\theta'\cos\phi' \\ \sin\theta'\sin\phi' \end{pmatrix} \quad (34)$$

into equation 31, and obtain:

$$\nu_\lambda = \frac{\bar{a}_\lambda}{2} + \frac{\bar{b}_\lambda}{2}(1-\cos^2\theta) + \frac{\bar{\ell}_\lambda}{2}(\cos^2\theta-1)\cos(2\phi'-\omega_\lambda)\,, \quad (35a)$$

where

$$\bar{a}_\lambda = (\bar{A}_\lambda + \bar{B}_\lambda + \bar{C}_\lambda)/3 = 2\left[\sum_{m=1}^{n} I_{H_m}(A_m + B_m + C_m)/3\right]_\lambda ;$$

$$\bar{b}_\lambda = (\bar{B}_\lambda + \bar{C}_\lambda - 2\bar{A}_\lambda)/6 = 2\left[\sum_m I_{H_m}(B_m + C_m - 2A_m)/6\right]_\lambda ;$$

$$\bar{\ell}_\lambda = (\bar{C}_\lambda - \bar{B}_\lambda)/2 = 2(\ell_{a\lambda}^2 + \ell_{\beta\lambda}^2)^{1/2} ; \quad (35b)$$

$$\cos\omega_\lambda = \frac{\ell_{a\lambda}}{\bar{\ell}_\lambda} \; ; \quad \sin\omega_\lambda = \frac{\ell_{\beta\lambda}}{\bar{\ell}_\lambda} \; ;$$

$$\ell_{a\lambda} = \left\{\sum_m I_{H_m}[(C_m - B_m)/2]\cos(2\xi_m)\right\}_\lambda ;$$

$$\ell_{\beta\lambda} = \left\{\sum_m I_{H_m}[(C_m - B_m)/2]\sin(2\xi_m)\right\}_\lambda .$$

If one rotates the $\hat{k}$, $\hat{i}'$, $\hat{j}'$ axes system through an angle $\omega_\lambda/2$ about the $\hat{k}$ axis, one can replace $\cos(2\phi'-\omega_\lambda)$ in equation 35a by $\cos 2\phi_\lambda$. (The new axes $\hat{k}$, $\hat{i}_\lambda$, $\hat{j}_\lambda$ are the principal axes of the $\underline{T}_\lambda$

dyadic. .) The principal values $\bar{A}_\lambda$, $\bar{B}_\lambda$, $\bar{C}_\lambda$ are readily obtained from equation 35b; the line shape, $g_\lambda(\bar{\nu})$, from the appropriately modified equation 26 (a, b, ℓ replaced by $\bar{a}_\lambda$, $\bar{b}_\lambda$, ℓ_λ).

In the above sections we have concerned ourselves with calculating the polycrystalline line shape in detail. Gross features of the spectra are incorporated in the second and higher moment expressions. Moment measurements can be particularly useful when $\underline{n}$ is large so that a detailed line shape study may be impractical. They can also be used as a check on the conclusions reached from a detailed line shape study.

The 2p'th moment of a polycrystalline spectrum is defined as

$$\left\langle (\Delta\nu)^{2p} \right\rangle_{\theta,\phi} = \left\langle \sum_\mu \nu_\mu^{2p}(\theta,\phi)\, R_\mu(\theta,\phi) \Big/ \sum_\mu R_\mu(\theta,\phi) \right\rangle_{\theta,\phi} . \qquad (36)$$

$\langle \quad \rangle_{\theta,\phi}$ denotes an averaging over all angles θ, ϕ.

The sum is over all possible transitions, ν_μ (2^{2n} in the case of n, I = 1/2, nuclear spins); R_μ is the corresponding intensity. Hanna and McConnell (12) have shown that the polycrystalline second moment of an arbitrary polynuclear radical consisting of n, I = 1/2,* nuclei interacting magnetically with the unpaired electron is:

---

* Our moment definition (eq. 36) gives values that are 2^{2p} smaller than that used by Hanna and McConnell. We shall not consider the moments of radicals having I > 1/2 nuclei. If desired, they can be readily derived, and are expected to be similar in content to equations 37 ff.

$$\langle(\Delta\nu)^2\rangle_{\theta,\phi} = \sum_{m=1}^{n} \langle(\Delta\nu)^2_m\rangle_{\theta,\phi} = \sum_m \frac{(A^2+B^2+C^2)_m}{12} \quad ; \tag{37}$$

$$(\Delta\nu)^2_m = 1/4\,(A^2\cos^2\theta + B^2\sin^2\theta\cos^2\theta + C^2\sin^2\theta\sin^2\phi)_m \quad .$$

The second moment is simply the sum of the second moment contributions of the individual nuclei, and is independent of the magnitudes of the nuclear Zeeman terms.

The fourth moment can be shown to be:

$$\langle(\Delta\nu)^4\rangle_{\theta,\phi} = \sum_m \langle(\Delta\nu)^4_m\rangle_{\theta,\phi} + 6\sum_{m>r} \langle(\Delta\nu)^2_m\,(\Delta\nu)^2_r\rangle_{\theta,\phi} \tag{38a}$$

where

$$\langle(\Delta\nu)^4_m\rangle_{\theta,\phi} = 1/30\left[(A^2+B^2+C^2)-(AB+AC+BC)\right]_m \nu_m^2 \tag{38b}$$

$$+\left[1/80\,(A^4+B^4+C^4)+(1/120\,(A^2B^2+A^2C^2+B^2C^2)\right]_m .$$

The relative orientations of the principal axes of the $\underline{T}_m$ dyadics now appear in the last term of equation 38a. We note that the fourth moment is field dependent since it involves the nuclear Zeeman frequencies; consequently, for sufficiently large external field it may be necessary to truncate the sum in equation 36. (The field dependence comes from the weak outer frequencies, which, with increasing H, become correspondingly smaller in intensity, and further removed from the strong, field insensitive, inner frequencies.)

SPECTRA OF POLYCONJUGATED HYDROCARBON RADICALS

We now apply the results of the above sections to polyconjugated hydrocarbon radicals. The spins of all the protons are assumed quantized along the external field. (This is the case at X-band if the unpaired electron spin is distributed more or less equally over four or more carbon atoms.)

The dotted curves in Figure I illustrate the polycrystalline line shape (eq. 26) that would be obtained from a $\dot{C}H$ radical fragment when I_H is a good quantum number. The unpaired electron is assumed to be essentially localized in a $2p_z$ orbital centered on the carbon atom; the x-axis coincides with the CH bond direction. The values for A, B, C are -61.5, -30, -92.5 Mc, respectively, and were obtained from the experimental work on the oriented malonic acid radical (3).

Two broad peaks separated by $|A| = 61.5$ Mc are obtained; the end point frequencies of each peak are $|B/2| = 15$ Mc, and $|C/2| = 46$ Mc. The asymmetry of the shoulders of the peaks is negligible since $|A - B|$ is approximately $|C - A|$. No overlap of the two resonance peaks occurs because A, B, C all have the same sign.

The solid curves in Figure I have been included to illustrate how a different set of values of A, B, C, which we have arbitrarily chosen to be 5, 78.5, and 111.5 Mc, would have altered the line shape.

The significant feature of the polycrystalline spectrum of the $\dot{C}H$ fragment is its remarkable similarity to the liquid solution spectrum. In a liquid solution the dipolar interactions of the $\dot{C}H$ fragment average out to zero, leaving only the isotropic Fermi term (1). The latter term gives two sharp hyperfine lines, separated by an amount

$$|a| = |(A + B + C)/3| = |B| = 60 \text{ Mc} .$$

Polyconjugated hydrocarbon radicals can generally be regarded as π-electron radicals. McConnell and Chesnut have shown that the Fermi contact interaction term, a_m, of the m'th proton of a π-electron hydrocarbon radical is approximately $-60\, p_m$ Mc. p_m is the electron spin density on the carbon atom to which the proton is bonded. The corresponding $\underline{T}_m$ dyadic is $-(60\hat{k}\hat{k} + 30\hat{i}\hat{i} + 90\hat{j}\hat{j})_m p_m$ Mc. Using this fact, and equation 35b, one can show that the polycrystalline line shapes of polyconjugated hydrocarbon radicals should be very similar to those obtained from the liquid state.*

This similarity was observed experimentally by Brown, Anderson, and Gutowsky in connection with their proton resonance studies of polycrystalline samples of DPPH and TPPAP (8). They found that the hyperfine term $\langle S_H \rangle \hat{e}_H \cdot \underline{T}_m \cdot \hat{e}_H I_{H_m}$ could be replaced by

---

* If the hydrocarbon contains C^{13} atoms, the polycrystalline and liquid resonance spectra would be different. The C^{13} nucleus can interact magnetically with the unpaired electron; the middle value of its $\underline{T}$ dyadic does not equal its Fermi contact term (13).

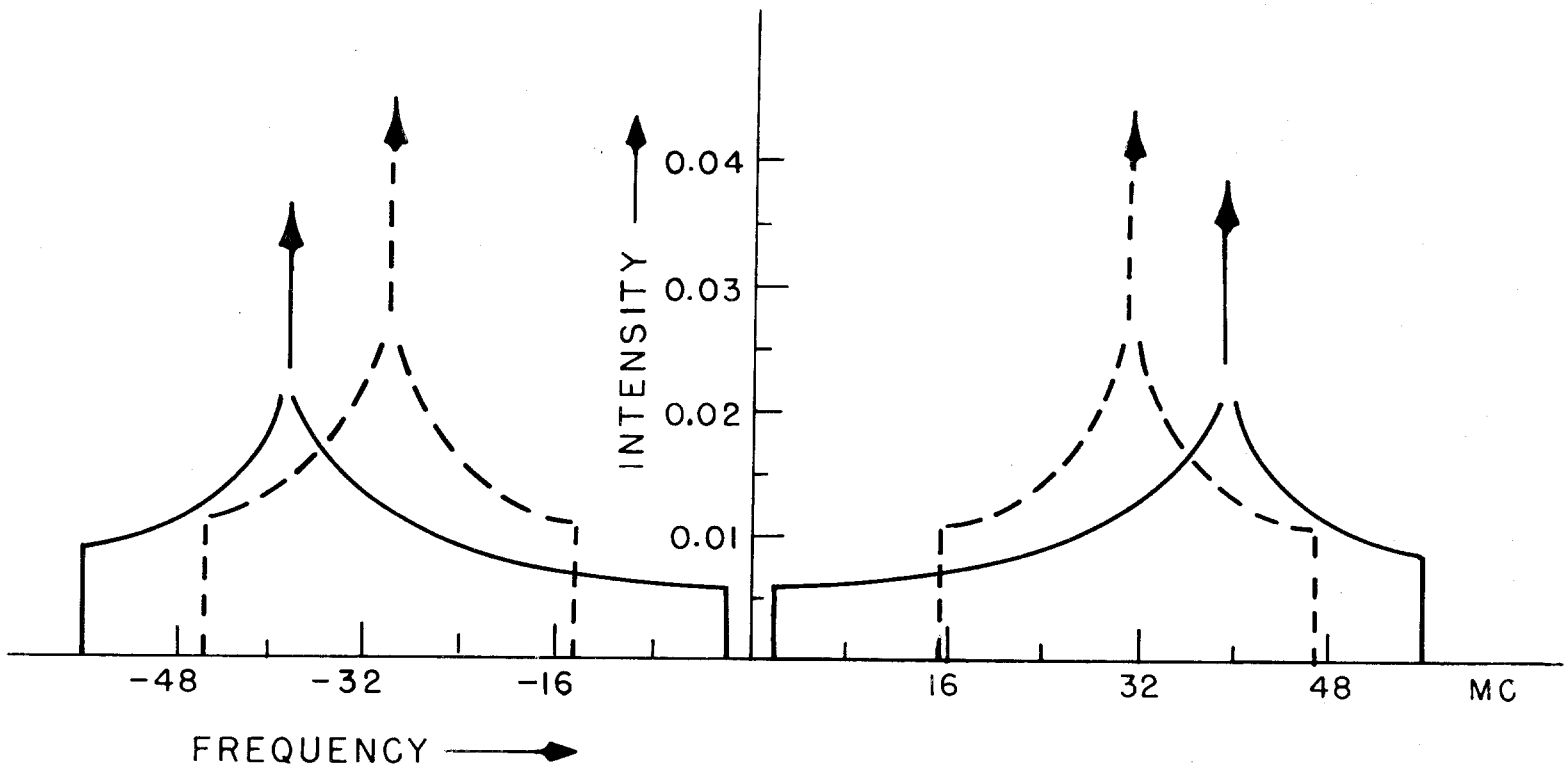

Figure I. The theoretical polycrystalline line shape of a $\dot{C}H$ radical fragment. The component line width, γ (Eq. 16), was set equal to zero. The dotted curve is based on the experimental values of A, B, C, which are -61.5, -30, -92.5 Mc , respectively. The solid curve illustrates how the line shape is modified by an arbitrarily different set of values for A, B, C taken as 5, 78.5, 111.5 Mc , respectively.

$h a_m \langle S_H \rangle I_{H_m}$ for purposes of determining resonance positions (see an earlier footnote); i.e., the anisotropic interaction could be effectively ignored. The extent of the resonance broadening and the shape of the lines obtained conform very well with the conclusions of this section.

CONCLUSION

We have shown how the polycrystalline spectra of an arbitrary polynuclear radical can be correlated with the magnetic dipolar interactions between the electron and nuclei. The theorem that enables us to do so was derived for a large external field relative to the internal dipolar fields; however, we suspect that this theorem, possibly in slightly modified form, may be applicable when the internal fields at the nuclei dominate the external field. When the internal and external fields are comparable, it is necessary to evaluate rather complicated integral expressions.

Polycrystalline spectra analysis can potentially give (1) the magnitudes and relative signs of the principal terms, $[A, B, C]_m$; and (2) the relative orientations of the diagonalizing vectors, $[\hat{k}, \hat{i}, \hat{j}]_m$.*

* In practice, one usually knows, either from theoretical considerations or previous experiments, the absolute orientations and signs of the principal vectors and principal values of some $\underline{T}_r$ dyadic; consequently, the ambiguity in the signs of $[A,B,C]_m$ and the orientations of $[\hat{k},\hat{i},\hat{j}]_m$ are resolved. There is still the unresolved ambiguity in the assignment of the principal values to the corresponding principal vectors. For example, we see from equation 35b that the line shape is invariant to an interchange of B_m, C_m in the case of π-electron radicals.

We have shown how this information can be extracted when the external field is sufficiently large. In practice, the determination of the $\underline{T}_m$ dyadic from the polycrystalline spectra may be rendered difficult for a number of reasons:

(1) If n is large, hand calculation would be impractical, and an electronic computer would be needed. Large n require very accurate spectra measurements if all the unknowns are to be determined. It is questionable whether such accuracy can be achieved;

(2) Significant line broadening mechanisms other than the dipolar can seriously qualify the conclusions we have reached. A large γ (eq. 16), for example, can shift resonance positions (7,10); an anisotropic g_e factor can destroy the symmetry of the line shape, $g(\bar{\nu})$, about $\bar{\nu} = \nu_e$ and also shift resonance positions (14).

REFERENCES

PART I

1. H. Sternlicht, J. Chem. Phys. 33, 1128 (1960).
2. D. J. E. Ingram, "Free Radicals as Studied by Electron Spin Resonance" (Butterworths Scientific Publications, Ltd., London, 1958).
3. H. M. McConnell, C. Heller, T. Cole, and R. W. Fessenden, J. Am. Chem. Soc. 82, 766 (1960).
4. D. K. Ghosh and D. H. Whiffen, Mol. Phys. 2, 285 (1959).
5. N. M. Atherton and D. H. Whiffen, Mol. Phys. 3, 1 (1960).
6. H. M. McConnell and J. Strathdee, Mol. Phys. 2, 129 (1959).
7. R. Lefebvre, J. Chem. Phys. 33, 1826 (1960).
8. T. H. Brown, D. H. Anderson, and H. S. Gutowsky, J. Chem. Phys. 33, 720 (1960).
9. H. M. McConnell and D. B. Chesnut, J. Chem. Phys. 28, 107 (1958); 27, 984 (1957).
10. S. M. Blinder, J. Chem. Phys. 33, 748 (1960).
11. A. Gray, G. Mathews, and T. McRobert, "A Treatise on Bessel Functions and Their Applications to Physics," (McMillan and Co., Ltd., London, 1952), p. 64.
12. M. W. Hanna and H. M. McConnell, "Free Radicals in Biological Systems" (Academic Press, New York, N. Y., 1961), p. 133.

13. T. Cole and C. Heller, J. Chem. Phys. 34, 1085 (L) (1961).

14. R. Lefebvre, J. Chem. Phys. 35, 762 (L), 1961.

PART II*

PARAMAGNETIC EXCITONS IN MOLECULAR CRYSTALS

INTRODUCTION

Within the past several years a number of successful paramagnetic resonance experiments have been performed on phosphorescent aromatic hydrocarbons. Hutchison and Mangum (2) observed electron spin resonance from triplet state naphthalene ($^3B^+_{2u}$) upon irradiating a single crystal of a solid solution of naphthalene in durene with ultraviolet light. Van der Waals and de Groot (3) obtained ESR spectra from rigid glass solutions of phosphorescing naphthalene, coronene, triphenylene, and 1,3,5-triphenylene. Efforts to obtain resonance spectra from pure phosphorescing aromatic crystals have, to the best of the author's knowledge, not yet been successful.

The ESR spectra of the pure crystals are of particular interest; it is possible that they may reveal the presence of triplet excitons. Both triplet (4,5) and singlet (6) excitation energy transfer processes are known to occur in aromatic systems in the solid state. Whereas the singlet-exciton concept has proved very useful in explaining energy transfer processes in molecular crystals (e.g., sensitized fluorescene, Davydov splittings), the nature and role of the triplet exciton in energy transfer processes involving triplet state molecules has yet to be clarified.

*Most of the contents of Part II (Chapter A) have appeared in an earlier paper (1).

A crystal consists of identical elementary units which may be molecules, atoms, or groups of molecules, atoms, or groups of molecules, atoms and ions. Upon exciting the crystal, say by optical means, the excitation quantum need not remain localized in any of these units. Because of interactions between the molecules, and the resonance caused by the translatory equivalence of the elementary units, a propagation or transfer of excitation energy occurs between the elementary units. Stationary states of the crystal, in fact, are characterized by having the excitation quantum distributed over a larger number of molecules.

Consider a crystal having one molecule per unit cell (7, 8). Let $|r\rangle$ represent a state of a crystal in which molecule r is in the excited state ϕ'_r, and all other N-1 molecules* are in their ground states, ϕ. The crystal energies are solutions of the NXN secular determinant:

$$\left| \langle r | \mathcal{H}_o | r' \rangle - \langle r | r' \rangle \varepsilon \right| = 0 . \qquad (1)$$

The stationary states are the corresponding N linear combinations of the one-molecule excited state functions $|r\rangle$. Here $\mathcal{H}_o$ is

---

*For convenience of mathematical treatment, it is customary to impose cyclic boundary conditions on the crystal. A sufficient number of translations of the crystal along any of the unit vectors eventually causes the crystal to repeat on itself. If N, the number of unit cells in this cyclic boundary, crystal, is taken to be very large, the physics of the problem is clearly unaffected.

the complete exact kinetic and electrostatic Hamiltonian for the problem:

$$\mathcal{H}_o = \sum_r h_r + 1/2 \sum_{r \neq s} V_{rs} . \qquad (2)$$

h_r denotes the Hamiltonian of the isolated molecule, r ; V_{rs}, the interaction of molecule r with molecule s. The sum is over all molecules of the crystal.

Since the crystal has translational symmetry, $\mathcal{H}_o$ is left invariant when the crystal is translated by a vector $\hat{g}$ connecting two lattice points. Furthermore, the various eigenstates of $\mathcal{H}_o$ serve as a basis for the unidimensional irreducible representation of the translation group. These considerations lead to the following expression for the eigenstates of $\mathcal{H}_o$:

$$|\hat{k}> = \frac{1}{N^{1/2}} \sum_n |n> \exp [i\, 2\pi\, \hat{k} \cdot \hat{R}_n] . \qquad (3)$$

A translation by an arbitrary lattice vector, $\hat{g}$, causes $|\hat{k}>$ to be multiplied by $\exp[i\, 2\pi\, \hat{k} \cdot \hat{g}]$. $\hat{R}_n$ denotes the position of the molecule n.

The cyclic crystal boundary conditions define a band or spectrum of permissible values for $\hat{k}$.* We note that

---

*The concept of the reciprocal lattice has been found to be very useful for denumerating the exciton states, and studying their sym-properties (9,10). Denote the primitive translation vectors (i.e., $\hat{}$ the unit cell vectors) of the crystal by $\hat{t}_1$, $\hat{t}_2$, $\hat{t}_3$; then the primitive translation vectors, $\hat{b}_1$, $\hat{b}_2$, $\hat{b}_3$, of the reciprocal lattice are given by

$$\hat{b}_i \cdot \hat{t}_j = \delta_{ij}$$

The permissible values of $\hat{k}$ lie within the parallelopiped unit cell defined by $\hat{b}_1$, $\hat{b}_2$, $\hat{b}_3$ (10) :

$$\langle \hat{k} | \mathcal{H}_o | \hat{k}' \rangle = 0 , \tag{4}$$

when $\hat{k} \neq \hat{k}'$, since $\hat{k}$ and $\hat{k}'$ belong to different irreducible representations of the translation group. The energy, $\mathcal{E} = E_{\hat{k}}$, of the $\hat{k}$'th state is

$$S + \sum_{\ell > n} M_{n\ell} \, e^{i 2\pi \hat{k} \cdot (\hat{R}_\ell - \hat{R}_n)} , \tag{5}$$

where $M_{n\ell}$ is the "transfer" integral

$$M_{n\ell} = \langle \phi'_n \, \phi_\ell \, | \, V_{n\ell} \, | \, \hat{A} \, \phi_n \, \phi'_\ell \rangle . \tag{6}$$

ϕ'_j denotes an excited state function located on molecule j; ϕ_j, the unexcited wave function. $\hat{A}$ is the well known antisymmetrization operator, $\sum_P (-1)^P P (\;)$. The sum is over all possible permutations, P, of pairs of electrons between molecules n and ℓ. S is independent of $\hat{k}$.

If one had a free particle of mass m, and momentum $\hat{p} = \hbar \hat{k}$, its energy would be

$$\hat{k} = K_i \hat{b}_i \; ; \; K_i = p_i / N_i \; ; \; p_i = \frac{-N_i}{2}, \frac{-N_i+1}{2}, \ldots 0 \ldots, \frac{N_i - 1}{2} .$$

The cyclic boundary condition requires that the crystal lattice repeats itself after N_i primitive translations, $\hat{t}_i$. If $\hat{k}$ lies outside the parallelopiped, no new irreducible representation, hence no new state, is introduced. This follows by noting that

$$\exp[i2\pi \hat{k} \cdot \hat{g}] = \exp[i2\pi \hat{k}' \cdot \hat{g}] \exp[i2\pi K_q \cdot \hat{g}] = \exp[i2\pi \hat{k}' \cdot \hat{g}] ,$$

where $\hat{k}'$ lies within the parallelopiped and K_q is a vector joining two reciprocal lattice points.

$$\frac{\hbar^2}{2m}\left(k_x^2 + k_y^2 + k_z^2\right). \tag{7}$$

When $\hat{k}$ is small, equation 5 reduces to

$$S + I_x k_x^2 + I_y k_y^2 + I_z k_z^2 , \tag{8}$$

For a crystal having cubic symmetry, $I_x = I_y = I_z = \hbar^2/2m^*$ m^* defines an effective mass. Thus, $\hat{k}$ can be regarded as a pseudo-momentum, and S would then be the self energy or zero point energy of this pseudo-particle. For non-cubic crystals, the effective mass will be anisotropic and depend upon the direction of propagation. An effective mass tensor is, therefore, introduced.

$$\left(\frac{1}{m^*}\right)_{ij} = \frac{1}{\hbar^2}\,\frac{\partial^2 E_{\hat{k}}}{\partial k_i\,\partial k_j} , \tag{9}$$

Equation 9 also defines the effective mass tensor when $\hat{k}$ is large. (For large $\hat{k}$, the anisotropic effective mass will also depend on velocity (i.e., upon k)).

The above discussion points out that excitation waves behave very much like matter waves. By taking a linear combination of the various $\hat{k}$ states that differ slightly in the direction and magnitude of $\hat{k}$, we can form a wave packet having a group velocity, $\hat{v}_g$, in the $\hat{k}$'th direction given by

$$\hat{v}_g = \hbar^{-1} \hat{\nabla}_k E_{\hat{k}} \quad ; \quad \hat{\nabla}_k = \hat{e}_x \frac{\partial}{\partial k_x} + \hat{e}_y \frac{\partial}{\partial k_y} + \hat{e}_z \frac{\partial}{\partial k_z} . \quad (10)$$

$\hat{e}_x$, $\hat{e}_y$, $\hat{e}_z$ are vectors of magnitude 1 in the x, y, z directions. The pseudo-particle having an effective mass, momentum and velocity, $\hat{v}_g$, is referred to as a Frenkel exciton.

The concept of excitation waves and the associated Frenkel exciton breaks down if there are either (1) pronounced self-trapping effects; or (2) pronounced scattering by lattice vibrations, crystal defects, and/or impurities. A diffusional model would be more appropriate for the energy transfer processes.

Self-trapping effects correspond to a nuclear deformation accompanying a propagating exciton wave packet, thus increasing its effective mass. The self-trapping effects may be intermolecular and/or intramolecular in origin (11,12). In the event of significant self-trapping, the excitation may be highly localized. The major mechanism for the transfer of energy might then be the thermal vibrations of the lattice which brings the "trapped exciton" into a new configuration more favorable for transfer to occur. Under such circumstances, we are dealing with a diffusional process involving thermal activation.

In the event of pronounced scattering by the lattice (case (2) above), the propagation of energy is again diffusional but now no thermal activation is required.

If the excited state, ϕ', is paramagnetic with spin multiplicity greater than one, ESR experiments can, under appropriate conditions, distinguish between wavelike and diffusionlike energy propagation modes. In Chapter A we examine the consequence of triplet (wave) exciton motion on the ESR spectra of molecular crystals*; in Chapter B we examine the consequence of the diffusional motion of a "trapped" exciton. Our treatment ignores interactions between excitons, and is valid only at low concentrations for which spin exchange effects are negligible.

Aromatic molecules in the triplet state are characterized by a zero-field splitting of the spin states. The removal of the threefold spin degeneracy may be complete or partial, the extent depending upon the symmetry of the molecule and the nature of the triplet state molecular wave function. In these molecules the interaction responsible for this behavior is primarily the (electron spin)-(electron spin) dipolar interaction (13,14).

$$\underset{\sim}{\mathcal{H}}_D' = g_e^2 \beta^2 \sum_{i<j} [(\hat{\underset{\sim}{s}}_i \cdot \hat{\underset{\sim}{s}}_j) r_{ij}^{-3} - 3(\hat{r}_{ij} \cdot \hat{\underset{\sim}{s}}_i)(\hat{r}_{ij} \cdot \hat{\underset{\sim}{s}}_j) r_{ij}^{-5}] . \qquad (11)$$

The sum is over the electrons of the molecule; g_e is the (assumed isotropic) electron g factor; β is the electronic Bohr magneton; $\hat{\underset{\sim}{s}}_i$ is the spin operator of electron i in units of $\hbar$; $\hat{r}_{ij}$ is the distance

---

*We explicitly consider crystalline benzene, naphthalene, and coronene.

vector directed from i to j. It is possible to put equation 11 in the following form

$$\underset{\sim}{\mathcal{H}}_S = D(\underset{\sim}{S}_z^2 - \underset{\sim}{S}^2/3) + E(\underset{\sim}{S}_x^2 - \underset{\sim}{S}_y^2) . \qquad (12)$$

D, E are constants; $\underset{\sim}{S}_z$, $\underset{\sim}{S}_x$, $\underset{\sim}{S}_y$ are the z, x, y spin component operators (in units of $\hbar$) for a "S" = 1 system. (A simple derivation of equation 12 is given in the Appendix.) In the case of the aromatic molecules considered, $\hat{z}$, $\hat{x}$, $\hat{y}$ refer to the molecular axes of symmetry; $\hat{z}$ could be taken as the normal to the molecular plane.

In the presence of an external magnetic field, $\hat{H}$, the electron spin Hamiltonian of the aromatic molecule can be represented as

$$\underset{\sim}{\mathcal{H}} = D(\underset{\sim}{S}_z^2 - \underset{\sim}{S}^2/3) + E(\underset{\sim}{S}_x^2 - \underset{\sim}{S}_y^2) + g_e|\beta|\sum_i \hat{\underset{\sim}{s}}_i \cdot \hat{H} \qquad (13)$$

$$+ \sum_{i,j} \hat{\underset{\sim}{s}}_i \cdot T_{ij} \cdot \hat{\underset{\sim}{I}}_j .$$

$g_e|\beta|\sum_i \hat{\underset{\sim}{s}}_i \cdot \hat{H}$ is the Zeeman interaction term, $\underset{\sim}{\mathcal{H}}_z$; $\sum_{i,j} \hat{\underset{\sim}{s}}_i \cdot T_{ij} \cdot \hat{\underset{\sim}{I}}_j$ is the nuclear hyperfine term (15). The Zeeman term by itself would give a one line resonance at a frequency $\nu_o = g_e|\beta| h^{-1} H_o$ (ESR experiments are usually carried out at X-band where $\nu_o \sim 9{,}500$ Mc/sec. and $H_o \sim 3{,}500$ gauss). The nuclear hyperfine interaction terms cause the appearance of a number of additional lines essentially symmetrically distributed about H_o and having an overall extension of ~30 gauss. The inclusion of the spin-spin interaction term (i.e., the "fine" field), however, alters the spectrum radically. Because $\underset{\sim}{\mathcal{H}}_S$ is large

($\sim$0.1 $cm.^{-1}$, or, equivalently, $\sim$1000 gauss), the orientation of the external field relative to the molecular axes of symmetry becomes important, and the ESR spectrum is highly anisotropic. In addition, instead of obtaining a single resonance with nuclear hyperfine structure, one now obtains a two line resonance with hyperfine structure.* The separation between these two lines can be as large as 1,000 gauss for certain magnetic field orientations.

The above conclusions were first corroborated by Hutchison and Mangum (2) who obtained four ESR lines from their solid solution of naphthalene molecules in durene. One pair of lines could be assigned to each of the two differently oriented sites of naphthalene molecules in durene. (For some special orientations of the external field, the four lines merge to give two lines. This occurs when the external field is along a symmetry element of the crystal.)

It is possible that low lying triplet excited states of pure aromatic single crystals will give ESR spectra that are qualitatively different from that expected for the isolated molecules that make up the crystal. Differences in the spectra will be shown to be most pronounced if (a) there are two or more molecules per unit cell that are not related by a center of symmetry, and if (b) the Davydov splitting

---

*Actually, a third resonance can be present. For large external fields along the z axis, $\hat{H} \gtrsim 3{,}000$ gauss, this line has low intensity and corresponds to a semi-forbidden transition between states having spin components, $S_z = 1, -1$. We neglect this transition for simplicity of discussion.

of the triplet exciton states is large compared to $|D|$ and $|E|$.* Unfortunately, the triplet Davydov splittings have not as yet been observed experimentally. If the magnitude of the splitting is such that condition (b) is satisfied, the paramagnetic resonance of a triplet exciton wave can consist of essentially only two lines, due to the dipole interaction of equation 12, for all orientations of the external magnetic field. Furthermore, since the triplet exciton is distributed over many molecules, the nuclear hyperfine structure is washed out in contrast to the nuclear hyperfine structure that is observed for isolated molecules.

A two line spectrum representing an average over the molecular sites in the unit cell does not necessarily prove the existence of coherent exciton waves. For example, if the excitation is highly localized requiring thermal activation for transfer to occur, we have a "random walk" or diffusional process. A two line spectrum will occur if

$$\tau^{-1} \gg |D, E| .$$

Here τ represents the characteristic time for the random walk between nontranslatory neighbors of the unit cell. In general, we anticipate that (barring any pronounced chemical dimerization of excited molecules in the crystal) the excitation transfer rate, τ^{-1}, will be large if the nontranslatory neighbor interactions are large.

---

*The Davydov splitting is a concept that has been most useful in understanding the optical spectra arising from singlet excitons molecular crystals. The exciton lines are sharp, and the separations between them are called Davydov splittings. The magnitude of the splittings is related to the resonance interactions between the nontranslatory equivalent molecules in the unit cell.

If the excitation wave undergoes pronounced scattering by lattice vibrations or impurities, the excitation motion is again best regarded as being diffusional. The wave packet width of such a "diffusional" exciton may still be large in the sense that the excitation quantum is distributed over a number of molecules, translatory and nontranslatory. In that event, it is meaningless to assign a characteristic time, τ, for the random walk between nontranslatory neighbors; nevertheless, we again expect a two line spectrum corresponding to an average over all molecular sites when the interaction between nontranslatory neighbors is much larger than $|D|$ and $|E|$.

A. WAVE EXCITONS

AN EFFECTIVE HAMILTONIAN

The theory of singlet Frenkel excitons in aromatic molecular crystals has been the subject of extensive theoretical study by Davydov, Fox and Schnepp; McClure; Simpson; Craig; and Winston. A comprehensive review and bibliography have been given by McClure (6). As pointed out earlier, singlet Frenkel excitons in aromatic crystals are usually treated by elementary degenerate perturbation theory (eqs. 2-6). The matrix elements $M_{n\ell}$ can often be approximated by simple multipole expansions (6). Overlap of the electronic parts of the wave functions centered on different molecules does not appear in the evaluation of $M_{n\ell}$.

The problem of triplet exciton states in molecular crystals appears to be a little less straightforward. This is because, at first sight, one would expect the triplet exciton bandwidths to be extremely narrow. (If we now let $|t\rangle$ represent a crystal state having molecule t in the lowest triplet excited state, then all matrix elements of the type $\langle t|\mathcal{H}_o|t'\rangle$ in equation 1 reduce to two-electron exchange integrals between orbitals on different molecules, and these are expected to be very small (16). Our order of magnitude estimates using Slater type functions bear this out.) However, it is likely that intermolecular charge transfer triplet excited states make significant contributions toward broadening the lowest "neutral" triplet exciton bands. Recent

work by Lyons (17) has pointed out the possible importance of intermolecular charge-transfer effects in molecular crystals in connection with photoconductivity. It may well be that triplet exciton intermolecular charge transfer states make an appreciable (~1%) contribution to the lowest triplet exciton wave functions, and therefore play an important role in determining the triplet exciton bandwidth.* We hesitate to offer any detailed numerical calculations in support of this contention in view of the great uncertainties in molecular electronic wave functions at large distances, and in molecular wave functions of ionized states in crystals. Our main purpose here is to show that the problem of triplet exciton band can be handled by a secular determinant analogous to that given above in equation 1 for singlet excitons by replacing the exact spin independent Hamiltonian, $\mathcal{H}_o$, by an effective spin independent Hamiltonian, $\mathcal{H}_f$, that includes the effects of the charge-transfer states on the triplet exciton bandwidths.

Let $|\hat{k}, \Omega>$ represent an intermolecular charge-transfer ionization wave with wave vector $\hat{k}$ and band index Ω. The $|\hat{k}, \Omega>$ are to be regarded as variational functions to be used to improve the triplet exciton functions based on the neutral one molecule triplet states $|t>$ having energy E^o. Second-order perturbation theory for degenerate systems leads to the following effective Hamiltonian

*A. Zmerli (18) has recently claimed to have obtained phosphorescence spectra from single crystals of acenaphthene which show a Davydov splitting of 30 cm^{-1}. If this is correct, and not a spurious result arising possibly from impurities, or molecules in lattice defect sites, the 30 cm^{-1} splitting may well be due to charge transfer effects.

$\mathcal{H}_f$ (19):

$$\mathcal{H}_f = \mathcal{H}_o + \sum_{t,t'} R_{tt'} \; |t\rangle\langle t'| \quad ; \tag{14}$$

$$R_{tt'} = - \sum_{\hat{k},Q} (E_{kQ} - E^o)^{-1} V_{kQt'} V_{tkQ} \; ; \tag{15}$$

$$V_{kQt'} = \langle \hat{k}, Q | \mathcal{H}_o | t' \rangle \; . \tag{16}$$

To second order the triplet exciton energies, $\mathcal{E}$, are given by the following N X N secular determinant:

$$\left| \langle t | \mathcal{H}_f | t' \rangle - \langle t | t' \rangle \mathcal{E} \right| = 0 \; . \tag{17}$$

The assumption that the triplet exciton band is dominated by contributions from the ionization states is then equivalent to the following inequality for neighboring molecular pairs:

$$\left| R_{tt'} \right| > \left| (\mathcal{H}_o)_{tt'} \right| \; . \tag{18}$$

The ionization waves, $|\hat{k}, Q\rangle$, can be formally approximated by

$$|\hat{k}, Q\rangle = \sum_{\hat{R}} a(\hat{R}, Q) \; |\hat{k}, \hat{R}, Q\rangle \; ; \tag{19a}$$

$$|\hat{k}, \hat{R}, Q\rangle = \frac{1}{N^{1/2}} \sum_m e^{i2\pi \hat{k} \cdot \hat{R}_m} \left| Q_{\hat{R}_m, \hat{R}_m + \hat{R}} \right\rangle \; . \tag{19b}$$

($\hat{R}$ held constant)

$|Q_{\hat{R}_a, \hat{R}_b}\rangle$ denotes an antisymmetrized state of the crystal in which an electron has been removed from the molecule at $\hat{R}_a$ and added to the molecule at $\hat{R}_b$. For the sake of simplicity we have only considered one site per unit cell. The site index, θ, has been suppressed in Q for convenience of notation. The exact ionized wave would be a linear combination of the one site ionized waves.

We shall assume in the present work that only nearest-neighbor terms are important in the effective Hamiltonian. This implies that ionized waves having $|\hat{R}| > |\hat{t}|$, where $\hat{t}$ is the largest of the primitive translations of the crystal (see below), make negligible contributions to $\mathcal{E}$. This approximation appears to be reasonable because (1) the lowest lying ionized waves presumable are those having $|\hat{R}| \leq |\hat{t}|$; and (2) overlap considerations reduce further the coupling effectiveness of those states having $|\hat{R}| > |\hat{t}|$.

EXCITON BAND DEGENERACIES

Let us now consider a crystal of N molecules, where the unit cells are numbered, n = 1, 2, 3, ..., and where the molecular sites in the unit cell are specified by θ. Every molecule in the crystal is then completely identified by the pair of numbers n, θ. Let $|n\ \theta\ M\rangle$ represent an antisymmetrical crystal wave function in which molecule $n\theta$ is excited to its lowest triplet electronic state, with spin component M, and all other molecules are in their ground states. If one temporarily neglects matrix elements of $\mathcal{H}_f$ connecting different sites (e.g.,

$\langle n\theta M|\mathcal{H}_f|n'\theta M\rangle$, then the functions that diagonalize the secular determinant, equation 17, are the one site exciton functions,

$$|\hat{k}\,\theta\,M\rangle = \frac{1}{N^{1/2}} \sum_n |n\,\theta\,M\rangle e^{i2\pi \hat{k}\cdot\hat{R}_{n\theta}} \quad . \tag{20}$$

When matrix elements that connect different sites ($\theta \neq \theta'$) are included in the secular determinant, equation 17 , then this determinant is diagonalized by the crystal exciton wave functions

$$|\hat{k}_\ell\ M\rangle = \sum_\theta C_{\theta\ell}\ |\hat{k}\,\theta\,M\rangle \ . \tag{21}$$

Here subscript ℓ is a triplet exciton band index. (The number of bands is the same as the number of molecular sites in the unit cell.) For convenience of notation the nuclear vibrational functions corresponding to polaron or self-trapping effects are not included explicitly in the above equations. This can be done in a relatively simple way by using a variational procedure; the net effect is to reduce the exciton bandwidths by a factor depending on the overlap of nuclear vibrational functions.

In order to calculate the resonance spectra of the aromatic crystals considered in this chapter, it is necessary to determine the regions of band degeneracies or near band degeneracies. To the extent that we are in a region of the BZ* sufficiently far from those values

*In an earlier section we introduced the reciprocal lattice parallelopiped unit cell. This unit cell does not show the symmetry of the crystal; consequently, it is usually redefined. The new symmetric unit cell, which has the same volume as the original parallelopiped, is called the Brillouin Zone (BZ). It is constructed by putting a reciprocal lattice

of $\hat{k}$ for which there is a degeneracy between the bands (thus ensuring us that the energy separation between the bands is large compared with the spin-spin interaction), we can use the following 3X3 determinant to obtain the spin energies of the crystal:

$$\left| < \hat{k}_\ell \; M | \underset{\sim}{\mathcal{H}}_D + \underset{\sim}{\mathcal{H}}_z | \hat{k}\ell \; M' > - E \, \delta_{MM'} \right| = 0 \qquad (22)$$

$\underset{\sim}{\mathcal{H}}_D$ is given in equation 11, and the sum is over all the electrons in the crystal. Since $\underset{\sim}{\mathcal{H}}_D + \underset{\sim}{\mathcal{H}}_z$ belongs to the totally symmetric representation of the translation operator, we need only consider elements between states having the same $\hat{k}$. In regions of degeneracy, or near degeneracy where the separation between the bands is comparable to the spin-spin interactions, it is necessary to replace equation 22 by

$$\left| <\hat{k}_\ell \; M | \underset{\sim}{\mathcal{H}}_f + \underset{\sim}{\mathcal{H}}_D + \underset{\sim}{\mathcal{H}}_z | \hat{k}_{\ell'} M' > - E \delta_{MM'} \, \delta_{\ell\ell'} \right| = 0 \qquad (23)$$

where ℓ now ranges over the degenerate or near degenerate bands.

Divide the BZ into two regions, Δ and Γ, whose spin energies are to be calculated by equations 22 and 23, respectively. The relative volumes of the Δ and Γ regions are determined by the relative magnitudes of the Davydov splittings of the band and the spin-spin interaction. *

---

point at the origin of the zone and then drawing the perpendicular bisecting planes of the lines joining the origin to each of the near lattice points (9). The smallest closed volume bounded by these planes is the "first" BZ. (In this paper we need only concern ourselves with this "first" BZ.)

*We take the magnitude of the spin-spin interactions (relative to the isolated molecule) to be (3):

$$2/3 \, (D^2 + 3E^2)^{1/2} .$$

The Davydov splitting between two bands corresponds to the difference in energy between the $\hat{k} = 0$ states of the two bands. Large Davydov splittings relative to the spin-spin interaction imply that the volume of the Δ region is large relative to the Γ region. The Δ region gives triplet resonance spectra that are essentially independent of $\hat{k}$ (as will be shown below), while the Γ region gives spectra that are highly dependent on $\hat{k}$. Furthermore, the Δ region spectra will represent an average over sites. (In the case of naphthalene, for example, two line spectra would be obtained for all magnetic field orientations.)

If the Davydov splittings are small compared with the spin-spin interaction, the Γ region will occupy all of the BZ. However, now the spectra will be independent of $\hat{k}$, and will correspond to that expected from an oriented gas for which there is no averaging over sites. (In the case of naphthalene, four line spectra would be obtained for a general external field orientation.)

The physical reason for the strong dependence of the ESR spectra on the magnitude of the Davydov splitting is briefly the following: The Davydov splitting is a measure of the resonance interaction between different site molecules. If we assign the set of spin states $|M_\theta>$, $|M_{\theta'}>$ to sites θ and θ', the resonance interaction and the resonance integrals, $<n\theta M_\theta|\mathcal{H}_f|n'\theta' M_{\theta'}>$, are maximized if the sets $|M_\theta>$, $|M_{\theta'}>$ are the same. The resonance interaction is responsible for defining a common, albeit arbitrary, axis of spin quantization for the two sites, and spin orientation

is preserved during the excitation transfer process. The spin-spin interaction, on the other hand, defines certain preferred directions for the spin relative to the molecular symmetry axes. If we imagine that the excitation is transferring back and forth between two different site molecules, which have different orientations, the spin-spin interaction, $\mathcal{H}_D$, competes with the resonance interaction, $\mathcal{H}_f$. The former picks out preferred directions relative to the molecular axes of the site molecule on which the excitation is temporarily confined; whereas the latter "strives" to quantize the spin along a common axis for the two sites. When the resonance interaction between the site molecules is larger than the spin-spin interaction, a common axes system is defined for the unit cell, and two line ESR spectra are obtained. If the spin-spin interaction dominates, the individual site molecular axes retain their importance, and oriented gas spectra with no site averaging are obtained.

Equation 23 expresses the fact that the spin and resonance interactions of our system can be strongly coupled. That is, the resonance interaction between sites can depend strongly on the spin dipolar interaction of the unpaired electrons. The eigenstates of such a system might be referred to as "spinonic" states to emphasize this coupling.

In the balance of this chapter we explore the consequence of large Davydov splittings relative to the spin-spin interaction. The volume of Γ space will be determined by the extent that band

degeneracies occur. Band degeneracies can be classified as to whether they are required by symmetry or are accidental. The Hamiltonian of the crystal $\mathcal{H}_o$ or $\mathcal{H}_f$ is invariant to time reversal and the space group operations. It is easily shown that in the case of the aromatic crystals treated here there can only be symmetry degeneracies arising from time reversal. Furthermore, one can show that accidental degeneracies can occur for benzene while they do not occur for naphthalene and coronene. The matter of accidental degeneracies will be discussed later.

The effect of time-reversal symmetry on the energy bands of spinless states has been examined by Herring (20). (The extension of Herring's arguments to spin 1 states is straightforward, and leads to no new conclusions that cannot be derived from his original paper assuming spinless states.) Using Herring's method one can show that time reversal requires that energy bands stick together in pairs for all reciprocal lattice wave vectors, $\hat{k}^b$ ($\hat{k}^b$ is any wave vector that terminates on the boundary plane of the BZ that is perpendicular to a twofold screw axis of the reciprocal lattice).

Benzene belongs to the orthorhombic crystal system (21) and the D_{2h}^{15} (Pbca) space group which has three mutually perpendicular screw axes, and three mutually perpendicular glide planes. The three primitive translations, $\hat{t}_i$, of the crystal are all mutually perpendicular; the three primitive translations, $\hat{b}_i$, of the reciprocal lattice space are all

mutually perpendicular. One encounters degeneracies at all boundary points of the BZ. Naphthalene (22) and coronene (23) belong to the simple monoclinic system and the C_{2h}^{15} ($P2_{1/a}$) space group, which has a twofold screw axis. The primitive translations that define the unit cell of the crystal are:

$$\begin{aligned} \hat{t}_1 &= \hat{c} = c \sin\beta\,\hat{e}_1 + c\cos\beta\,\hat{e}_2 ; \\ \hat{t}_2 &= \hat{a} = a\,\hat{e}_2 ; \\ \hat{t}_3 &= \hat{b} = b\,\hat{e}_3 . \end{aligned} \tag{24}$$

$\hat{e}_1$, $\hat{e}_2$, $\hat{e}_3$ are three mutually perpendicular unit vectors. The $\hat{b}$ axis is parallel to the screw axis.

Figure II-1 shows a cross section of the BZ for the simple monoclinic system. It extends a distance $\hat{b}_3/2$ above and below the plane of the paper. The distinct values of $\hat{k}$ (see earlier footnotes) are given by:

$$\hat{k} = K_1\hat{b}_1 + K_2\hat{b}_2 + K_3\hat{b}_3 \quad ; \quad -1/2 \leq K_1, K_2, K_3 < 1/2 . \tag{25}$$

There is a degeneracy for all points on the BZ boundary plane perpendicular to the screw axis in $\hat{k}$ space (i.e., a degeneracy occurs for all points on the planes $K_3 = \pm 1/2$). In addition, it is possible to show that there are degeneracies in the naphthalene and coronene systems along the lines

$$k^{(1)} = \pm 1/2\,\hat{b}_2 + K_3\hat{b}_3 \; ; \; k^{(2)} = \pm 1/2\,\hat{b}_1 \pm 1/2\,\hat{b}_2 + K_3\hat{b}_3 . \tag{26}$$

(These lines lie in boundary planes.)

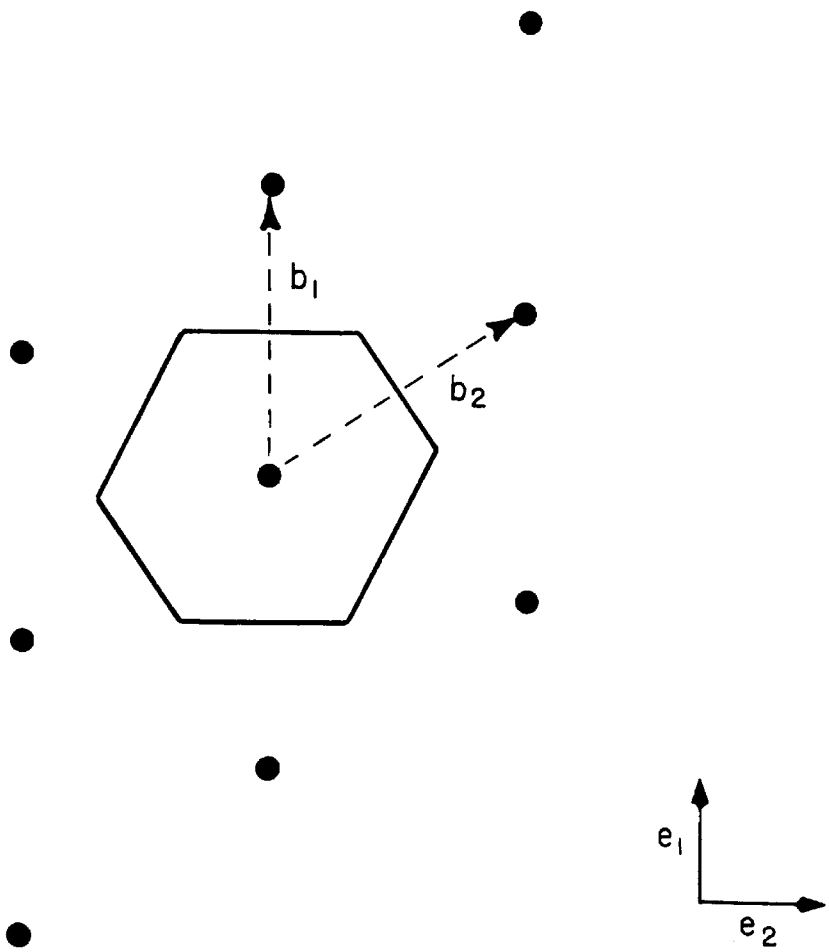

BRILLOUIN ZONE
(SIMPLE MONOCLINIC SYSTEM)

Figure II-1

The simplest way to demonstrate the above time reversal degeneracies without recourse to any elaborate symmetry arguments is to expand the exciton matrix elements, $\langle \hat{k}^b \theta M | \underset{\sim}{\mathcal{H}}_f | \hat{k}^b \theta' M' \rangle$, $\langle \hat{k}^{(i)} \theta M | \underset{\sim}{\mathcal{H}}_f | \hat{k}^{(i')} \theta' M' \rangle$ $(\theta \neq \theta')$, in terms of the molecular matrix elements $\langle n \theta M | \underset{\sim}{\mathcal{H}}_f | n' \theta' M' \rangle$. If one makes use of the fact that $\underset{\sim}{\mathcal{H}}_f$ is real, then one can show that when θ and θ' are related by a twofold screw axis operation, the exciton matrix elements $(\theta \neq \theta')$ are zero.* For the benefit of the interested reader, however, the time reversal symmetry proofs are given in the Appendix.

If the spin-spin interactions, $\underset{\sim}{\mathcal{H}}_D$, are included, the above band degeneracies still occur because $\underset{\sim}{\mathcal{H}}_D$ is also invariant to time reversal. The band degeneracies can be removed, however, by an external magnetic field. (Our system no longer shows time reversal symmetry--the new symmetry element is the product of time reversal and inversion of the magnetic field direction.)

One can show that there are no degeneracies required by the spatial symmetries of these aromatic crystals. To do this it is necessary to introduce the concept of the group of the wave vector $\hat{k}'$. This group comprises all those symmetry operations of the space group which leaves $\hat{k}'$ invariant. It can be shown (24) that a nonaccidental degeneracy of the band at certain values of $\hat{k}(\hat{k} = \hat{k}')$ can only occur if $\hat{k}'$ is left invariant by some symmetry operation. $\hat{k}'$ must therefore be either parallel to a rotation (or screw) axis or in the plane of a

*In an analogous manner we can show that the diagonal matrix elements (Eq. 23) of the θ, θ' sites are equal. As a result, we are led to a degeneracy that is essentially the same as that discussed by Herring (20).

reflection (or glide) plane. $|\hat{k}'_{\ell} M\rangle$ will denote a crystal exciton function where $\hat{k}'$ is along a symmetry element.

A member of the group of the wave vector $\hat{k}'$ can be denoted by $\{\underset{\sim}{B}|\hat{g}\}$, $\underset{\sim}{B}$ being a rotation, proper or improper; $\hat{g}$ any combination of lattice translations and translations between sites. The various $\underset{\sim}{B}$'s of this group are isomorphous with a point group. The irreducible representation of this point group determines the transformation behavior of $|\hat{k}'_{\ell} M\rangle$. If there is a two-dimensional irreducible representation of this point group, there must be two wave functions $|\hat{k}'_1 M\rangle$ and $|\hat{k}'_2 M\rangle$ of the same energy and $\hat{k}$ value, $\hat{k}'$ (10).

$$\{\underset{\sim}{B}|\hat{g}\}\begin{pmatrix}|\hat{k}'_1 M\rangle\\ |\hat{k}'_2 M\rangle\end{pmatrix} = \exp(i2\pi\hat{k}'\cdot\hat{g})\,\underset{\sim}{R}(B)\begin{pmatrix}|\hat{k}'_1 M\rangle\\ |\hat{k}'_2 M\rangle\end{pmatrix} \qquad (27)$$

Here $\underset{\sim}{R}(B)$ is a two-dimensional irreducible matrix of the group of $\hat{k}'$. If the point group has an n-dimensional representation, then there must be n functions of the same $\hat{k}'$ (but from n different bands) that have the same energy, and which form a basis for the n-dimensional irreducible representation.

The crystal systems treated in this paper are either monoclinic or orthorhombic. For these systems all irreducible representations of the group of the wave vector $\hat{k}'$ are unidimensional. This follows most quickly by noting that the point groups, (D_{2h}, C_{2h}), underlying the crystal space groups we are considering all have unidimensional representations. The point groups associated with the group of the wave

vector for the orthorhombic and monoclinic systems must either be also D_{2h} and C_{2h}, or subgroups of D_{2h} and C_{2h}, respectively; hence they too are unidimensional. Overlap of the bands is, of course, permissible.

As pointed out by several authors (25, 26), it is possible to determine the coefficients $C_{\theta\ell}$ (eq. 21) when $\hat{k} = 0$, and determine relationships among the coefficients when $\hat{k}$ is along a symmetry element of the crystal by applying group theoretical arguments. When $\hat{k} = 0$ the crystal wave functions $|\hat{k}_\ell M\rangle$ serve as a basis for an irreducible representation of the factor group. We have for naphthalene (or coronene)

$$|\hat{k}_\ell M\rangle = [\,|\hat{k}\,I\,M\rangle + (-1)^\ell\,|\hat{k}\,II\,M\rangle]\,/\,\sqrt{2}\,, \qquad \ell = 1, 2 \tag{28}$$

and for benzene

$$|\hat{k}_\ell M\rangle = 2^{-\frac{1}{2}} \sum_{\theta = I(1)}^{IV(4)} \mathrm{Sin}\,(\pi\ell\theta/2 + \pi/4)\,|\hat{k}\theta M\rangle\,. \qquad (\ell = 1, 2, 3, 4) \tag{29}$$

(Benzene has four molecular sites per unit cell.)

When $\hat{k}$ is not zero but is along a symmetry element, say parallel to the screw axis in the direction of $\hat{b}$, we again find simple relationships. For naphthalene (or coronene) we have

$$C_{I\ell} = \pm\, C_{II\ell}\,, \tag{30a}$$

and for benzene

$$C_{I\ell} = \pm C_{III\,\ell} \; ; \; C_{II\,\ell} = \pm C_{IV\,\ell} \; . \tag{30b}$$

(The sites have been labeled so that site I is transformed into site III and site II into site IV by the screw axis operation.) Symmetry arguments cannot be used as a means to determine the coefficients for a general $\hat{k}$. Any linear combination of the one-site functions will have the same transformation properties as any other combination. It is then necessary to solve a secular determinant for the coefficients. If one assumes, however, that only nearest neighbor interactions are important, the coefficients, $C_{\theta\ell}$, are the same as for the $\hat{k} = 0$ states. With naphthalene as an example, equation 14 leads to the following secular determinant:

$$\begin{vmatrix} H_{I,I}(\hat{k}) - \mathcal{E} & H_{I,II}(\hat{k}) \\ H_{II,I}(\hat{k}) & H_{II,II}(\hat{k}) - \mathcal{E} \end{vmatrix} = 0 \; , \tag{31}$$

where

$$H_{I,I}(\hat{k}) = H_{II,II}(\hat{k}) = 2A \cos 2\pi \hat{k}\cdot\hat{a} + 2B \cos 2\pi \hat{k}\cdot\hat{b} + 2C \cos 2\pi \hat{k}\cdot\hat{c} \tag{32}$$

$$H_{I,II}(\hat{k}) = H_{II,I}(\hat{k}) = 4P \cos(\pi \hat{k}\cdot\hat{a}) \cos(\pi \hat{k}\cdot\hat{b}); \; C_{I\ell} = \pm C_{II\ell} \; .$$

The above expression (eq. 32) suggests that the two bands stick together on the planes $K_2 = \pm 1/2$, $K_3 = \pm 1/2$, since $H_{I,II}$ is zero there.

Time reversal only required a degeneracy on the planes $K_3 = \pm 1/2$ and along the lines defined by equation 26. Taking into account non-nearest neighbor interactions, we find that the bands separate for all points except those dictated by time-reversal symmetry.

The Davydov splitting is is 8P. P consists of a sum of two terms: the "direct" term, $< \phi'_{nI}\, \phi_{nII} | \mathcal{H}_o | \underset{\sim}{A}\, \phi_{nI}\, \phi'_{nII} >$, and the "indirect" term arising from the ionization state contributions. The "direct" term involves an exchange interaction and is presumably small. If only those ionization states characterized by an electron-hole separation $\hat{a}/2 + \hat{b}/2$ need be taken into account, then the "indirect" term can be approximated by $-2\ \Delta E^{-1}\ f_1 f_2$. ΔE denotes the energy difference between the ionized state and the lowest neutral triplet. f_1, f_2 are defined by

$$f_1 = < \phi'_{nI}\, \phi_{nII} |\ V_{I,II}\ | \underset{\sim}{A} \phi^+_{nI}\, \phi^-_{nII} >$$

$$f_2 = < \phi'_{nI}\, \phi_{nII} |\ V_{I,II}\ | \underset{\sim}{A} \phi^-_{nI}\, \phi^+_{nII} > \qquad (33)$$

$\phi'_{n\theta}$ is the neutral triplet wave function of molecule $n\theta$. $V_{I,II}$ denotes the interaction between sites I and II of the unit cell. $\phi^+_{n\theta}\, \phi^-_{n\theta'}$ represents an ionized triplet state; an electron is promoted from the highest filled bonding orbital of molecule $n\theta$ to the lowest antibonding orbital of molecule $n\theta'$.

In the case of naphthalene (or coronene) one easily sees that there can be no accidental degeneracies. In the case of benzene it is possible to establish that accidental degeneracies can occur within the BZ. Taking into account nonnearest neighbor contributions to the band energies, and noting that time-reversal requires pairwise degeneracy on the surfaces of the BZ, we find that there can be (1) curves of degeneracies in the $K_1 = 0$ and/or $K_2 = 0$ and/or $K_3 = 0$ planes, and (2) points of degeneracy on the symmetry axes. The ordering of the band degeneracies and the symmetry of the corresponding wave functions at $\hat{k} = 0$ determine the planes in which the degeneracy curves lie. If, however, one omits nonnearest neighbor interactions, one finds surfaces of "accidental" degeneracies. These surfaces extend throughout the BZ and intersect the boundary planes along the boundary edges. If the nonnearest neighbor interactions exceed the spin-spin dipolar interactions, the regions of "accidental" degeneracies are confined only to the neighborhoods of the aforementioned curves and points. (The reader is referred to the Appendix for a proof of the above remarks.)

Clearly, if the Davydov splittings are large, the total region of the BZ occupied by those values of $\hat{k}$ that are sufficiently close to the curves or points of accidental degeneracies, so that equation 23 is required to calculate the spin energies, is quite small. It is small in fact in comparison to the region occupied by those $\hat{k}$'s that are sufficiently near the boundaries of the BZ where time reversal degeneracies occur.

RESONANCE SPECTRA

In using equation 22 to calculate the spin energies in the Δ region of the BZ, we encounter matrix elements of the form

$$\langle \hat{k}_\ell M | \mathcal{H}_D | \hat{k}_\ell M' \rangle = \sum_\theta |C_{\ell\theta}|^2 \langle n\theta M | \mathcal{H}_D | n\theta M' \rangle + \sum_\theta F(k_\ell \theta MM') + \sum_{\theta<\theta'} G(k_\ell \theta\theta' MM') , \tag{34}$$

where

$$F(\hat{k}_\ell \theta MM') = \sum_{t(t\neq n)} |C_{\ell\theta}|^2 \langle n\theta M | \mathcal{H}_D | t\theta M' \rangle \times \exp[2\pi i \hat{k}\cdot(\hat{R}_{t\theta} - \hat{R}_{n\theta})] ;$$

$$G(k_\ell \theta\theta' MM') = \sum_t \{ C_{\ell\theta}^* C_{\ell\theta'} \langle n\theta M | \mathcal{H}_D | t\theta' M' \rangle \times \exp[2\pi i \hat{k}\cdot(\hat{R}_{t\theta'} - \hat{R}_{n\theta})] + C_{\ell\theta} C_{\ell\theta'}^* \langle t\theta' M | \mathcal{H}_D | n\theta M' \rangle \times \exp[2\pi i \hat{k}\cdot(\hat{R}_{n\theta} - \hat{R}_{t\theta'})] \} . \tag{35}$$

As pointed out above, $|C_{\ell\theta}|^2 = 1/2$ for the aromatic crystals discussed in this chapter. The terms $F(k_\ell \theta MM')$, $G(k_\ell \theta\theta' MM')$ arise from the spin dipolar interactions between triplet molecules, and they are expected to be small. If one ignores the F and G terms, it becomes a simple matter to calculate the matrix elements $\langle \hat{k}_\ell M | \mathcal{H}_D | \hat{k}_\ell M' \rangle$. (An estimate of F and G will be made later on.) With naphthalene as a representative example, we integrate over the space coordinates and obtain a matrix element involving only spin

functions and spin operators.

$$\langle \hat{k}_\ell M | \mathcal{H}_D | \hat{k}_\ell M' \rangle$$

$$\sim 1/2 \left\{ \langle M \left[D(S_z^2 - 1/3 S^2) + E(S_x^2 - S_y^2) \right]_I M' \rangle \right. \tag{36}$$

$$\left. + \langle M \left[D(S_x^2 - 1/3 S^2) + E(S_x^2 - S_y^2) \right]_{II} M' \rangle \right\} .$$

Here $D = +0.1006\ cm^{-1}$; $E = -0.0138\ cm^{-1}$.

The x axis corresponds to the long axis of the molecule; the y axis corresponds to the short axis of the molecule. The subscripts I and II indicate that the x, y, z axes coincide with the molecular axes at sites I and II, respectively. To facilitate the computation the spin functions were taken as quantized along the $\hat{b}$ axis (screw axis) with unit vectors $\hat{e}_z$, $\hat{e}_y$, $\hat{e}_x$ in the direction of $\hat{b}$, $\hat{a}$, and $\hat{c}'$ ($\hat{c}'$ being perpendicular to $\hat{a}$ and $\hat{b}$). It is a simple matter to transform the spin operators from their respective molecular axis systems $(x,y,z)_I$ or $(x,y,z)_{II}$ to the $\hat{e}_x$, $\hat{e}_y$, $\hat{e}_z$ Cartesian system and calculate the matrix elements.

The following spin Hamiltonian was found to be equivalent to the $\mathcal{H}_D$ operator ($\mathcal{H}_S$ expressed in cm^{-1}):

$$\mathcal{H}_S = \frac{(\mathcal{H}_S)_I + (\mathcal{H}_S)_{II}}{2} = -0.00588(S_z^2 - 1/3 S^2) - 0.0345(S_x^2 - S_y^2)$$

$$+ 0.0332(S_x S_y + S_y S_x). \tag{37}$$

($\hat{e}_x$, $\hat{e}_y$, $\hat{e}_z$ Cartesian system).

This spin Hamiltonian can be further simplified by rotating through an angle $\theta = 68°$, counterclockwise about the $\hat{b}$ axis, thus

transforming the Cartesian system from $\hat{e}_z$, $\hat{e}_x$, $\hat{e}_y$ to $\hat{e}_z$, $\hat{e}_{x'}$, $\hat{e}_{y'}$. $\mathcal{H}_s$ becomes

$$\mathcal{H}_s = -0.00588(S_z^2 - 1/3\, S^2) + 0.0478\,(S_{x'}^2 - S_{y'}^2). \tag{38}$$

For coronene we have

$$\mathcal{H}_s = 0.0273(S_z^2 - 1/3\, S^2) - 0.0229\,(S_x^2 - S_y^2), \tag{39}$$

where the x, y, z axes are taken as coinciding with $\hat{c}'$, $\hat{a}$, $\hat{b}$, respectively. For benzene the following spin Hamiltonian is obtained:*

$$\mathcal{H}_s = D[0.168(S_z^2 - 1/3\, S^2) - 0.228(S_x^2 - S_y^2)]. \tag{40}$$

Here x, y, z axes coincide with $\hat{b}$, $\hat{a}$, $\hat{c}$, respectively (21). Figure II-2 gives the exciton spin energies relative to those of the free molecules and summarizes the above results.

We now estimate the F and G terms (eq. 35) for naphthalene, the results being qualitatively the same for the other systems. $F(k_\ell \theta MM')$ involves terms of the type $\langle n\theta M|\, \mathcal{H}_D \,|t\theta M'\rangle$, which can, after slight manipulation, be approximated by the following equation, when $M = M' = 1$.

$$\begin{aligned}
&\langle n\theta 1 \Big|\, \mathcal{H}_D \,\Big|_{t\neq n} t\theta 1\rangle \\
&\sim 1/2\, g_e^2\, \beta^2 \langle u_{n\theta'}(1)\, u_{t\theta}(2) \,|\, r_{12}^{-3} \,|\, u_{n\theta}(1)\, u_{t\theta'}(2)\rangle \\
&\quad - 3 g_e^2\, \beta^2 \langle u_{n\theta'}(1)\, u_{t\theta}(2)\, \alpha(1)\beta(2)| \\
&\quad \times (\hat{s}_1 \cdot \hat{r}_{12})(\hat{s}_2 \cdot \hat{r}_{12}) r_{12}^{-5} \,|u_{n\theta}(1)\, u_{t\theta'}(2)\beta(1)\alpha(2)\rangle .
\end{aligned} \tag{41}$$

*The spin Hamiltonian of benzene molecule is $D(S_z^2 - 1/3\, S^2)$, z being normal to the molecular plane. Hameka (28) calculated D to be 0.15 cm^{-1} for a $^3B_{1u}^+$ state.

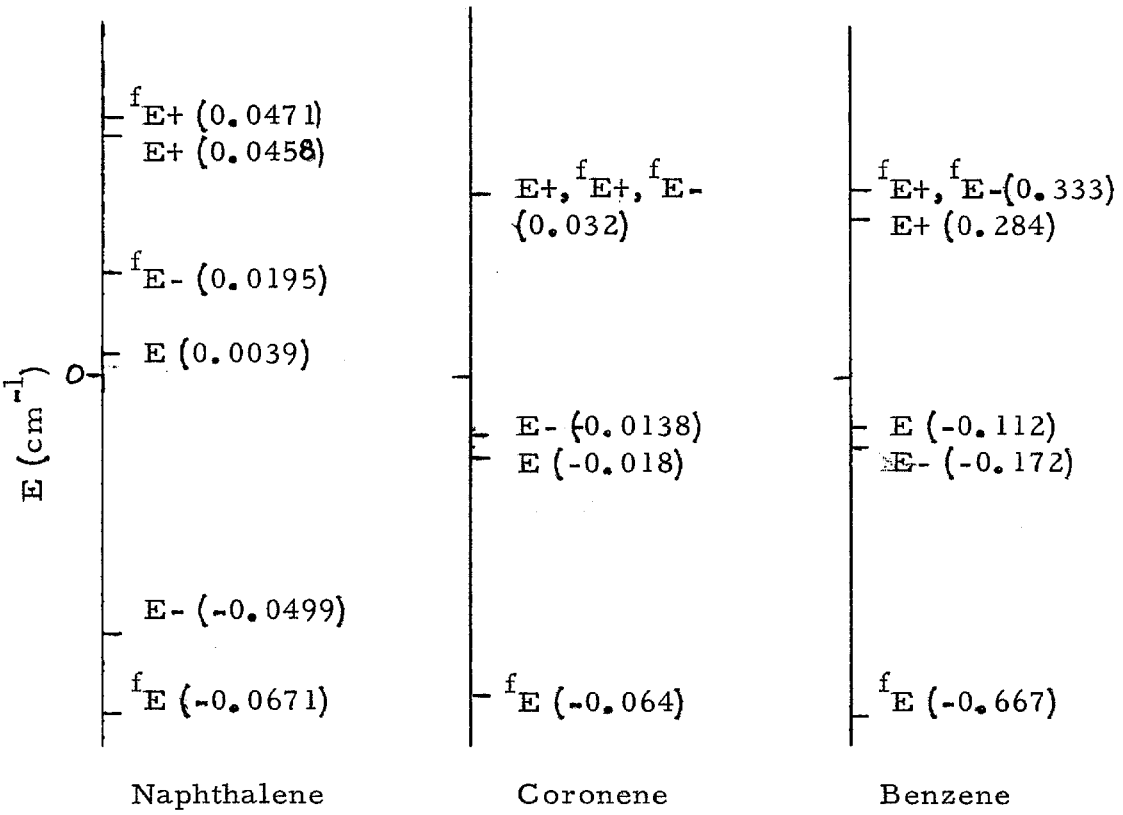

Fig. II-2. Zero-field energies of the triplet exciton states of crystalline naphthalene, coronene and benzene. ^{f}E, $^{f}E_{\pm}$ denote the zero-field energies of the isolated molecules; E, $E_{\pm}$ denote the triplet exciton spin energies. ^{f}E, E refer to the energies of the M = 0 states. Energies are in cm^{-1} except for benzene where the units are D (see text).

$u_{n\theta'}$ denotes the "excited" orbital of molecule $n\theta$ (the lowest unfilled molecular orbital of the unexcited molecule); $u_{n\theta}$, the highest filled orbital of the unexcited molecule. An estimate can be made of the value of the terms in equation 41 by replacing $(r_{12})^{-3}$ by $(R_{nt}^{2} r_{12})^{-1}$ and $(\hat{s}_1 \cdot \hat{r}_{12})(\hat{s}_2 \cdot \hat{r}_{12}) r_{12}^{-5}$ by $(\hat{s}_1 \cdot \hat{e}_{nt})(\hat{s}_2 \cdot \hat{e}_{nt}) R_{nt}^{-2} r_{12}^{-1}$ and then using the Davydov-type dipole approximation. $\hat{e}_{nt}$ is a unit vector connecting the centers of molecules $n\theta$ and $t\theta$; $\hat{R}_{nt} = \hat{R}_{n\theta} - \hat{R}_{t\theta}$.

This approximation is good when the distance between centers of molecules is several times larger (say 8 to 10 times larger) than the dimensions of the molecule. Unfortunately this is not true for nearest neighbors, and only roughly true for next-nearest neighbors. It is expected, however, that the above substitution will be within an order of magnitude of the correct value. (This technique cannot be used in the case of benzene because the dipole transition matrix vanishes and an octapole matrix is necessary (26). The conclusions based on the naphthalene crystal should be qualitatively applicable to the benzene crystal.) The six nearest naphthalene neighbors need only be considered, and the dipole transition matrix element can be obtained from the experimental oscillator strength for the transition $^1A_{1g}^{-} \longrightarrow {}^1B_{2u}^{+}$ (27). (The lowest triplet of naphthalene is the $^3B_{2u}^{+}$ state.) We obtain the maximum value of 4.8×10^{-4} cm^{-1} for $\left| \sum_{\theta} F(k_\ell \theta 11) \right|$ when $\hat{k} = 0$. The other matrix elements, $F(k_\ell \theta MM')$, are of the same order of magnitude. The term

$$\left| \sum_{\theta<\theta'} G(k_\ell \theta\theta' 11) \right|$$

can be evaluated in a similar manner as above and gives a maximum value of about 5×10^{-6} cm^{-1} for $\hat{k} = 0$.

One therefore obtains about 0 to 4.8×10^{-4} cm^{-1} as the range of values for

$$\left| \sum_{\theta} F(k_\ell \theta MM') + \sum_{\theta<\theta'} G(k_\ell \theta\theta' MM') \right| .$$

It is most probable that the approximations used underestimate the actual range. It may well be that the true maximum value is a factor 5 to 10 times larger than 4.8×10^{-4} cm^{-1}.

We note that when $\hat{k} = \hat{k}^b$, a vector terminating on the boundary of the BZ, where time-reversal symmetry requires that the bands stick together in pairs in the absence of an external magnetic field, the spin-Hamiltonian (eq. 12) is significantly different from that of the Δ region. One expects in the cases of naphthalene and coronene that the spectra obtained from the $\hat{k}^b$ states to be very nearly the same as those from an "oriented gas" of isolated molecules except for the absence of hyperfine structure. In the case of benzene, the spectra from the $\hat{k}^b$ states are not approximately the same as those from an "oriented gas" of isolated benzene molecules, although they are different from that of the interior (Δ region). The spectra from the "oriented gas" would show no averaging over sites. Its fine structure would consist of (a) eight lines for an arbitrary $\hat{H}$, and (b) two lines when $\hat{H}$ is along $\hat{a}$, $\hat{b}$, or $\hat{c}$. The spectra

from the $\hat{k}^b$ states on the other hand should consist of four lines for an arbitrary $\hat{H}$, except when $\hat{H}$ is along $\hat{a}$, $\hat{b}$, or $\hat{c}$, whereupon two line spectra should be obtained. In general, the ESR spectra are highly dependent on $\hat{k}$ in the Γ region.

We have proceeded above on the assumption that the Davydov splittings are large, and have calculated the spin energies to first order. It is worthwhile pointing out the qualitative changes in the ESR spectra that are introduced by the second order corrections to the spin energies. Again using the two site naphthalene (coronene) as an example, we denote the eigenstates as $|\hat{k}_\ell \Psi_i>$. The spin functions $|\Psi_i>$ diagonalize the "averaged" spin Hamiltonian,

$$1/2\ [(\mathcal{H}_s)_I + (\mathcal{H}_s)_{II}] + \mathcal{H}_z .$$

Second order corrections to the spin energy of the $|\hat{k}_\ell \Psi_i>$ state arise from the $|k_{\ell'} \Psi_j>$ states $(\ell' \neq \ell)$. We have as the corresponding energy correction:

$$\sum_j \frac{\left|<\hat{k}_{\ell'} \Psi_j|\ \mathcal{H}_D + \mathcal{H}_z\ |\hat{k}_\ell \Psi_i>\right|^2}{E(\hat{k}_\ell \Psi_i) - E(\hat{k}_{\ell'} \Psi_j)} \sim \sum_j \frac{\left|<\Psi_j|\ V|\ \Psi_i>\right|^2}{E(\hat{k}_\ell \Psi_i) - E(\hat{k}_{\ell'} \Psi_j)}$$

where $V = 1/2\ [(\mathcal{H}_s)_I - (\mathcal{H}_s)_{II}]$. Since the Davydov splitting is assumed large, the denominator can be approximated by $\pm \left| 8P \cos \pi \hat{k} \cdot a \cos \pi\ \hat{k} \cdot b \right| = \Delta E(\hat{k})$ for all i, j. The + holds if the ℓ state is higher in energy, the - otherwise.)

The observed resonances correspond to intraband transitions;

$\left[\text{i.e.,}\quad |k_\ell \Psi_i> \longrightarrow |k_\ell \Psi_j> \;;\text{ and }\quad |k_\ell, \Psi_i> \longrightarrow |\hat{k}_\ell, \Psi_j>\right]$. A single resonance occurs for the $|\Psi_i> \longrightarrow |\Psi_j>$ transition to first order; however, to second order two lines will be present, displaced an amount

$$\left|\Delta E(\hat{k})^{-1} \sum_s \left[\, |<\Psi_s | V | \Psi_i>|^2 - |<\Psi_s | V | \Psi_j>|^2 \,\right]\right|$$

to the right and left of the position calculated to first order. This will be generally true for all external field orientations. If we take ΔE to be $\sim 5\ cm^{-1}$ and the bracketed term to be $\sim 0.05\text{-}0.1\ cm^{-1}$, we have two lines displaced ~ 5 to 10 gauss to the right and left of the first order resonance position. (The overall resonance line shape is obtained, of course, by averaging over the density of $\hat{k}$ states.)

The $\Delta \leftrightarrow \Gamma$ Scattering Process

An exciton having a wave vector $\hat{k}$ can interact with the lattice and be "scattered" into a state of a different $\hat{k}$ value. The most important perturbing sources are presumably those which destroy the translatory symmetry of the crystal: i.e., lattice crystal defects, impurities. (One would have to include any excited singlet state molecules present as impurities.) Collisions between excitons may be another scattering factor. Although the above scattering mechanisms are most probably spin independent, they, nevertheless, can cause spin relaxation. For example, we noted earlier that the stationary spin

states of the Δ region of the BZ are in general different from those of the Γ region. If an exciton is scattered so that its $\hat{k}$ vector moves from the Δ region to the Γ, and back to the Δ region, this scattering process can clearly be a spin relaxation mechanism. Below we make an estimate of the potency of this relaxation mechanism. We assume that the energy minimum of the exciton bands occurs in the Δ region, and that the volume of the Δ region is large compared with the Γ region. Thus, even at low temperatures, the ESR lines can be essentially regarded as arising from Δ exciton states.

The spin Hamiltonian of a particular $\hat{k}$ state, say $\hat{k}^r$, in the absence of any interactions with the lattice would be

$$\underset{\sim}{\mathcal{H}} = g|\beta|\hat{H}\cdot\hat{\underline{S}} + [D(\underline{S}_z^2 - \underline{S}^2/3) + E(\underline{S}_x^2 - \underline{S}_y^2)]_r$$

$$\mathcal{H} = g|\beta|\hat{H}\cdot\hat{\underline{S}} + \underset{\sim}{\mathcal{H}}_s^r \quad . \tag{42}$$

(The eigenspin states are $|_r\gamma>$.)

We now assume that a perturbation term, $_r\underline{V}(t)$, can be added to equation 42 to take into account the scattering caused by the lattice. The scattering process is regarded as one which takes our $\hat{k}^r$ exciton and randomly "carries it" through the other $\hat{k}$ states, $\hat{k}^{r'}$, as a result of which it experiences the corresponding zero-field Hamiltonians, $(\underset{\sim}{\mathcal{H}}_s^{r'})$, of the $\hat{k}^{r'}$ state.

If our $\hat{k}^r$ exciton is initially in spin state $|_r\gamma'>$, $_rR_{\gamma\gamma'}$, the transition rate from $|_r\gamma'>$ to $|_r\gamma>$, is

$$ {}_{r}R_{\gamma\gamma'} = \lim_{T\to\infty} \frac{1}{\hbar^2 T} \left| \int_0^T {}_{r}V_{\gamma\gamma'}(t)\, e^{-i\,{}_{r}\omega_{\gamma\gamma'}\, t}\, dt \right|^2 \qquad (43) $$

$(\gamma \neq \gamma')$

by first order perturbation theory. ${}_{r}\omega_{\gamma\gamma'} = E_{r\gamma'} - E_{r\gamma}$ and ${}_{r}V_{\gamma\gamma'}(t) = \langle {}_{r}\gamma | \underline{V}(t) | {}_{r}\gamma' \rangle$. Applying the Wiener-Khinchine theorem (29), we have that

$$ {}_{r}R_{\gamma\gamma'} = \hbar^{-2} \int_{-\infty}^{\infty} \langle {}_{r}V^{*}_{\gamma\gamma'}(0)\ {}_{r}V_{\gamma\gamma'}(\tau) \rangle_{ave}\, e^{-i\,{}_{r}\omega_{\gamma\gamma'}\,\tau}\, d\tau \,, \qquad (44) $$

where

$$ \langle {}_{r}V^{*}_{\gamma\gamma'}(0)\ {}_{r}V_{\gamma\gamma'}(\tau) \rangle_{ave} = \lim_{T\to\infty} T^{-1} \int_{-T/2}^{T/2} {}_{r}V^{*}_{\gamma\gamma'}(t)\ {}_{r}V_{\gamma\gamma'}(t+\tau)\, dt \,. \qquad (45) $$

We preferably obtain $\langle {}_{r}V^{*}_{\gamma\gamma'}(0)\ {}_{r}V_{\gamma\gamma'}(\tau) \rangle_{ave}$ by averaging over a representative statistical ensemble.

Let $P_{\sigma\sigma'}(t)$ denote the probability of finding the "wandering" exciton in state σ' $(\hat{k}^{\sigma'})$ at time $t + t_o$ when it was in state σ at time t_o. Let $P(\sigma)$ denote the a priori probability of finding the exciton in state σ. $(P(\sigma) = P_{\sigma'\sigma}\ (t\to\infty)$. We expect the distribution of the $P(\sigma)$'s to be essentially the same as the Boltzmann distribution.) Let ${}_{r}\underline{\gamma}_{\sigma}$ denote the spin perturbation when the exciton is scattered into the σ state.

$$ {}_r\underset{\sim}{V}_\sigma = \underset{\sim}{\mathcal{H}}_s^\sigma - \underset{\sim}{\mathcal{H}}_s^r \, . \tag{46} $$

Then $\langle {}_rV^*_{\gamma\gamma'}(0) \quad {}_rV_{\gamma\gamma'}(t) \rangle_{ave}$ is given by the following expression:

$$ \sum_{\sigma,\sigma'} ({}_rV_\sigma)^*_{\gamma\gamma'} \quad ({}_rV_{\sigma'})_{\gamma\gamma'} P(\sigma)P_{\sigma\sigma'}(t) = \sum_{\sigma,\sigma'} {}_r(\mathcal{H}_s^\sigma)^*_{\gamma\gamma'} \quad {}_r(\mathcal{H}_s^{\sigma'})_{\gamma\gamma'} P(\sigma)P_{\sigma\sigma'}(t) \, , \quad (\gamma \neq \gamma') \tag{47} $$

where

$$ {}_r(\mathcal{H}_s^\sigma)_{\gamma\gamma'} = \langle {}_r\gamma | \underset{\sim}{\mathcal{H}}_s^\sigma | {}_r\gamma' \rangle \, . $$

Furthermore,

$$ \frac{1 - P_{\sigma\sigma}(s)}{s} \to C_\sigma \; ; \quad \frac{P_{\sigma\sigma'}(s)}{s} \longrightarrow C_\sigma \lambda_{\sigma\sigma'} \, . \quad (s \to 0) \tag{48} $$

Here $\lambda_{\sigma\sigma'}$ can be interpreted as the conditional probability that, if a change occurs from state σ during a time interval, s, this change takes the system from state σ to σ' . C_σ denotes the probability for a change to occur from state σ during the time interval, s. The $P_{\sigma\sigma'}(t)$'s are obtained by solving the Chapman-Kolmogorov equations (31)

$$ \frac{dP_{\sigma\sigma'}(t)}{dt} = -C_{\sigma'} P_{\sigma\sigma'}(t) + \sum_\ell P_{\sigma\ell}(t) \, C_\ell \lambda_{\ell\sigma'} \, . \tag{49} $$

(σ held fixed)

We thus obtain the following expression for $_{r}R_{\gamma\gamma'}$:

$$\hbar^2 {}_{r}R_{\gamma\gamma'} = \sum_{\sigma,\sigma'} {}_{r}(\mathcal{H}_s^{\sigma})^*_{\gamma\gamma'} \; {}_{r}(\mathcal{H}_s^{\sigma'})_{\gamma\gamma'} P(\sigma) \int_{-\infty}^{\infty} P_{\sigma\sigma}(\tau) \, e^{-i\,{}_{r}\omega_{\gamma\gamma'}\tau} \, d\tau \tag{50}$$

$$P_{\sigma\sigma'}(\tau) = \frac{1}{2\pi i} \int_{q-i\,\infty}^{q+i\,\infty} e^{s\tau} [\, \mathbb{1}\theta^{-1}(s)\,]_{\sigma\sigma'} \, ds \; .$$

$q > 0$, and all singularites occur to the left of q. $\mathbb{1}$ is the unit matrix. θ^{-1} is the inverse of the matrix $\theta(s)$, a typical element of which is

$$[\theta(s)]_{j\ell} = (C_\ell + s)\,\delta_{j\ell} - C_j \lambda_{j\ell} \; , \tag{51}$$

The overall transition rate from level γ', $\bar{R}_{\gamma'}$, is obtained by summing over all states $\gamma (\gamma \neq \gamma')$ and doing a Boltzmann average over all states $\hat{k}^r$ in the Δ region.

The results so far are strictly formal since we do not know the C_j's and $\lambda_{j\ell}$'s. We approximate the above in the following way. Ignore the small dependence of $\underset{\sim}{\mathcal{H}}_s$ on $\hat{k}$ in region Δ. Designate $\underset{\sim}{\mathcal{H}}_s$ in this region as $\underset{\sim}{\mathcal{H}}_s^{\Delta}$. Use an average $\underset{\sim}{\mathcal{H}}_s^{\Gamma}$ for region Γ. Our perturbation $\underset{\sim}{V}(t)$ is now $[\, \underset{\sim}{\mathcal{H}}_s^{\Gamma} - \underset{\sim}{\mathcal{H}}_s^{\Delta} \,]\, f(t)$. $f(t)$ is a random function capable of taking on two values, 1 and 0. We denote the probability per unit time for the $\Gamma \longrightarrow \Delta$ transition as $C_\Gamma = \tau_\Gamma^{-1}$, and that for $\Delta \longrightarrow \Gamma$ as $C_\Delta = \tau_\Delta^{-1}$. Our spin transition rate is now approximated as:

$$R_{\gamma\gamma'} = 2\hbar^{-2} \left| (\mathcal{H}_s^{\Gamma})_{\gamma\gamma'} \right|^2 \int_0^{\infty} \langle f(0)\, f(\tau) \rangle_{ave} \cos \omega_{\gamma\gamma'} \tau \, d\tau \quad , \tag{52}$$

$$(\mathcal{H}_s^{\Gamma})_{\gamma\gamma'} = \langle {}_{\Delta}\gamma | \mathcal{H}_s^{\Gamma} | {}_{\Delta}\gamma' \rangle \ .$$

$\langle f(0)\, f(\tau) \rangle_{ave}$ can be evaluated using equations 47 ff.

$$\langle f(0)\, f(\tau) \rangle_{ave} = \left(\frac{\tau_C}{\tau_{\Delta}} \right)^2 + \exp\left[- \frac{\tau}{\tau_C} \right] \left(\frac{\tau_C^2}{\tau_{\Gamma} \tau_{\Delta}} \right) . \tag{53}$$

We have set $(\tau_{\Gamma})^{-1} + (\tau_{\Delta})^{-1} = \tau_C^{-1}$. $R_{\gamma\gamma'}$ becomes

$$R_{\gamma\gamma'} = 2\hbar^{-2} \left| (\mathcal{H}_s^{\Gamma})_{\gamma\gamma'} \right|^2 \tau_C^3 \left[(\tau_{\Gamma} \tau_{\Delta})(\omega_{\gamma\gamma'}^2 \tau_C^2 + 1) \right]^{-1} . \tag{54}$$

When $\tau_{\Delta} > \tau_{\Gamma}$ and $|\omega_{\gamma\gamma'}| \tau_C > 1$, we have $\tau_C \sim \tau_{\Gamma}$ and that

$$R_{\gamma\gamma'} = 2\hbar^{-2} \left| (\mathcal{H}_s^{\Gamma})_{\gamma\gamma'} \right|^2 (\omega_{\gamma\gamma'}^2 \tau_{\Delta})^{-1} . \tag{55}$$

We expect $\tau_{\Delta} > \tau_{\Gamma}$ since $\tau_{\Gamma} / \tau_{\Delta} \sim \frac{\text{volume } \Gamma \text{ region}}{\text{volume } \Delta \text{ region}} < 1$.

At X-band $|\omega_{\gamma\gamma'}| \sim 1 \times 10^{11}$ rad/sec. The inequality $|\omega_{\gamma\gamma'}| \tau_C > 1$ implies that $\tau_{\Gamma} > 1 \times 10^{-11}$ secs. This inequality is consistent with our assumption that we have a wave exciton system. (On physical grounds, one does not expect the scattering rate to exceed the interaction between molecules which gives rise to the excitation propagation. If the resonance interaction between molecules is ~ 5-10 cm^{-1} (or $\sim 5 \times 10^{-11}$ secs in reciprocal frequency units), τ_{Γ} is expected to be

greater than 5×10^{-11} secs. If $\tau_\Gamma \approx 5 \times 10^{-11}$ sec, the lattice perturbation becomes comparable to the resonance interaction between molecules, and a significant departure from the wave exciton model is to be expected. A diffusion model would be more appropriate; our first order time dependent perturbation treatment is no longer valid.)

We see from equation 55 that (1) $R_{\gamma\gamma'}$ decreases as τ_Δ increases (i.e., as the Davydov splitting increases); (2) $R_{\gamma\gamma'}$ decreases with increasing $\omega_{\gamma\gamma'}$ (i.e., with increasing external fields). In addition $R_{\gamma\gamma'}$ is a minimum along symmetry elements of the crystal. We conclude that the relaxation rate can best be reduced by applying a sufficiently strong external field along a symmetry element of a crystal having large Davydov splittings. This is precisely what one expects on intuitive grounds without recourse to the methods of this section.

We apply equation 55 to the naphthalene crystal. The external field is taken as $\sim 3{,}000$ gauss and is directed along the $\hat{b}$ axis. We do not know what value to assign τ_Δ. If we set its range to be such that $1 \times 10^{-4} > \tau_\Delta > 1 \times 10^{-6}$ sec, we obtain a spin relaxation time, R^{-1}, where 1×10^{-4} sec $< R^{-1} < 1 \times 10^{-2}$ sec. This gives negligible line broadening but does give a spin relaxation rate that compares favorably with the low temperature spin lattice relaxation times of organic free radicals. *

At this point a few words concerning the validity of this section

---

*The spin-lattice relaxation time of malonic acid, for example, is ~ 0.1 secs at helium temperatures.

is in order. We have reduced the effect of the scattering process to a perturbation, $\underset{\sim}{V}(t)$, which we add to equation 42. That a reduction of this nature is possible, and that it can be approximated by the perturbation model we have used, clearly requires justification. This is beyond the scope of this paper. We justify ourselves by saying that (1) our choice of $V(t)$ makes the relaxation problem tractable, and (2) we are only interested for the time being in an order of magnitude estimate, which our $V(t)$ probably gives. We await experimental clarification before proceeding further in rigor. Our method does suggest that observable spin relaxation effects may occur from the $\Delta \longleftrightarrow \Gamma$ scattering process.

CONCLUSION

We have calculated the ESR spectra to be expected for triplet (wave) exciton states of benzene, naphthalene, and coronene. (The exciton concentration is assumed low. At high exciton concentrations one expects an exchanged narrowed spin resonance line centered at $g_e = 2$.) The Davydov splittings between the bands play an important role in determining the nature of the spectra. If the splittings are small compared to the spin-spin interactions, the spectra are expected to be essentially the same as that obtained from an "oriented gas" of isolated molecules. In the exciton case, however, no nuclear hyperfine structure would be present. If the splittings are comparable to the spin-spin interaction, the spectra are highly dependent on the exciton wave vector $\hat{k}$, and characterized, therefore, by very broad line resonances. If the Davydov splittings are large, we now find that the spectra are essentially independent of the wave vector $\hat{k}$, except for small regions of time reversal and accidental degeneracies and certain small terms (F, G). Two-line spectra (with no hyperfine structure), representing an average over the molecular sites in the unit cell, are obtained to first order. If the energy minimum occurs for a $\hat{k}$ vector, $\hat{k}^b$, on a boundary plane of the BZ where there are time reversal degeneracies, a significant change in spectra would occur by lowering the temperature sufficiently so that the $\hat{k}$ states near $\hat{k}^b$ are preferentially populated. The spectra would now be highly dependent on $\hat{k}$ near $\hat{k}^b$ and would not show the full averaging over the molecular sites in the unit cell.

Because of possible lattice perturbations, one must consider two time-dependent exciton-lattice interactions that can lead to spin lattice relaxation. First, an exciton can be scattered so that its $\hat{k}$ vector moves from the Δ region of the BZ to the Γ region, and back to the Δ region. Since the stationary spin states in the two regions are in general different, this exciton scattering is clearly a relaxation mechanism. We note that in certain special cases this relaxation mechanism ceases to be effective. If, for example, in the case of naphthalene, the steady applied field is along the twofold screw axis (or perpendicular to it), and if the applied field is so strong that the Zeeman energy is large relative to the zero-field splittings, then the stationary spin states in the Δ and Γ regions are essentially the same, and the Δ to Γ scattering does not lead to relaxation.

A second type of relaxation mechanism arises when the electronic excitation density on the various molecules of the unit cell varies with time. This may be achieved by mixing exciton states with the same $\hat{k}$ vector. This mixing clearly can be brought about by intermolecular and intramolecular lattice vibrations that make various molecules in the unit cell nonequivalent to one another. Certain degenerate intermolecular vibrations may be particularly effective in this respect. But here again this relaxation mechanism can be made relatively ineffective in certain cases by the application of a strong, steady external field in special crystal directions.

In the case that an exciton diffusion model is more appropriate, it is again the jumping of excitation between the various molecules of the unit cell that is doubtless the most important source of spin-lattice relaxation and line broadening. It is comparatively easy to make order-of-magnitude estimates of resonance linewidths Δ_ν due to this effect

$$\Delta_\nu \sim Z^2 \tau . \tag{56}$$

Here Z is of the order of the zero-field splitting and τ is the characteristic time for random walk between nontranslatory neighbors in the unit cell. If the triplet exciton Davydov splittings are of the order of 1-10 cm^{-1}, then we may reasonably expect that the diffusion rate (τ^{-1}) will be at least as large as this. Thus, tolerable resonance linewidths are expected from equation 56 when Z is in the range 0.01-0.1 cm^{-1}. Again, for strong external fields and special crystal orientations, the present relaxation mechanism can be almost completely eliminated for some crystal systems.

ADDENDUM

Although we have based our discussion on a particular set of aromatic molecular crystals, our conclusions are expected to be valid for other systems. The recent work of D. B. Chesnut and W. D. Phillips (31), and D. B. Chesnut and J. P. Arthur (32) suggests that triplet excitons are present in the crystalline tetracyanoquinodimethane (TCNQ) ion-radical salts. These salts have thermally accessible triplets. At low concentration (i.e., low temperatures) triplet resonance spectra showing "fine" field structure are obtained. No nuclear hyperfine structure is present. The "fine" field in each case is believed to arise from the spin dipolar interaction between two unpaired electrons distributed over many TCNQ molecules (33). Increasing the temperature results in an exchanged narrowed resonance near $g_e = 2$. The crystal structure of these salts is not known in detail, but the majority are believed to be triclinic.

The crystal structure of the $(Cs^+)_2 (TCNQ)_3^=$ salt (32) is believed to be monoclinic with two sites per unit cell. The Cs^+ ions separate the nontranslatory TCNQ neighbors. The ESR spectra show no averaging over sites. Two lines are obtained for each of the two differently oriented TCNQ groups. This suggests that the interaction between the nontranslatory neighbors is quite small ($\lesssim 0.001\ cm^{-1}$). The Cs^+ ions most likely "insulate" the nontranslatory TCNQ molecules, causing a reduced resonance interaction between them.

B. DIFFUSING EXCITONS

INTRODUCTION

In this chapter we shall enlarge on the earlier, somewhat limited discussion of diffusing excitons. In particular, we are interested in the resonance line shape as a function of the characteristic time, τ, for the random walk between nontranslatory neighbors of the unit cell.* A solution of this problem is important for a number of reasons. In the first place, the diffusing triplet exciton may be frequently encountered experimentally. For example, in the event of significant self-trapping effects, thermal activation may be required for the energy propagation. If there are important differences between the diffusing and wave triplet exciton ESR spectra, one should know what they are. In the second place, all previous calculations of the line shape of a resonating unit transferring randomly between different sites have, to the best of the author's knowledge, been done only for large external magnetic fields and negligibly small "fine" fields. Consequently, it is of interest to extend the calculations to the triplet state case, where the fine field, the spin-spin dipolar fields of the unpaired electrons, can be comparable to, or larger than, the external field. Furthermore, the solution of our triplet state problem would give us insight into handling other problems.

*We treat only the case where the excitation quantum is confined to one or more translatory molecules at any instant of time. If the excitation is simultaneously distributed over a number of translatory and nontranslatory neighbors, the problem is in general more formidable.

For example, the problem of the exchange narrowing of resonance lines when the "fine" fields are comparable to the Zeeman energy most likely can be treated by an extension of the techniques presented here.

The triplet state ESR behavior for small or intermediate external magnetic fields differs from the high field (Zeeman) cases previously considered in the literature in an important respect. In the latter case, transfer between equivalent magnetic sites, which may or may not be translatory equivalent, does not affect the resonance spectra—lines are not broadened, narrowed or shifted. In the former case, transfer of excitation between two equivalent magnetic (but translatory non-equivalent) sites can result in significant changes in spectra, as pointed out earlier. As a result, the well-known rules (37,38) which correlate the line shape and transfer rates for the Zeeman case, need not hold necessarily for the triplet case.

One of our aims in the forthcoming pages will be to obtain a better understanding of the above point of difference. (A clarification of the above will, as we shall see, enable us to distinguish experimentally between diffusing and wave excitons provided certain criteria are fulfilled.) Another of our aims will be to obtain a qualitative understanding of the line shape when the non-translatory sites cease to be magnetically equivalent. (This occurs when the external magnetic field is neither parallel to a screw nor rotation axis, not in the plane of a glide or mirror plane.)

A detailed quantitative analysis of line shape turns out to be impractical because of the number of variables that are important: namely, (1) the relative orientation of the non-translatory equivalent molecules of the unit cell; (2) the values of D and E, the spin-spin interaction parameters of the isolated molecule; (3) the orientation and strength of the external magnetic field; (4) the transfer rates. What we shall therefore do is calculate the resonance line shape as function of transfer rate for a simple but realistic model. A number of general conclusions will then be deduced. Calculations will be done using both the density matrix and "frequency modulation" methods.

Density Matrix Method: Calculation Procedure

If an oscillatory field, $H_1 \cos\omega t$, is applied, say, in the y-direction, the power, $P(\omega)$, absorbed per unit volume by the spin system is given by the well-known expression

$$P(\omega) = \frac{-N}{V} \overline{\langle \hat{\mathcal{M}}(t) \rangle \cdot \frac{d\hat{\mathcal{H}}}{dt}} = \frac{NH_1\omega^2}{2\pi V} \int_0^{2\pi/\omega} \langle \mathcal{M}_y(t) \rangle \sin\omega t \, dt \quad (56)$$

$\langle \mathcal{M}_y(t) \rangle$ is the expectation value for the y-component of the magnetization vector operator as a function of time. $\underset{\sim}{\mathcal{M}}_y$ is defined as

$$\underset{\sim}{\mathcal{M}}_y = -g_e|\beta|\underset{\sim}{S}_y \, . \quad (57)$$

N/V is the number of triplet molecules per unit volume; $\underset{\sim}{S}_y$ is the y component of spin in units of $\hbar$ ["S" = 1] . $\langle \mathcal{M}_y(t) \rangle$ is given by

$$\langle \mathcal{M}_y(t) \rangle = -\mathrm{Tr}\,[g_e |\beta| S_y \rho(t)]\,. \qquad (58a)$$

$\rho(t)$ is the density matrix evaluated at time t. Tr denotes the trace of the matrix product of S_y and $\rho(t)$.* If the N triplet resonating units are distributed among a number of sites, A, B,..., we set

$$\langle \mathcal{M}_y(t) \rangle = \sum_j \mathrm{Tr}\,[g_e |\beta| S_y \rho_j(t)]\ ;\ j = A, B, \ldots \qquad (58b)$$

In the absence of any transfer or relaxation processes, the density matrices for the various sites satisfy the well-known commutator relationships,

$$\frac{\hbar}{i}\frac{d\rho_j}{dt} = [\rho_j, \mathcal{H}_j + g_e |\beta| S_y H_1 \cos\omega t]\,. \qquad (59)$$

$\mathcal{H}_j$ is the Schrodinger spin Hamiltonian of the j'th site. It consists of the Zeeman term and the electron spin dipolar interactions.** Equation 59 must now be modified to include relaxation terms. The interaction with the lattice requires adding a term to equation 59 that we formally represent as $\frac{\hbar}{i}\left(\frac{d\rho_j}{dt}\right)_L$. If there is transfer between the non-

---

*The interested reader is referred to a review article by U. Fano (34) for a detailed discussion of the properties of the density matrix.

**For the sake of simplicity, we do not include the hyperfine interactions caused by the nuclear spins interacting with the unpaired electron spins. This omission is consistent with the assumption that the transfer rates to be subsequently considered are much greater than the hyperfine splittings. This results in a washing out of the hyperfine structure. Actually the omission of the hyperfine interaction terms would still be justified even if transfer rates between non-translatory neighbors are less than the hyperfine splitting, provided that the transfer rate between translatory neighbors is much greater than the hyperfine splitting. (The physical picture would then be that diffusion occurs primarily between translatory neighbors with an occasional random walk between non-translatory neighbors.)

translatory sites we replace equation 59 with a set of coupled matrix equations. (For simplicity we consider only transfer between two sites, A and B.) Our modified equations are

$$\frac{\hbar}{i}\frac{d\rho_A}{dt} = [\rho_A, \mathcal{H}_A + g_e|\beta|S_y H_1 \cos\omega t] - \frac{\hbar}{i}\frac{\rho_A}{\tau_A} + \frac{\hbar}{i}\frac{\rho_B}{\tau_B} + \frac{\hbar}{i}\left(\frac{d\rho_A}{dt}\right)_L; \tag{60a}$$

$$\frac{\hbar}{i}\frac{d\rho_B}{dt} = [\rho_B, \mathcal{H}_B + g_e|\beta|S_y H_1 \cos\omega t] - \frac{\hbar}{i}\frac{\rho_B}{\tau_B} + \frac{\hbar}{i}\frac{\rho_A}{\tau_A} + \frac{\hbar}{i}\left(\frac{d\rho_B}{dt}\right)_L . \tag{60b}$$

τ_A, τ_B represent the characteristic times for the random walk from A to B and B to A respectively.

Equations 60a and 60b are regarded as being phenomenologically correct; no effort will be made to rigorously justify the equations. We note that they are consistent with the propagation model presented in the previous chapter; that is, we expect the mechanism responsible for and the rate of excitation propagation to be independent of the spin orientation of the triplet molecule and to proceed through virtual triplet ionization states. This requires that the orientation of the "transferring" spins be preserved. (The spin orientation immediately before transfer must be precisely that immediately after transfer.)

Equations analogous to equations 60a,b have appeared elsewhere in the literature (38). These analogous equations have all been expressed in a coordinate system rotating with the Larmor frequency about an axis parallel to the external field. Such a procedure

facilitates the solution of the coupled equations, but is only legitimate when the spin-spin interaction is sufficiently small so that resonance occurs virtually at the Larmor frequency. We, therefore, must look for a solution of equations 60a,b in a fixed laboratory system because of the large spin-spin interaction.

In order to solve the coupled matrix equations, we expand ρ_A and ρ_B in powers of H_1, the magnitude of the oscillatory field.

$$\rho_A = \rho_A^{(0)} + H_1\rho_A^{(1)} + H_1^2\rho_A^{(2)} + \dots \quad ; \tag{61a}$$

$$\rho_B = \rho_B^{(0)} + H_1\rho_B^{(1)} + H_1^2\rho_B^{(2)} + \dots \quad . \tag{61b}$$

We assume that the oscillatory field is sufficiently small so that the system's response is linear in H_1. (That is, the system is far from saturation.) Equations 60a,b can be decomposed into the following set:

$$\frac{\hbar}{i}\frac{d\rho_A^{(0)}}{dt} = 0 = [\rho_A^{(0)}, \mathcal{H}_A] - \frac{\hbar}{i}\frac{\rho_A^{(0)}}{\tau_A} + \frac{\hbar}{i}\frac{\rho_B^{(0)}}{\tau_B} + \frac{\hbar}{i}\left(\frac{d\rho_A^{(0)}}{dt}\right)_L \quad ; \tag{62a}$$

$$\frac{\hbar}{i}\frac{d\rho_B^{(0)}}{dt} = 0 = [\rho_B^{(0)}, \mathcal{H}_B] - \frac{\hbar}{i}\frac{\rho_B^{(0)}}{\tau_B} + \frac{\hbar}{i}\frac{\rho_A^{(0)}}{\tau_A} + \frac{\hbar}{i}\left(\frac{d\rho_B^{(0)}}{dt}\right)_L \quad ; \tag{62b}$$

$$\frac{\hbar}{i}\frac{d\rho_A^{(1)}}{dt} = [\rho_A^{(1)}, \mathcal{H}_A] + g_e|\beta|[\rho_A^{(0)}, S_y]\cos\omega t - \frac{\hbar}{i}\frac{\rho_A^{(1)}}{\tau_A} + \frac{\hbar}{i}\frac{\rho_B^{(1)}}{\tau_B} \quad ; \tag{62c}$$

$$\frac{\hbar}{i}\frac{d\rho_B^{(1)}}{dt} = [\rho_B^{(1)}, \mathcal{H}_B] + g_e|\beta|[\rho_B^{(0)}, S_y]\cos\omega t - \frac{\hbar}{i}\frac{\rho_B^{(1)}}{\tau_B} + \frac{\hbar}{i}\frac{\rho_A^{(1)}}{\tau_A} \quad . \tag{62d}$$

The terms $\left(\frac{d\rho_A^{(1)}}{dt}\right)_L$ and $\left(\frac{d\rho_B^{(1)}}{dt}\right)_L$ were dropped from equations 62c and 62d, respectively, since the relaxation terms, $\frac{\rho_A^{(1)}}{\tau_A}$ and

$\frac{\rho_B^{(1)}}{\tau_B}$, will dominate the lattice terms for reasonably large transfer rates. Unique solutions can be found for $\rho_A^{(1)}$ and $\rho_B^{(1)}$ when the lattice terms are dropped, provided $\rho_A^{(0)}$ and $\rho_B^{(0)}$ can be defined unambiguously. The line shape is proportional to $\int_0^{2\pi/\omega} \mathrm{Tr}(\mathcal{H}_y \rho_A^{(1)} + \mathcal{H}_y \rho_B^{(1)}) \sin\omega t \, dt$

There is, however, some ambiguity in what we mean by $\rho_A^{(0)}$ and $\rho_B^{(0)}$ when the eigenstates of $\mathcal{H}_A$ and $\mathcal{H}_B$ are significantly different from each other, and the transfer rates are neither sufficiently large nor sufficiently small. The difficulty can be ascribed to not knowing $\left(\frac{d\rho_A^{(0)}}{dt}\right)_L$ and $\left(\frac{d\rho_B^{(0)}}{dt}\right)_L$ as a function of τ_A^{-1} and τ_B^{-1}. Offhand, it would seem that a knowledge of these terms need not be important, since, again, the transfer terms $\frac{\rho_A^{(0)}}{\tau_A}$, $\frac{\rho_B^{(0)}}{\tau_B}$ are expected to dominate the lattice relaxation terms. A little reflection shows that they cannot be ignored. If one drops the lattice terms, one finds that no unique solutions for $\rho_A^{(0)}$ and $\rho_B^{(0)}$ can be found. For example, one set of solutions that would satisfy equations 62a,b is

$$\rho_A^{(0)} = \tau_A \mathbb{1}; \qquad \rho_B^{(0)} = \tau_B \mathbb{1} . \tag{63}$$

($\mathbb{1}$ is the 3×3 unit matrix.)

The form that the lattice interaction terms take is a difficult one to answer. For very long transfer times we expect $\rho_A^{(0)}$ to approach $f_A \rho_A^E$ and $\rho_B^{(0)}$ to approach $f_B \rho_B^E$. ρ_A^E, ρ_B^E are the canonical ensemble matrices defined by the well-known expressions

$$\rho_A^E = \frac{e^{-\mathcal{H}_A/KT}}{Tr\, e^{-\mathcal{H}_A/KT}} \quad ; \quad \rho_B^E = \frac{e^{-\mathcal{H}_B/KT}}{Tr\, e^{-\mathcal{H}_B/KT}} \quad . \tag{64}$$

f_A, f_B are the fraction of triplet molecules found at sites A, B.

$$\frac{f_A}{f_B} = \frac{\tau_A}{\tau_B} \quad . \tag{65}$$

When the transfer rates are very large, A and B are a strongly coupled system. The lattice undoubtedly relaxes A and B to a suitably averaged canonical ensemble. Equations 62a,b must be solved subject to the above boundary conditions for the lattice interaction terms.

Although it may be difficult to define $\rho_A^{(0)}$ and $\rho_B^{(0)}$ accurately under some circumstances, an approximate determination of $\rho_A^{(0)}$ and $\rho_B^{(0)}$ probably suffices for a reasonably accurate calculation of the line shape. The argument is as follows:

The terms $[\rho_A^{(0)}, S_y] \cos\omega t$ and $[\rho_B^{(0)}, S_y]\cos\omega t$ can be regarded as driving forces; the resonance response behavior of $\rho_A^{(1)}$ and $\rho_B^{(1)}$ are determined primarily by $[\rho_A^{(1)}, \mathcal{H}_A]$, $[\rho_B^{(1)}, \mathcal{H}_B]$ and $\frac{\rho_A^{(1)}}{\tau_A}$, $\frac{\rho_B^{(1)}}{\tau_B}$. The line shape will therefore be rather sensitive to changes in $\mathcal{H}_A$, $\mathcal{H}_B$, τ_A^{-1}, τ_B^{-1} but not as sensitive to changes in the driving force. (The calculations can always be checked by seeing whether the calculated line shape is correct in the limits of fast and slow transfer rates.)

We now proceed to do some illustrative calculations.

Density Matrix Method: Model

Equations 62c,d represent a set of 18 simultaneous differential equations. Clearly some simplifications are in order to make the problem more tractable. The model we use is sketched in Figure II-3. $\hat{H}_o$, the external magnetic field, is directed along a two-fold rotation (or screw) axis. The molecular planes of A and B make angles of $\theta = \pi/4$ with the symmetry axis. (The results obtained for angles other than $\pi/4$ are discussed in a later section.) $\hat{x}_A$, $\hat{x}$ come out of plane of paper; $\hat{x}_B$ goes into plane of paper. In the absence of an external field or any transfer processes, we shall assume that the spin-spin interaction aligns the triplet spins of the individual molecules along their respective normals. Sites A and B are magnetically equivalent for all values of the external magnetic field. The spin Hamiltonians of sites A and B are

$$\begin{aligned} \mathcal{H}_A &= D(S_z{}^2_A - S^2/3) + g_e|\beta|\, \hat{H}_o \cdot \hat{S}_A \ ; \\ \mathcal{H}_B &= D(S_z{}^2_B - S^2/3) + g_e|\beta|\, \hat{H}_o \cdot \hat{S}_B \ . \end{aligned} \tag{66}$$

Case I: $H_o = 0$

A common axis system, $\hat{x}$, $\hat{y}$, $\hat{z}$, is chosen to represent the spin Hamiltonians of A and B. In this common coordinate system we have

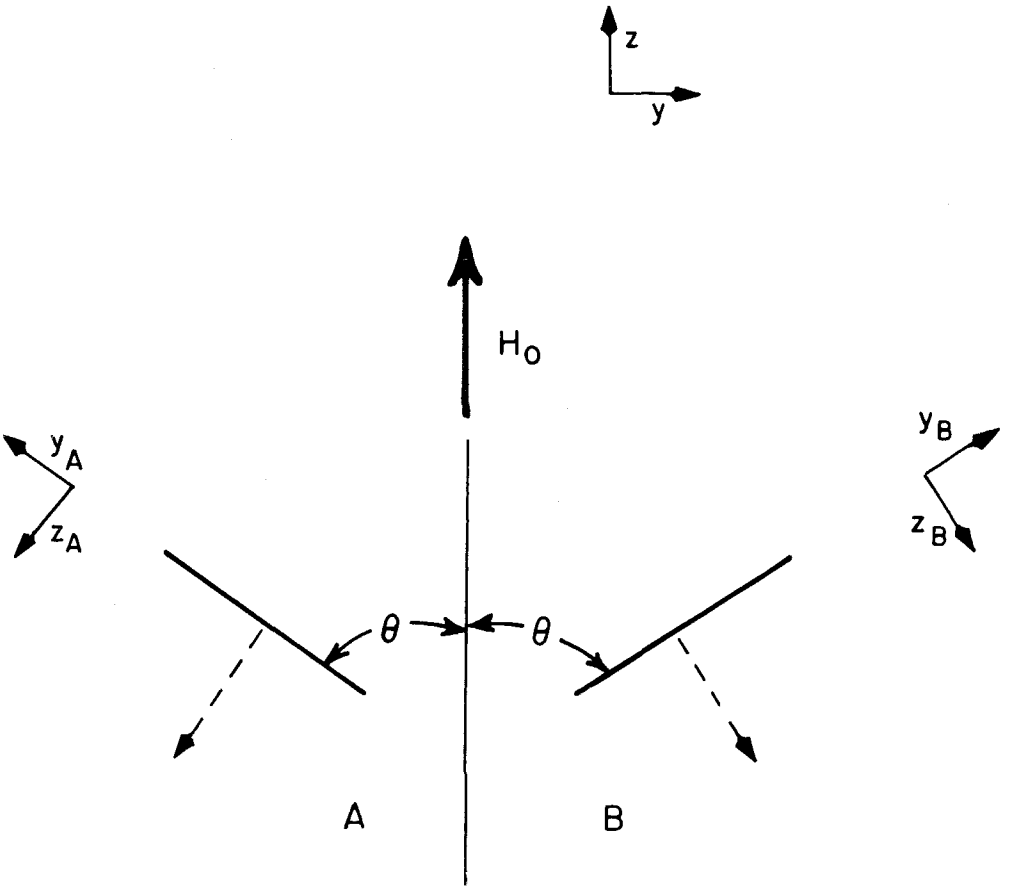

Figure II-3. Two molecular sites per unit cell. The external field, $\hat{H}_o$, is directed along the symmetry axis of the crystal. The molecular planes of A and B are perpendicular to the plane of the paper.

$$\mathcal{H}_A = D/4\left\{(S^2_z - S^2/3) - (S^2_x - S^2_y)\right\} + \frac{D\sqrt{2}}{4}(S_yS_z + S_zS_y)\,;$$
$$\mathcal{H}_B = D/4\left\{(S^2_z - S^2/3) - (S^2_x - S^2_y)\right\} - \frac{D\sqrt{2}}{4}(S_yS_z + S_zS_y)\,. \qquad (67)$$

We reexpress equation 67 in a matrix representation diagonal in S_z; [i.e., $S_z = \begin{pmatrix} 1 & 0 \\ 0 & -1 \end{pmatrix}$]

$$\mathcal{H}_A = D\begin{pmatrix} 1/12 & 0 & -1/4 \\ 0 & -1/6 & 0 \\ -1/4 & 0 & 1/12 \end{pmatrix} + \frac{D\sqrt{2}}{4}\,i\begin{pmatrix} 0 & -1 & 0 \\ 1 & 0 & 1 \\ 0 & -1 & 0 \end{pmatrix} = \mathcal{H}^o + V\,;$$
$$\mathcal{H}_B = D\begin{pmatrix} 1/12 & 0 & -1/4 \\ 0 & -1/6 & 0 \\ -1/4 & 0 & 1/12 \end{pmatrix} - \frac{D\sqrt{2}}{4}\,i\begin{pmatrix} 0 & -1 & 0 \\ 1 & 0 & 1 \\ 0 & -1 & 0 \end{pmatrix} = \mathcal{H}^o - V\,. \qquad (68)$$

We set $\tau_A = \tau_B = \tau$. The energy spectra in the limits of infinitesmally slow and infinitely fast transfer are

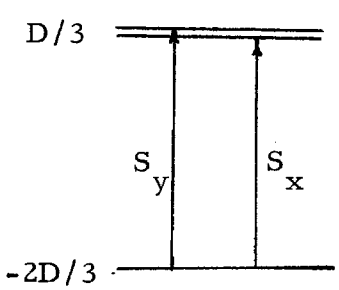

$\tau \longrightarrow \infty$

The upper level is two-fold degenerate

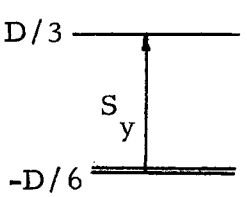

$\tau \longrightarrow 0$

The groundstate level is two-fold degenerate

(69)

An oscillatory field in the y direction is the only transition inducing

field for all values of τ . The resonance energies are D for the slow transfer (monomer) case, and D/2 for the rapid transfer (dimer) case.

The solution of the density matrix equations 62a-d are obtained with the help of symmetry arguments. A rotation of π radians about the z-axis changes molecule A into molecule B. Similarly, a reflection through the z-x plane converts A into B. These symmetry properties lead to the following set of relationships:

Rotation Symmetry

$$C\,\rho_A^{(0)}\,C^{-1} = e^{i\pi s_z}\,\rho_A^{(0)}\,e^{-i\pi s_z} = \rho_B^{(0)}\ ; \tag{70a}$$

$$-C\,\rho_A^{(1)}\,C^{-1} = -e^{i\pi s_z}\,\rho_A^{(1)}\,e^{-i\pi s_z} = \rho_B^{(1)}\ . \tag{70b}$$

Reflection Symmetry

$$\sigma\,\rho_A^{(0)}\,\sigma^{-1} = e^{i\pi s_y}\,\rho_A^{(0)}\,e^{-i\pi s_y} = \rho_B^{(0)}\ ; \tag{70c}$$

$$\sigma\,\rho_A^{(1)}\,\sigma^{-1} = e^{i\pi s_y}\,\rho_A^{(1)}\,e^{-i\pi s_y} = \rho_B^{(1)}\ . \tag{70d}$$

The (-) sign in equation 70b arises from the fact that S_y in equations 62c,d changes sign upon rotating the system π radians about the z axis. The implication of equations 70b and 70d is that

$$\rho_A^{(1)} = \begin{pmatrix} k_1 & k_o & ik_3 \\ k_o^* & 0 & -k_o^* \\ -ik_3 & -k_o & -k_1 \end{pmatrix}\ ;\ \rho_B^{(1)} = \begin{pmatrix} -k_1 & k_o & -ik_3 \\ k_o^* & 0 & -k_o^* \\ ik_3 & -k_o & k_1 \end{pmatrix}\ . \tag{71}$$

k_1 , k_3 are real.

For convenience $\rho_A^{(0)}$ was set equal to $\rho_B^{(0)}$. (This is consistent with the symmetry relationships and is approximately true for all transfer rates.)

$$\rho_A^{(0)} = \rho_B^{(0)} = \frac{0.5\, e^{\frac{-(\mathcal{H}_A+\mathcal{H}_B)}{2\,KT}}}{Tr\, e^{-(\mathcal{H}_A+\mathcal{H}_B)/2\,KT}} \; ; \; \frac{\mathcal{H}_A+\mathcal{H}_B}{2} = D\begin{pmatrix} 1/12 & 0 & -1/4 \\ 0 & 1/6 & 0 \\ -1/4 & 0 & 1/12 \end{pmatrix}. \tag{72}$$

This approximation is only valid for sufficiently fast transfer rates, and does not hold in the intermediate or slow transfer limit. The error introduced by the use of equation 72 was estimated from equations 62a,b to be of the order

$$\frac{1/T_2}{2/\tau + 1/T_2} \; \frac{D\sqrt{2}}{24\,KT} \begin{pmatrix} 0 & -1 & 0 \\ 1 & 0 & 1 \\ 0 & -1 & 0 \end{pmatrix} . \tag{73}$$

T_2 is a relaxation time associated with the lattice integration. Since we are interested in values of τ such that $\tau / T_2 \ll 1$ our approximation appears to be a good one.

Using the above expressions, we obtain that the rate of energy absorption is given by

$$P(\omega) = \frac{N}{V}\, 2\, H_1^{\,2}\, \omega\, g_e^2\, \beta^2\, (KT)^{-1}\, \mathcal{X}(\omega) , \tag{74}$$

where

$$\mathcal{K}(\omega) = \frac{1}{12}\left(\frac{\bar{D}^4}{\tau}\right)\frac{(\omega^3 + 2\omega/\tau^2)}{[\omega^4-(4/\tau^2+\bar{D}^2)\omega^2+\frac{\bar{D}^2}{\tau^2}]^2 + (\frac{2\bar{D}^2\omega}{\tau} - \frac{4\omega^3}{\tau})^2} \quad . \tag{75}$$

$$\bar{D} = D/\hbar$$

Figure II-4 is a plot of $\mathcal{K}$ for various values of τ^{-1}. We note that when $\tau^{-1} \gtrsim \bar{D}$ we obtain a resonance peak at the dimer position, $\omega = \bar{D}/2$. When $\tau^{-1} = 0.3\,\bar{D}$ the line shape is rather broad and extends both to the right and left of $\bar{D}/2$. The broad resonance arises from the fact that the ground state level is no longer degenerate and fairly sharply defined, but rather has split and broadened.

Referring to equation 75 we see that as $\tau^{-1} \longrightarrow \infty$ we obtain a sharp lorentzian line located at $\omega = \bar{D}/2$ and having a width, $(\bar{D}^2/8)\gamma$.

$$\mathcal{K} \longrightarrow \left(\frac{\bar{D}}{24}\right)\frac{(\bar{D}^2/8)\gamma}{(\omega-\bar{D}/2)^2 + \{(\bar{D}^2/8)\gamma\}^2} \quad . \tag{76}$$

(When $\tau^{-1} \gtrsim 10\,\bar{D}$ we find that the resonance line is virtually lorentzian)

When $\tau^{-1} \longrightarrow 0$ we obtain a sharp lorentzian line located at the monomer position, $\omega = \bar{D}$, and having a width, $1/\tau$. The intensity, however, is off by a factor of two. The reason is, of course, that we have set $\rho_A^{(0)} = \rho_B^{(0)}$ and used an "averaged" canonical ensemble. When $\bar{D} \gg 1/\tau \sim 0$, the lattice interaction dominates and it would be more appropriate to use the isolated molecule canonical ensemble (that

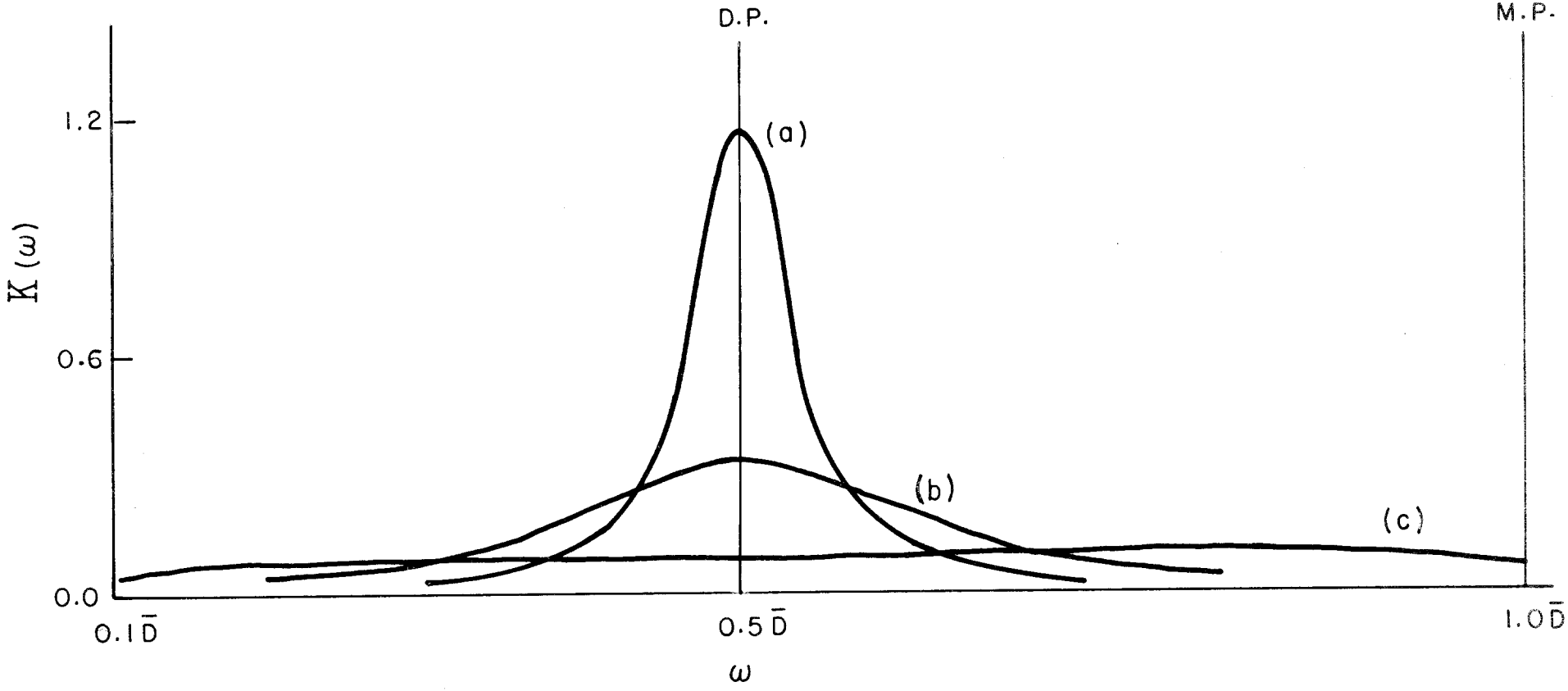

Figure II-4. Absorption curves as a function of transfer rate, τ^{-1}, in the absence of the external field, H_0. D.P., M.P. refer to the dimer ($\tau \longrightarrow 0$) and monomer ($\tau \longrightarrow \infty$) resonance positions. (a), (b), (c) are the line shapes when $\tau^{-1} = 3.5\ \bar{D}$, $1.0\ D$, $0.3\ D$, respectively.

is, $\rho_A^{(0)} = 1/2\ \rho_A^{E}$; $\rho_B^{(0)} = 1/2\ \rho_B^{E}$) .

Case II: Intermediate Field. $g_e|\beta|\ H_o = 3D$

$\mathcal{H}_A$ and $\mathcal{H}_B$ now include the Zeeman term $g_e|\beta|\ H_o S_z = 3D\begin{pmatrix} 1 & 0 \\ 0 & -1 \end{pmatrix}$

The equations we solve are the density matrix equations (equations 62a-d) with one slight modification: an oscillatory field along the x-direction rather than the y-direction was chosen for convenience of calculation. (One can show that for sufficiently high fields, $H_o \gtrsim \frac{3D}{g_e|\beta|}$, an oscillatory field in either the x or y direction gives essentially the same spectra.) An external magnetic field modifies the symmetry properties of our system. We now have

$$C\ \rho_A^{(0)}\ C^{-1} = \rho_B^{(0)} \quad ; \tag{77a}$$

$$-C\ \rho_A^{(1)}\ C^{-1} = \rho_B^{(1)} \quad ; \tag{77b}$$

$$I_{H_o} \sigma\ \rho_A^{(0)} \sigma^{-1} = \rho_B^{(0)} \quad ; \tag{77c}$$

$$-I_{H_o} \sigma\ \rho_A^{(1)} \sigma^{-1} = \rho_B^{(1)} \quad . \tag{77d}$$

I_{H_o} reverses the direction of the external field, and needs to be introduced because S_z, appearing in the Zeeman term, changes sign upon reflection through the z-x plane. We again set

$$\rho_A^{(0)} = \rho_B^{(0)} = \frac{e^{-(\mathcal{H}_A + \mathcal{H}_B)/2KT}}{\mathrm{Tr}\ e^{-(\mathcal{H}_A + \mathcal{H}_B)/2KT}} \quad . \tag{78}$$

This appears to be a justifiable substitution for sufficiently large transfer rates.

An effective use of the symmetry conditions expressed by equations 77a-d would require some sort of expansion of $\rho_A^{(1)}$ and $\rho_B^{(1)}$ in powers of $D/g_e|\beta| H_o$. Unfortunately no convenient expansion series could be devised. As a result only equations 77a,b were used. We obtain

$$\rho_A^{(1)} = \begin{pmatrix} k_{11} & k_{12} & k_{13} \\ k_{21} & k_{22} & k_{23} \\ k_{31} & k_{32} & k_{33} \end{pmatrix}; \quad \rho_B^{(1)} = \begin{pmatrix} -k_{11} & k_{12} & -k_{13} \\ k_{21} & -k_{22} & k_{23} \\ -k_{31} & k_{32} & -k_{33} \end{pmatrix} . \tag{79}$$

The results of the calculation are displayed in Figures II-5 and II-6 for the $|1^-> \longrightarrow |0>$ transition. The expression for the corresponding line shape is given in the Appendix. The computation was very laborious despite the use of the rotation symmetry condition. If no convenient expansion series in $D/g_e|\beta| H_o$ can be devised, a computer would have to be used for the general case where H_o is not along a symmetry element.

The density matrix equations yielded the monomer and dimer resonance positions correct to within 0.05% for all transitions; the corresponding intensities, to within an accuracy of ~ 96%. Again

$$P(\omega) = \frac{N}{V} \; 2H_1^2 \, \omega \, g_e^2 \, \beta^2 (KT)^{-1} \mathcal{K}(\omega).$$

The separation between the monomer and dimer resonance peaks for

the $|\bar{1}> \longrightarrow |0>$ transition is $0.062\,\bar{D}$. The line widths for this transition in the monomer and dimer limits are $\sim 0.088\,\tau^{-1}$ and $0.192\,\bar{D}^2\tau$ respectively (see Appendix).

Comparing Figures II-4 and II-5,6, we see that a larger transfer rate is required to displace the resonance from the monomer to the dimer side for the present case II than for case I. In addition the case II line width in the dimer limit is almost twice that of case I. This is surprising because the monomer-dimer resonance peak separation of the former is $\sim 1/10$ that of the latter.

The results of the above calculations suggest that if H_o is increased, the system's response would become more lethargic; i.e., a larger transfer rate, τ^{-1}, would be required to effect a displacement from the monomer to the dimer side. Thus, when $H_o \sim 10D$, one suspects that when τ^{-1} is $\sim\bar{D}$, the resonance peak might now occur at the monomer position. (This indeed turns out to be true, as will be proven in the next section.)

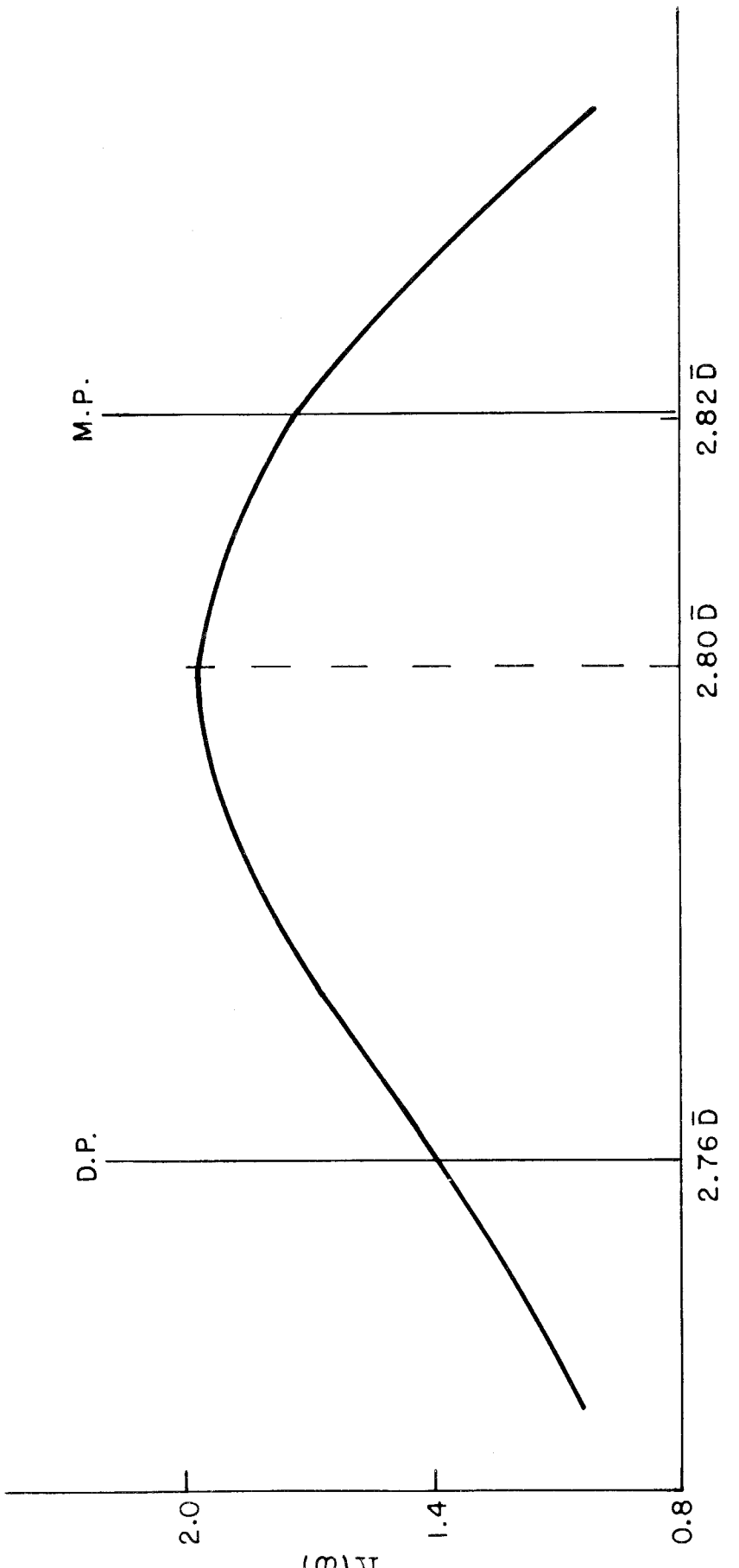

Figure II-6. An enlargement of absorption curve (c) of Figure II-5.

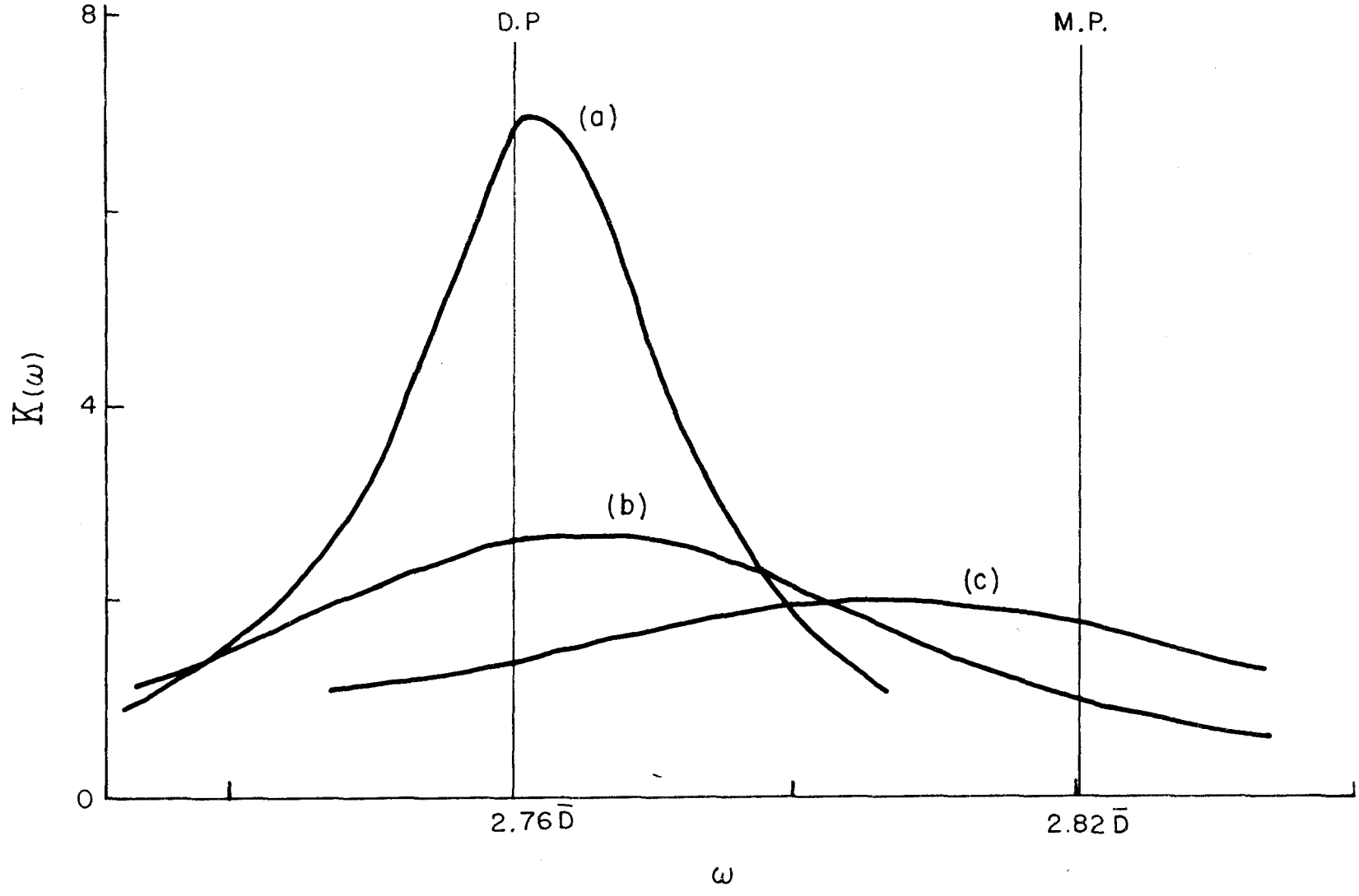

Figure II-5. Absorption curves for the $|\bar{1}> \longrightarrow |0>$ transition when $H_o = 3D\,(g_e\,|\beta|\,)^{-1}$, and is along the symmetry axis (Fig. II-3). The transfer rates, τ^{-1}, corresponding to the curves (a), (b), (c) have the values 10.5 $\bar{D}$, 3.5 $\bar{D}$, $\bar{D}$, respectively.

The "Frequency Modulation" Method

The probability amplitude that the small oscillatory field, $\hat{H}(t) = 2H_1 \cos\omega t\, \hat{e}_y$, will induce a transition from the spin state $|i> \longrightarrow |j>$ at time T is given by

$$1/\hbar \int_{-\infty}^{T} <j|\ \mathcal{M}^{H}(t)\ |i> H_1 e^{-i\omega t}\, dt = 1/\hbar \int_{-\infty}^{T} \mathcal{M}^{H}_{ji}(t) H_1 e^{-i\omega t}\, dt\,. \qquad (80)$$

$\mathcal{M}^{H}(t)$ is the $\mathcal{M}_y$ operator in the Heisenberg representation, and is defined as

$$\mathcal{M}^{H}(t) = \exp\left[\, i/\hbar \int_{o}^{t} \mathcal{H}_s\, dt' \,\right] \mathcal{M}_y \exp\left[-i/\hbar \int_{o}^{t} \mathcal{H}_s\, dt'\right]\,. \qquad (81)$$

$\mathcal{H}_s$ is the Schrodinger spin Hamiltonian.

The physical meaning of equation 80 is that the wave function is $|i>$ at $t = 0$, whereupon it evolves, or propagates, to time t with the propagation factor $\exp\left[-i/\hbar \int_{o}^{t} \mathcal{H}_s\, dt'\right]$; it interacts with the "potential," $\mathcal{M}_y \exp[-i\omega t]$, at time t and then propagates to time T with the propagation factor $\exp\left[-i/\hbar \int_{t}^{T} \mathcal{H}_s\, dt'\right]$. The matrix element is then taken between this state and the evolved state $|j>$, i.e., $\exp\left[-i/\hbar \int_{o}^{T} \mathcal{H}_s\, dt'\right] |j>$. Since the system can interact with the oscillatory field at any time $-\infty < t \leq T$, we take the time integral of the resulting matrix element to obtain the probability amplitude.

When $\mathcal{H}_s$ is independent of time, the rate of energy absorption, $P(\omega)$, is given by the well-known expression:

$$P(\omega) = \frac{N}{V} \hbar\omega (\rho^E_{ii} - \rho^E_{jj}) \lim_{T\to\infty} 1/\hbar^2 \frac{\left| \int_{-T/2}^{T/2} \mathcal{M}^{\mathcal{H}}_{ji}(t)\, H_1\, e^{-i\omega t}\, dt \right|^2}{T} \quad (82)$$

$$= 2\pi H_1^2 \frac{N}{V} \hbar\omega (\rho^E_{ii} - \rho^E_{jj}) \frac{|(\mathcal{M}_y)_{ji}|^2}{\hbar} \delta(\hbar\omega + E_i - E_j).$$

δ is the delta function.

Conservation of energy assures a very sharp resonance when $\hbar\omega = E_j - E_i$.

We are interested in the case where a random walk of the triplet excitation occurs between sites A and B. As a result, $\mathcal{H}_s$ is a time dependent Hamiltonian in the sense that it stochastically takes on the values, $\mathcal{H}_A$ and $\mathcal{H}_B$. We can talk about transitions between fairly well defined states provided that the time dependent part of $\mathcal{H}_s$ can be regarded as a sufficiently small perturbation. If the eigenstates of $\mathcal{H}_A$ are considerably different from those of $\mathcal{H}_B$, we require that the transfer rate be either sufficiently fast or slow in order to avoid ambiguity. In the former case, we define $|i>$, $|j>$ to be eigenstates of a suitably average Hamiltonian; in the latter case, we take $|i>$, $|j>$ to be eigenstates of $\mathcal{H}_A$, and $|i'>$, $|j'>$ to be eigenstates of $\mathcal{H}_B$.

If the time dependent part of $\mathcal{H}_s$ is small for the entire range of transfer rates, we simply define $|i>$, $|j>$ to be eigenstates of the time independent part of $\mathcal{H}_s$. $I(\omega)$, the line shape for the absorption in the presence of the stochastic transfer of excitation is taken as

$$I(\omega) = \lim_{T\to\infty} (T)^{-1} \left| \int_{-T/2}^{T/2} \mathcal{M}^{\mathcal{H}}_{ji}(t)\, e^{-i\omega t}\, dt \right|^2 . \qquad (83)^*$$

$I(\omega)$ is still not in its most convenient form. Using a well-known transformation (the Wiener-Khinchine formula (29)), we reexpress $I(\omega)$ as equation 84

$$I(\omega) = \int_{-\infty}^{\infty} \langle (\mathcal{M}_y)^*_{ji}\, \mathcal{M}^{\mathcal{H}}_{ji}(t) \rangle_{ave}\, e^{-i\omega t}\, dt . \qquad (84)$$

$\langle (\mathcal{M}_y)^*_{ji}\, \mathcal{M}^{\mathcal{H}}_{ji}(t) \rangle_{ave}$ is referred to as the correlation function, $K_{ji}(t)$, and is defined as

$$K_{ji}(t) = \lim_{T\to\infty} \frac{1}{T} \int_{-T/2}^{T/2} \mathcal{M}^{\mathcal{H}}_{ij}(t_1)\, \mathcal{M}^{\mathcal{H}}_{ji}(t_1 + t)\, dt_1 . \qquad (85)$$

(In practice, the time average is replaced by an ensemble average.)

Further manipulation of equation 84 is required. We set

---

*The above statements are consistent with the conclusions of Bloom and Margenau (39) who have shown that the proper criteria for the use of equation 83 is that the density matrix be essentially diagonal in the $|i>$, $|j>$ representation.

$$\mathcal{H}_s = \frac{\mathcal{H}_A+\mathcal{H}_B}{2} + \left(\frac{\mathcal{H}_A-\mathcal{H}_B}{2}\right) f(t) = \mathcal{H}^o + V f(t). \tag{86}$$

$f(t)$ is a stochastic variable that takes on the values ± 1. (When $f(t)$ is 1 (-1), $\mathcal{H}_s$ is $\mathcal{H}_A(\mathcal{H}_B)$.)

$|i>$ and $|j>$ are chosen as eigenfunctions of $\mathcal{H}^o$. $\mathcal{M}^{\mathcal{H}}(t)$ is rewritten in the interaction representation, with $\mathcal{H}^o$ diagonal.

$$\mathcal{M}^{\mathcal{H}}(t) = U(t) \exp[i/\hbar\, \mathcal{H}^o t]\, \mathcal{M}_y \exp[-i/\hbar\, \mathcal{H}^o t]\, U^{-1}(t) . \tag{87}$$

$U(t)$ and $U^{-1}(t)$ are time ordered operators defined by

$$U(t) = e^{i\int_o^t \bar{V}(t')\, f(t')\, dt'} = 1 + i\int_o^t \bar{V}(t_1)\, f(t_1)\, dt_1$$

$$+ (i)^2 \int_o^t dt_1 \int_o^{t_1} \bar{V}(t_2)\, \bar{V}(t_1)\, f(t_2)\, f(t_1)\, dt_2 + \ldots \tag{88a}$$

$$\ldots + (i)^n \int_o^t dt_1 \int_o^{t_1} dt_2 \ldots \int_o^{t_{n-1}} \bar{V}(t_n)\bar{V}(t_{n-1}) \ldots \bar{V}(t_1) f(t_n) \ldots$$

$$f(t_1)\, dt_n + \ldots$$

and

$$U^{-1}(t) = e^{-i\int_o^t \bar{V}(t')f(t')dt'} = 1 - i\int_o^t \bar{V}(t_1)dt_1 + (-i)^2\int_o^t dt_1\int_o^{t_1} \bar{V}(t_1)\bar{V}(t_2)f(t_2)f(t_1)dt_2 \tag{88b}$$

$$+\ldots+(-i)^n\int_o^t dt_1\int_o^{t_1} dt_2\ldots\int_o^{t_{n-1}} \bar{V}(t_1)\bar{V}(t_2)\ldots\bar{V}(t_n)f(t_n)\ldots f(t_1)dt_n+\ldots$$

$$\bar{V}(t') = \exp\left[i/\hbar\, \mathcal{H}^o t'\right]\frac{V}{\hbar}\exp\left[-i/\hbar\, \mathcal{H}^o t'\right].$$

Using the above, we can rewrite the correlation function as

$$K_{ji}(t) = \left|(\mathcal{M}_y)_{ji}\right|^2 < U_{jj}(t)\, U^{-1}_{ii}(t) >_{ave} e^{i\lambda_{ji} t}$$

$$+ \sum_{m,r}{}' (\mathcal{M}_y)^*_{ji}(\mathcal{M}_y)_{mr} < U_{jm}(t)\, U^{-1}_{ri}(t) >_{ave} e^{i\lambda_{mr} t} \tag{89}$$

$$\hbar\lambda_{ji} = E^o_j - E^o_i$$

$m = j$, $r = i$ are omitted from the primed sum. The latter sum arises from the fact that the transfer process mixes the eigenfunctions of $\mathcal{H}^o$. We note that, in general, the primed sum can be ignored if V is diagonal, or if the external field, H_o, is large enough. If V is diagonal, U, U^{-1} are diagonal. If V is not diagonal, but H_o is large, we separate V into a diagonal part, V_1, and an off diagonal part, V_2. The V_2 part contributes a rapidly oscillating term. For example, U would have the form

$$U(t) = \exp\left[i\int_o^t V_1 f(t')dt' + i\int_o^t e^{i/\hbar \mathcal{H}^o t'} V_2 e^{-i/\hbar \mathcal{H}^o t'} f(t')\, dt'\right] . \quad (90)$$

The integral involving V_2 cannot exceed $i(V_2/g_e \beta H_o)t$, whereas the integral involving V_1 cannot exceed $iV_1 t$. Consequently, for large H_o, the V_1 integral dominates, and the off diagonal terms of $U(t)$ and $U^{-1}(t)$ will be quite small.*

Equation 89 can be evaluated by a number of different techniques. One useful method, for example, involves multiplying the appropriate matrix elements of $U(t)$ and $U^{-1}(t)$ together and incorporating the "average" brackets into the resulting integrals. The subsequent evaluation would require knowing the correlation functions of the $f(t)$'s. That is, we shall need $\langle f(t)\rangle_{ave}$, $\langle f(t_i)f(t_j)\rangle_{ave}$, $\langle f(t_i)f(t_j)f(t_k)f(t_\ell)\rangle \cdots$ etc. The $f(t)$'s define a stochastic process having a characteristic time τ (τ_A is assumed equal to τ_B for convenience). It is generally well known (29) that

$$\langle f(t)\rangle_{ave} = 0 \; ; \; \langle f(t_1)f(t_2)\rangle_{ave} = \exp\left[\omega_e(t_1 - t_2)\right] . \quad (91)$$

$$\omega_e = 2\tau^{-1} \qquad t_1 < t_2$$

The higher order correlation functions can be derived easily enough. We have

---

*The primed sum was not examined critically in this thesis since it gives a negligible correction to the line shape for those cases studied. Offhand it does appear that the $|i> \rightarrow |j>$ transition might make a contribution to the line shape in the neighborhood of λ_{mr} (the predominant contribution to the line shape comes from the $|r> \longrightarrow |m>$ transition) if the external field is not large.

$$\langle f(t_1)f(t_2)f(t_3)f(t_4)\rangle_{ave} = \exp[\omega_e(t_1-t_2)]\exp[\omega_e(t_3-t_4)];\ t_1<t_2<t_3<t_4$$

$$\langle f(t_1)f(t_2)\cdots f(t_{2n-1})f(t_{2n})\rangle_{ave} = \exp[\omega_e(t_1-t_2)]\cdots\exp[\omega_e(t_{2n-1}-t_{2n})] \qquad (92)$$

$$t_1<t_2\cdots t_{2n-1}<t_{2n}$$

$$\langle f(t_1)f(t_2)\cdots f(t_{2n-1})\rangle_{ave} = 0 .$$

Zero Field Case

We now repeat the calculations for the model presented in the Density Matrix section. $\mathcal{H}^o$ and V in the S_z representation are given by equation 68 . The eigenstates of $\mathcal{H}^o$ are

$$|x_+\rangle = \frac{|1\rangle + |\bar{1}\rangle}{\sqrt{2}} \quad ; \quad |x_o\rangle = |0\rangle ; \quad |x_-\rangle = \frac{|1\rangle - |\bar{1}\rangle}{\sqrt{2}} . \qquad (93)$$

We reexpress $\mathcal{H}^o$ and V in the x_+, x_o, x_- representation

$$\mathcal{H}^o = \begin{array}{c} \\ x_+ \\ x_o \\ x_- \end{array}\begin{array}{c} \begin{array}{ccc} x_+ & x_o & x_- \end{array} \\ \begin{pmatrix} -D/6 & 0 & 0 \\ 0 & -D/6 & 0 \\ 0 & 0 & D/3 \end{pmatrix} \end{array} ; \quad V = iD/2\begin{pmatrix} 0 & -1 & 0 \\ +1 & 0 & 0 \\ 0 & 0 & 0 \end{pmatrix} . \qquad (94)$$

The only allowed transition caused by the oscillatory field in the y direction is the $|x_o\rangle \longrightarrow |x_-\rangle$ transition. Our expression for the correlation function for the induced absorption is, by equation 89

$$K_{-o}(t) = g_e^2 \beta^2 \left[\langle U_{--}(t) U_{oo}^{-1}(t) \rangle_{ave} e^{i\bar{D}t/2} - \langle U_{-o}(t) U_{-o}^{-1}(t) \rangle_{ave} e^{-i\bar{D}t/2} \right]. \tag{95}$$

(For convenience of notation, we have set $U_{-o}(t)$ etc., equal to $\langle x_- | U | x_o \rangle$ etc. This notation convention is used throughout the remainder of this chapter.)

We note from equation 94 that V has no diagonal matrix elements. Furthermore, $V_{r-} = 0$, $r = +, 0, -$. The consequence of this is that $U_{-o}(t) = U_{-o}^{-1}(t) = 0$ and that $U_{--}(t) = 1$ for all times, t. Therefore,

$$K_{-o}(t) = g_e^2 \beta^2 \langle U_{oo}^{-1}(t) \rangle_{ave} e^{i\bar{D}/2\, t}. \tag{96}$$

Using equations 88a and 94 we find that

$$\langle U_{oo}^{-1}(t) \rangle = \langle e^{i\bar{D}/2 \int_o^t f(t')\, dt'} \rangle_{ave}. \tag{97}$$

This expression is precisely that which one would have found if one considered the case of a single electron transferring between two sites that differ by an amount D in their Zeeman energies. (The orientation of the effective magnetic fields at the two sites is the same.) The equivalence of our triplet system, in which there is no external field, and the above transferring electron case is accidental. It arises from the model we have used for our calculations; i.e., it is caused by the

fact that the y, z directions in the laboratory system are magnetically equivalent when $\theta = \pi/4$. (We shall discuss briefly the general case in a latter section.)

Equation 97 has been studied by Anderson (37), and the interested reader can refer to the appropriate sections in his paper. The consequence of a correlation function of the form of equation is that in the dimer limit a lorentzian line of width $(\bar{D}^2/8)\tau$ occurs at $\omega = \bar{D}/2$; while in the monomer limit, lorentzian lines of width τ^{-1} are obtained at $\omega = \bar{D}$ and $\omega = 0$.

The last resonance at $\omega = 0$ is unobservable for the following reason. It arises because the oscillatory field in the y direction connects the two upper degenerate states in the monomer limit. Since the population of these states is the same, there clearly is no net absorption of energy from the radiation field. (Our calculation only concerned itself with the induced absorption and neglects the induced emission contribution.) The line shape that results from using equation 97 is also essentially that calculated by the density matrix method.

The Hamiltonians $\mathcal{H}_A$ and $\mathcal{H}_B$ differ significantly from each other. In the light of what was earlier said in connection with equation 83, one might suspect the validity of using equations 94-97 over the entire range of τ. It is a simple matter to repeat the line shape calculation in the limit of $\tau \longrightarrow \infty$, using eigenstates of $\mathcal{H}_A$ and $\mathcal{H}_B$.

Our results were the same as those calculated above--because of this and equation 73 we feel confident in the applicability of equations 94 to 97 to the entire τ range for this example (the $H_o = 0$, $\theta = \pi/4$ case).

Intermediate Field. $g_e|\beta| H_o = 3D$

The eigenstates of $\mathcal{H}^o$ are now

$$|x_+\rangle = 0.999\ |1\rangle - 0.041\ |\bar{1}\rangle\ ; \quad |x_o\rangle = |0\rangle\ ; \qquad (98)$$
$$|x_-\rangle = -0.041\ |1\rangle - 0.999\ |\bar{1}\rangle\ .$$

$\mathcal{H}^o$ and V have the following forms in the x_+, x_o, x_- representation

$$\mathcal{H}^o = \begin{array}{c|ccc} & x_+ & x_o & x_- \\ \hline x_+ & 3.094D & 0 & 0 \\ x_o & 0 & -D/6 & 0 \\ x_- & 0 & 0 & -2.927D \end{array} \quad ; \quad V = \frac{iD\sqrt{2}}{4} \begin{array}{|ccc|} \hline 0 & 0.958 & 0 \\ -0.958 & 0 & -1.041 \\ 0 & 1.041 & 0 \\ \hline \end{array} \ . \qquad (99)$$

The correlation function is

$$K_{o-}(t) = \left|(\mathcal{M}_x)_{o-}\right|^2 \langle U_{oo}(t)\, U^{-1}_{--}(t)\rangle_{ave}\, e^{i\,2.76\bar{D}t} + (\mathcal{M}_x)^*_{o-}\,(\mathcal{M}_x)_{+o} \langle U_{o+}(t)\, U^{-1}_{o-}(t)\rangle_{ave}\, e^{i\,3.26\bar{D}t} \ . \qquad (100)$$

(The oscillatory field is in the x-direction to be consistent with the earlier density matrix calculation)

As pointed out above, the off diagonal elements of U and U^{-1} are expected to make a small, negligible contribution to $K_{o-}(t)$ when

the Zeeman energy, $g_e|\beta| H_o$, is large compared with V. (A calculation of $< U_{o+}(t)\, U_{o-}^{-1}(t) >_{ave}$ indeed shows that it is negligible.) We have

$$K_{o-}(t) \sim \frac{g_e^2 \beta^2}{2} < U_{oo}(t)\, U_{--}^{-1}(t) >_{ave} e^{i\, 2.76 \bar{D} t} \; ; \qquad (101)$$

$$\left(\left| (M_x)_{o-} \right|^2 \sim \frac{g_e^2 \beta^2}{2} \right) .$$

Setting

$$\lambda_{o-} = -\lambda_{-o} = 2.76 \bar{D} \; ; \quad \lambda_{+o} = -\lambda_{o+} = 3.26 \bar{D} \; ; \qquad (102)$$

$$G(t_i - t_j) = \left\{ \left| V_{o-} \right|^2 e^{i\lambda_{-o}(t_i - t_j)} + \left| V_{o+} \right|^2 e^{i\lambda_{+o}(t_i - t_j)} \right\} .$$

We obtain the following expressions for $U_{oo}(t)$ and $U_{--}^{-1}(t)$

$$U_{oo}(t) = 1 - \left(\frac{1}{\hbar}\right)^2 \int_o^t dt_1 \int_o^{t_1} G(t_1 - t_2) f(t_1) f(t_2) dt_2 \qquad (103a)$$

$$+ \left(\frac{1}{\hbar}\right)^4 \int_o^t dt_1 \int_o^{t_1} dt_2 \cdots \int_o^{t_3} G(t_1 - t_2) G(t_3 - t_4) f(t_1) \cdots f(t_4) dt_4 + \cdots$$

$$\cdots + \left(\frac{i}{\hbar}\right)^{2n} \int_o^t dt_1 \int_o^{t_1} dt_2 \cdots \int_o^{t_{2n-1}} G(t_1 - t_2) G(t_3 - t_4) \cdots G(t_{2n-1} - t_{2n}) f(t_1)$$

$$\cdots f(t_{2n}) dt_{2n} + \cdots \; ;$$

$$U_{--}^{-1}(t) = 1 - \left(\frac{|V_{o-}|}{\hbar}\right)^2 \int_o^t dt_1 \int_o^{t_1} e^{i\lambda_{-o}(t_1-t_2)} f(t_1)f(t_2)dt_2$$

(103b)

$$+ \left(\frac{1}{\hbar}\right)^4 |V_{o-}|^2 \int_o^t dt_1 \int_o^{t_1} dt_2 \cdots \int_o^{t_3} e^{i\lambda_{-o}(t_1-t_4)} G(t_3-t_2)f(t_1)\cdots f(t_4)dt_4$$

$$+\cdots +(-i/\hbar)^{2n} |V_{o-}|^2 \int_o^t dt_1 \int_o^{t_1} dt_2 \cdots \int_o^{t_{2n-1}} e^{i\lambda_{-o}(t_1-t_{2n})} G(t_3-t_2)\cdots G(t_{2n-1}-t_{2n-2})$$

$$\times f(t_1)f(t_2)\cdots f(t_{2n})\, dt_{2n}$$

$$+\cdots$$

$\langle U_{oo}(t)\, U_{--}^{-1}(t) \rangle_{ave}$ is evaluated using equations 91 and 92 .

Upon ignoring small correction terms, we find that

$$K_{o-}(t) = \frac{g_e^2 \beta^2}{2} \quad e^{-t/\Gamma} \quad e^{i\lambda_{o-}t} \,) \tag{104}$$

where

$$\Gamma^{-1} = \frac{1}{\hbar^2} \quad \frac{[\,2\,|V_{o-}|^2 + |V_{o+}|^2]\omega_e + i\,[\,|V_{o+}|^2 \lambda_{o-} - 2\,|V_{o-}|^2 \lambda_{+o}]}{\omega_e^2 + \lambda_{o-}\lambda_{+o} + i\,(\lambda_{o-} - \lambda_{+o})\omega_e} \,. \tag{105}$$

$(\omega_e = 2\tau^{-1})$

The above holds for all values of ω_e . (The above also defines the correlation function for the $|0> \rightarrow |+>$ transition provided we interchange the +, - subscripts.)

*Equation 105 can be expressed somewhat more compactly as

$$\Gamma^{-1} = \frac{1}{h^2}\left(\frac{2\,|V_{o-}|^2}{\omega_e + i\lambda_{o-}} + \frac{|V_{o+}|^2}{\omega_e + i\lambda_{o+}}\right) \qquad \text{(Cf. eq. 109b).}$$

The line width is given by the real part of Γ^{-1}; the line shift from the dimer position, λ_{o-}, by the imaginary part.

When $\omega_e >> g_e |\beta| H_o$, we obtain:

$$\text{line width} \sim \frac{[2|V_{o-}|^2 + |V_{o+}|^2]}{\hbar^2 \omega_e} ; \tag{106a}$$

$$\text{resonance peak at} \sim \lambda_{o-} + \frac{[2|V_{o-}|^2 \lambda_{o-} - |V_{o+}|^2 \lambda_{+o}]}{\hbar^2 \omega_e^2} . \tag{106b}$$

Our earlier density matrix calculations suggested that the resonance peak at a fixed ω_e tends toward the monomer position with increasing H_o. We indeed see that this is true.* When $g_e |\beta| H_o >> \omega_e$, we obtain:

$$\text{line width} \sim \frac{[2|V_{o-}|^2 + |V_{o+}|^2] \omega_e}{(\lambda_{o-} - \lambda_{+o}) \hbar^2} ; \tag{107a}$$

$$\text{resonance peak} \sim \lambda_{o-} + \left(1/\hbar^2\right) \left[\frac{2|V_{o-}|^2}{\lambda_{o-}} - \frac{|V_{o+}|^2}{\lambda_{+o}} \right] \tag{107b}$$

We note that equation 107b gives the monomer position correct to second order. Equations 104 ff. are valid over the entire range of ω_e, $o \leq \omega_e < \infty$, whenever V represents a perturbation on H_o that need only be taken into account up to second order.

* This lethargic behavior is associated with the fact that V has no diagonal elements. When V does have diagonal elements, the line shape behavior is somewhat different (cf. eqs. 109-113).

Presumably the higher order terms are contained in those correction terms ignored to obtain equations 104 and 105 .

We now compare the results obtained from the above with those previously obtained using the density matrix method.

When $g_e|\beta| H_o = 3D$; $\omega_e = 20 \bar{D}$, we find that the line width is $0.018 \bar{D}$, and that the resonance peak is shifted $0.001 \bar{D}$ away from the dimer position toward the monomer position.

When $\omega_e \longrightarrow 0$ we obtain that the line width is $0.084 \tau^{-1}$ and that the resonance is shifted $0.062 \bar{D}$ toward the monomer position.

When $\omega_e = 2 \bar{D}$ we use the complete expression (eq. 105) and find that the line width is $0.060 \bar{D}$, and that the resonance occurs at $2.8 \bar{D}$. These results are in excellent agreement with the values previously calculated using the density matrix method.*

We note that when $D \sim 0.1\ cm^{-1}$, $g_e|\beta| H_o \sim 0.3\ cm^{-1}$, a line width of 20 gauss is obtained when the transfer rate, ω_e, is $2\ cm^{-1}$. These are values that one might very likely encounter experimentally when working with aromatic systems.

Upon evaluating K_{o-}, we found the following interesting behavior: there is very little correlation between $U_{oo}(t)$ and $U_{--}^{-1}(t)$ permitting $< U_{oo}(t)\ U_{--}^{-1}(t)>_{ave}$ to be expressed approximately as $<U_{oo}(t) >_{ave} <U_{--}^{-1}(t) >_{ave}$. This decomposition is apparently associated with the fact that V contains no diagonal terms. If there were diagonal terms, V_{oo} and V_{--}, as does occur when H_o is no longer along a

*We expect good agreement. The density matrix method represents a differential equation approach to the line shape; the frequency modulation method an integral equation approach.

symmetry axis or plane, there is correlation between $U_{oo}(t)$ and $U^{-1}_{--}(t)$.

General Case

We now present an expression for the correlation function, $K_{o-}(t)$, valid for all orientations and magnitudes of $\hat{H}_o$, and for all values of ω_e, provided $\underset{\sim}{V}$ represents a perturbation on $(\mathcal{H}_A + \mathcal{H}_B)/2 = \mathcal{H}^o$ that need only be taken into account up to second order. $\underset{\sim}{V}$ can have diagonal terms; the "isolated" molecule dipolar spin Hamiltonian can be of the more general form $D(S^2_z - S^2/3) + E(S^2_x - S^2_y)$.* The derivation is straightforward. We find that the effect of the diagonal terms of $\underset{\sim}{V}$ can be separated from the off-diagonal terms. The correlation function is

$$K_{o-}(t) = (K_{o-})_{diag} \quad (K_{o-})_{off\text{-}diag} \qquad (108)$$

where

$$(K_{o-})_{off\text{-}diag} = \left|(\mathcal{H}_i)_{o-}\right|^2 e^{-t/\Gamma} e^{i\lambda_{o-}t}; \qquad (109a)$$

$$(i = x, y, z)$$

$$\hbar^2 \Gamma^{-1} = \frac{2\left|V_{o-}\right|^2}{\omega_e + i\lambda_{o-}} + \frac{\left|V_{o+}\right|^2}{\omega_e + i\lambda_{o+}} + \frac{\left|V_{+-}\right|^2}{\omega_e + i\lambda_{+-}} . \qquad (109b)$$

$(K_{o-})_{diag}$ is precisely the same correlation function one would have obtained if one considered the case of a single electron transferring between two sites that differ by an amount $2\left|V_{oo} - V_{--}\right|$ in their

*We remind the reader that the subscripts, o, -, +, now refer to the eigenstates, $|x_o\rangle$, $|x_-\rangle$, $|x_+\rangle$ of the general Hamiltonian, $\mathcal{H}^o$.

Zeeman energies. We can express $(K_{o-})_{diag}$ as

$$(K_{o-})_{diag} = \bar{\phi} \cdot \exp\left\{\left[i\frac{(V_{oo}-V_{--})}{\hbar}\bar{\Lambda} + \bar{\pi}\right]t\right\} \cdot \bar{1} = \left\langle \exp\left[i\frac{(V_{oo}-V_{--})}{\hbar}\int_0^t f(t')dt'\right]\right\rangle_{ave} \quad (110)$$

$\bar{\phi}$, $\bar{\Lambda}$, $\bar{\pi}$, $\bar{1}$ denote matrices in Markoffian Space:

$$\bar{\phi} = (1/2\ 1/2); \quad \bar{\Lambda} = \begin{pmatrix} 1 & 0 \\ 0 & -1 \end{pmatrix}; \quad \bar{\pi} = \tau^{-1}\begin{pmatrix} -1 & 1 \\ 1 & -1 \end{pmatrix}; \quad \bar{1} = \begin{pmatrix} 1 \\ 1 \end{pmatrix} \quad (111)$$

The interested reader is again referred to the paper by Anderson for a detailed discussion of the properties of $(K_{o-})_{diag}$. For large transfer rates, we have that

$$(K_{o-})_{diag} = e^{\frac{-[\hbar^{-2}(V_{oo}-V_{--})^2 t]}{\omega_e}} = e^{-t/\gamma} . \quad (112)$$

The line width of the $|x_-> \longrightarrow |x_o>$ transition is then

$$\gamma^{-1} + \Gamma^{-1} = \frac{(V_{oo}-V_{--})^2 + 2|V_{o-}|^2 + |V_{o+}|^2 + |V_{+-}|^2}{\hbar^2 \omega_e} . \quad (113)$$

(The above equations are expressed assuming that $E^o_{\lambda-} < E^o_{\lambda o}$; if $E^o_{\lambda-} > E^o_{\lambda o}$, the -, o subscripts must be interchanged.)

Equation 113 holds even if V is large compared with $\mathcal{H}^o$, provided ω_e is large compared with the differences between the eigenstate energies of $\mathcal{H}^o \pm V$. We observed this in our earlier calculations for the Zero Field case. The diagonal terms of V were all zero, and,

in addition, $V_{-+} = V_{o+} = \lambda_{o+} = 0$. By equation 113 our line width in the limit of fast transfer should be $\frac{|V_{o+}|^2}{\hbar^2 \omega_e} = \frac{\bar{D}^2 \tau}{8}$, which it was. As $\hat{H}_o$ is moved off the symmetry axis (Fig. II-3), the line widths tend to become large. Maximum broadening would occur when $\hat{H}_o$ is directed along the normal of either molecule A or B. When $g_e |\beta| H_o = 3D$ we find for the $|x_-> \longrightarrow |x_o>$ transition that the line width approaches $0.33 \bar{D}^2 \tau$ as $\omega_e \longrightarrow \infty$. (The off diagonal terms of $\underset{\sim}{V}$ contributed about 10%, so that in the limit of infinitely large H_o the line width would be $\sim 0.30 \bar{D}^2 \tau$.)

If the molecular planes of A and B make an angle of 2θ with each other, instead of $\pi/2$, we find that the line widths need to be multiplied by $\sim \sin^2 2\theta$.

Comparison of Wave and Diffusional Exciton Spectra

In Table I we compare the line widths expected from a wave exciton with that for a diffusing exciton having a narrow wave packet. The calculations are based on the methods outlined in this and the previous chapter, and refer to the model illustrated in Figure II-3. The $|x_-> \longrightarrow |x_o>$ transition is explicitly considered. The magnitude of the spin-spin interaction, D, was set equal to 0.1 cm^{-1}. 2θ was set equal to $\pi/2$ so as to give maximum broadening for a fixed τ^{-1}. τ^{-1} stands for both the transfer rate of the diffusing exciton and the Davydov splitting between the $\hat{K}$ bands in the case of the wave exciton.

In addition we assume (1) a low concentration of excitons so that there are no significant exchange effects, and (2) that there are no important non-nearest neighbor interactions. Contributions from regions of time reversal and accidental degeneracies are neglected for wave excitons.

We note that a pronounced qualitative difference between wave and diffusional excitons occurs when the transfer rate, $\tau^{-1} = \tau_{(2)}^{-1}$, is an order of magnitude larger than the spin-spin interaction. In the wave exciton case, two line spectra, somewhat displaced from the dimer position, are obtained. (Second order corrections cause a slight difference in the spin energies of the two $\hat{k}$ bands (see previous chapter).) In the diffusion exciton case we see that a single resonance line is obtained at the dimer position. (Upon increasing H_o along the symmetry axis, we note that lines broaden and then start to narrow only at very high magnetic fields.)

An experimental demonstration of the above is beset by numerous difficulties over which one has so little control. The spin-spin interaction cannot be too small; the orientation of the molecules in the unit cell relative to each other must be within an appropriate range; the transfer rate cannot be too large or too small.

If $\tau_{(1)}^{-1}$ or $\tau_{(4)}^{-1}$ represents the correct order of magnitude of the transfer rate, one most likely would have to resort to additional experiments to distinguish between the two types of excitons. An

investigation of relaxation rates, or a study of the exchange narrowing that should occur with increasing exciton concentration might lead to useful distinguishing criteria. In addition, resonance experiments carried out at very low temperatures might be helpful.

TABLE I

Line Widths of Diffusional and Wave Exciton ESR Spectra

	$\tau_{(1)}^{-1} = 10\ cm^{-1}$	$\tau_{(2)}^{-1} = 1\ cm^{-1}$		$\tau_{(3)}^{-1} = 0.1\ cm^{-1} = D$		$\tau_{(4)}^{-1} \leq 0.01\ cm^{-1}$	
	Diffusional *or* Wave	Diffusional	Wave	Diffusional	Wave[+]	Diffusional	Wave[+]
$H_o = 0$	Narrow (~2 gauss); resonance occurs at the dimer positions, (D.P.) for any arbitrary $\hat{H}_o$.	12 gauss (D.P.)	2 line spectra displaced 15-50 gauss to right and left of (D.P.)	~250 gauss (~D.P.)	Resonance lines are expected to be broad for any arbitrary $\hat{H}_o$.	$\lesssim$ 100 gauss (M.P.)	Resonance occurs at monomer positions (M.P.) for any arbitrary $\hat{H}_o$.
$H_o = 3,000$ gauss and directed along crystal symmetry axis.[++]		19 gauss (D.P.)		60 gauss (M.P.)*		$\lesssim$ 7 gauss (M.P.)	
$H_o = 3,000$ gauss and directed along the normal of molecule A.		33 gauss (D.P.)		~1,000 gauss		$\lesssim$ 100 gauss (M.P.)	
$H_o = 10,000$ gauss and directed along crystal symmetry axis.[++]		14 gauss (~D.P.)		7 gauss (M.P.)		~1 gauss (M.P.)	

[+] Not examined in great detail.

[++] Similar results hold when $\hat{H}_o$ is in symmetry plane.

*(M.P.)= Resonance occurs at monomer positions.

REFERENCES

1. H. Sternlicht and H. M. McConnell, J. Chem. Phys. 35, 1793 (1961).
2. C. A. Hutchison and B. W. Mangum, J. Chem. Phys. 29, 952 (1958); 34, 908 (1961).
3. J. H. van der Waals and M. S. de Groot, Mol. Phys. 2, 333 (1959); 3, 190 (1960).
4. M. A. El-Sayed, M. T. Wauk, and G. W. Robinson, Mol. Phys. 5, 205 (1962).
5. J. B. Farmer, C. L. Gardner, and C. A. McDowell, J. Chem. Phys. 34, 1058(L) (1961).
6. D. S. McClure, "Solid-State Physics" (Academic Press Inc., New York, 1959), Vol. 8, p. 1.
7. J. Frenkel, Phys. Rev. 37, 17, 1276 (1931).
8. A. S. Davydov, J. Exptl. Theoret. Phys. (U.S.S.R.) 18, 210 (1948).
9. L. Brillouin, "Wave Propagation in Periodic Structures" (Dover Publications, New York, N. Y., 1953), Chapters VI, VII.
10. G. F. Koster, "Solid-State Physics" (Academic Press Inc., New York, 1957), p. 211.
11. A. V. Hippel, Zeits. f. Physik 93, 86 (1934).
12. W. T. Simpson and D. L. Peterson, J. Chem. Phys. 26, 588 (1957).

13. H. M. McConnell, Proc. Natl. Acad. Sci. U.S. 45, 172 (1959).

14. M. Gouterman and W. Moffitt, J. Chem. Phys. 30, 1107 (1959).

15. H. M. McConnell, C. Heller, T. Cole, and R. W. Fessenden, J. Am. Chem. Soc. 82, 766 (1960).

16. R. E. Merrifield, J. Chem. Phys. 23, 402 (1955).

17. L. E. Lyons, J. Chem. Soc. 1957, 5001.

18. A. Zmerli, J. Chem. Phys. 34, 2130 (1961).

19. L. D. Landau and E. M. Lifshitz, "Quantum Mechanics; Non-Relativistic Theory" (Addison-Wesley Publishers, Inc., Reading, Mass., 1958), p. 138.

20. C. Herring, Phys. Rev. 52, 361 (1937).

21. E. G. Cox and J. A. Smith, Nature 173, 75 (1954).

22. J. M. Robertson and J. G. White, Acta Cryst. 2, 233 (1949).

23. J. M. Robertson and J. G. White, J. Chem. Soc. 1945, 607.

24. L. P. Bouckaert, R. Smoluchowski, and E. Wigner, Phys. Rev. 50, 58 (1936).

25. H. Winston, J. Chem. Phys. 19, 156 (1951).

26. D. Fox and O. Schnepp, J. Chem. Phys. 23, 767 (1955).

27. R. Pariser, J. Chem. Phys. 24, 250 (1956).

28. H. F. Hameka, J. Chem. Phys. 31, 315 (1959).

29. M. C. Wang and G. E. Uhlenbeck, Rev. of Mod. Phys. 17, 323 (1945).

30. W. Feller, "An Introduction to Probability Theory and Its Applications" (John Wiley & Sons, Inc., New York, N. Y., 1950), p. 386 ff.

31. D. B. Chesnut and W. D. Phillips, J. Chem. Phys. 35, 1002 (1961).

32. D. B. Chesnut and J. P. Arthur, J. Chem. Phys. (to be published).

33. H. M. McConnell and R. L. Bell, J. Chem. Phys. (to be published).

34. U. Fano, Rev. Mod. Phys. 29, 78 (1957).

35. E. P. Wigner, "Group Theory and Its Application to the Quantum Mechanics of Atomic Spectra" (Academic Press Inc., New York, N. Y. 1959), Chapter 26.

36. H. Eyring, J. Walter, and G. F. Kimball, "Quantum Chemistry" (John Wiley & Sons, Inc., New York, N. Y., 1957), p. 206.

37. P. Anderson and P. R. Weiss, Rev. Mod. Phys. 25, 269 (1953); P. Anderson, Phys. Soc. of Japan 9, 316 (1954).

38. J. A. Pople, W. G. Schneider, and H. J. Bernstein, "High Resolution Nuclear Magnetic Resonance" (McGraw-Hill, Inc., New York, N. Y., 1959), Chapter 10.

39. S. Bloom and H. Margenau, Phys. Rev. 90, 791 (1953).

APPENDIX

a. The Simplified Spin-Spin Operator

We assume that the multiplicity of the triplet state is well defined; that is, there is negligible mixing with states of different multiplicity. Denote the antisymmetrized wavefunction of the 2n electron system by $|\psi^m>$. $|\psi^m>$ is a function of cartesian and spin variables and is the exact eigenstate of the "spin" free Hamiltonian. The spin, "S", of $|\psi^m>$ is 1, its spin component is M. We let $|m>$ designate a spin function having "S" = 1 and spin component M. $\mathcal{H}_S$ and $\mathcal{H}_D$ are said to be "equivalent" operators if the eigenenergies of the two operators are the same. That is, the same set of E's satisfies equation a.1 .

$$\underbrace{\left| <\psi^m | \mathcal{H}_D | \psi^{m'}> - E\,\delta_{mm'} \right|}_{(I)} = 0 = \underbrace{\left| <m | \mathcal{H}_S | m'> - E'\,\delta_{mm'} \right|}_{(II)} \qquad (a.1)$$

(I) and (II) are 3X3 determinants. Determinant (I) can be derived from a sum of 9 linearly independent spin operators. (The number of linear independent operators (matrices) equivalent to an arbitrary operator (a NXN hermitian matrix) is N^2. The reader is referred to a review article by U. Fano (34) for further details concerning such operators.)

The eigenenergies of $\mathcal{H}_D$ can be derived from the following sum of 9 linearly independent hermitian spin operators:

$$(\mathcal{H}_D)_{\text{equiv}} = \tilde{C}_1 \underset{\sim}{S}_x + \tilde{C}_2 \underset{\sim}{S}_y + \tilde{C}_3 \underset{\sim}{S}_z + \left[r_1(\underset{\sim}{S}_x \underset{\sim}{S}_y + \underset{\sim}{S}_y \underset{\sim}{S}_x) + r_2(\underset{\sim}{S}_x \underset{\sim}{S}_z + \underset{\sim}{S}_z \underset{\sim}{S}_x) + r_3(\underset{\sim}{S}_y \underset{\sim}{S}_z + \underset{\sim}{S}_z \underset{\sim}{S}_y) \right] + \left[r_4 \underset{\sim}{S}_z^{\,2} + r_5 \underset{\sim}{S}_y^{\,2} + r_6 \underset{\sim}{S}_x^{\,2} \right] . \qquad (a.2)$$

The coefficients are all constants. S_x, S_y, S_z denote the x, y, z spin component operators of the "S" = 1 system. The sum in brackets defines a symmetrix tensor. By redefining the x, y, z axes system, it can be diagonalized.

$$(\mathcal{H}_D)_{\text{equiv}} = C_1 S_x + C_2 S_y + C_3 S_z + A S_z^2 + B S_y^2 + C S_z^2 . \qquad (a.3)$$

We further note that $\mathcal{H}_D$ is invariant to time inversion. Inverting time causes the spin angular momentum of electron i, $\hat{S}_i$, to go into $-\hat{S}_i$. Since $\mathcal{H}_D$ involves products of spin angular momentum it is time invariant. Consequently, $(\mathcal{H}_D)_{\text{equiv}}$ must also be time invariant. This requires C_1, C_2, C_3 to be all zero since $\underset{\sim}{S}_x$, $\underset{\sim}{S}_y$, $\underset{\sim}{S}_z$ change sign upon time inversion. Using the further fact that $\mathcal{H}_D$ is a traceless operator we can put

$$(\mathcal{H}_D)_{\text{equiv}} = \mathcal{H}_S = D(\underset{\sim}{S}_z^2 - \underset{\sim}{S}^2/3) + E(\underset{\sim}{S}_x^2 - \underset{\sim}{S}_y^2) . \qquad (a.4)$$

We can demonstrate the above assertions in a somewhat more formal manner. Let θ denote the time inversion operator. Since θ commutes with $\mathcal{H}_D$,

$$\theta \mathcal{H}_D = \mathcal{H}_D \theta \; ; \; \theta \mathcal{H}_D \theta = \mathcal{H}_D . \qquad (a.5)$$

We use the fact that $\theta^{-1} = \theta$ for a 2n electron system (35). The equivalent operator $(\mathcal{H}_D)_{\text{equiv}}$ must also satisfy the relationship equation a.5. We examine the transformation properties of one of the 9 linear operators appearing in equation a.2; remaining operators can be handled in an analogous manner.

The time inversion operator, θ, can be written as (35):

$$\theta = \prod_{j=1}^{2n} \sigma_{jy} K . \qquad (a.6)$$

K is an operator complexing all terms to its right. σ_{jy} denotes the y component Pauli spin matrix of electron j, $\sigma_{jy} = \begin{pmatrix} 0 & -i \\ i & 0 \end{pmatrix}_j$.
We have

$$\theta S_z^2 \theta = \left(\prod_j \sigma_{jy}\right)\left(1/2 \sum_\ell \sigma_{\ell z}\right)^2 \left(\prod_m \sigma_{my}\right)^* . \qquad (a.7)$$

Since $\sigma_{\ell z}^2 = \begin{pmatrix} 1 & 0 \\ 0 & 1 \end{pmatrix}_\ell$ commutes with θ, and $\theta^2 = 1$, we need only examine terms like $1/2 \sum_{\ell > k} \sigma_{\ell z} \sigma_{kz}$. We obtain

$$\theta S_z^2 \theta = 1/4 \sum_\ell \sigma_{\ell z}^2 + 1/2 \sum_{\ell > k} \sigma_{\ell y} \sigma_{ky} \sigma_{\ell z} \sigma_{kz} \sigma_{\ell y}^* \sigma_{ky}^* ; \qquad (a.8)$$

$$= 1/4 \sum_\ell \sigma_{\ell z}^2 + 1/2 \sum_{\ell > k} (\sigma_{\ell y} \sigma_{\ell z} \sigma_{\ell y}^*)(\sigma_{ky} \sigma_{kz} \sigma_{ky}^*) ;$$

$$= 1/4 \sum_\ell \sigma_{\ell z}^2 + 1/2 \sum_{\ell > k} \sigma_{\ell z} \sigma_{kz} = S_z^2 .$$

Proceeding in this fashion, we find that $\mathcal{H}_D$ is "equivalent" to $\mathcal{H}_S$.

b. Time-Reversal Degeneracies

We use here a theorem proved by Herring (20); namely, the condition for a time-reversal band degeneracy to occur when $\hat{k} = \hat{k}'$ is that

$$\sum_{Q_o} X(\underset{\sim}{Q}_o^2) = o \text{ or } -g \,. \qquad (b.1)$$

$\underset{\sim}{Q}_o$ is a space group symmetry operator that takes $\hat{k}'$ into $-\hat{k}' + \hat{K}_q$. $\hat{K}_q$ is an arbitrary lattice vector in reciprocal lattice space. ($\hat{K}_q$ may be zero, of course.) $\underset{\sim}{Q}_o^2$ is consequently an operator belonging to the group of the k' vector, $G^{k'}$. (In the text we denoted such an operator by $\{\beta | \hat{t}\}$, equation 27.) $X(\underset{\sim}{Q}_o^2)$ is the trace of $\underset{\sim}{Q}_o^2$ in the irreducible representation of $G^{k'}$. The sum is over all distinct $\underset{\sim}{Q}_o$'s. (Only one distinct $\underset{\sim}{Q}_o$, $\bar{\underset{\sim}{Q}}_o$, is assigned to the set of operators obtained by multiplying $\bar{\underset{\sim}{Q}}_o$ by all arbitrary lattice translation symmetry operators despite the fact that all members of this set take $\hat{k}'$ into $-\hat{k}'$ or its equivalent.) The trace must be o or -g for a degeneracy to occur. g is the order of the irreducible representation of $G^{\hat{k}'}$.

Let us now consider the lines $\hat{k}^{(1)}$ and $\hat{k}^{(2)}$ (eq. 26).

Take

$$\hat{k}^{(1)} = 1/2\, \hat{b}_2 + K_3 \hat{b}_3 \,. \qquad (b.2)$$

The only space group operators that take $\hat{k}^{(1)}$ into $-\hat{k}^{(1)}$ or its equivalent are the glide plane operator $\{\sigma_n | \hat{a}/2\}$ and the inversion operator $\{I | 0\}$. [E.g., reflect $\hat{k}$ through the glide plane to give

$$\{\sigma_n | \hat{a}/2\}\ \hat{k}^{(1)} = \sigma_n \hat{k}^{(1)} = 1/2\, \hat{b}_2 - K_3 \hat{b}_3 = -\hat{k}^{(1)} + \hat{K}_q \,. \qquad (b.3)$$

(The glide plane is perpendicular to $\hat{b}_3$). $\hat{K}_q$ is $\hat{b}_2$.]

Setting $\{\sigma_n | \hat{a}/2\} = \underset{\sim}{Q}_{o1}$ and $\{I | 0\} = \underset{\sim}{Q}_{o2}$, we have

$$\underset{\sim}{Q}_{o1}^2 = \{\sigma_n | \hat{a}/2\}^2 = \underset{\sim}{T}(\hat{a}) \;;\; \underset{\sim}{Q}_{o2}^2 = \{I | 0\}^2 = \underset{\sim}{T}(0) \,. \qquad (b.4)$$

$\underset{\sim}{T}(\hat{R}_n)$ belongs to the translation group and represents a translation of the crystal lattice through a vector, $\hat{R}_n$. Furthermore

$$X(\underset{\sim}{Q}_{o1}^{2}) = X[\underset{\sim}{T}(\hat{a})] = e^{i2\pi\hat{k}^{(1)}\cdot\hat{a}} = -1;$$
$$X(\underset{\sim}{Q}_{o2}^{2}) = X[\underset{\sim}{T}(0)] = 1; \quad \sum_{Q_o} X(\underset{\sim}{Q}_{o}^{2}) = 0. \qquad \text{(b.5)}$$

Q.E.D.

A similar proof applies to the equivalent line $-1/2\,\hat{b}_2 + K_3\hat{b}_3$, and to $\hat{k}^{(2)}$. The only other degenerate lines in the monoclinic system lie in the planes $K_3 = \pm 1/2$.

We now proceed to show that there are time-reversal degeneracies at all points of $K_3 = (\pm)\,1/2$. Consider the arbitrary vector, $\hat{k}^b$ that terminates in the boundary plane, $K_3 = 1/2$:

$$\hat{k}^b = K_1\hat{b}_1 + K_2\hat{b}_2 + \hat{b}_3/2. \qquad \text{(b.6)}$$

The only operators that take $\hat{k}^b$ into $-\hat{k}^b$ or its equivalent are the screw axis operator $\{\underset{\sim}{C}_2 | \hat{b}/2\} = \underset{\sim}{Q}_{o1}$, and the inversion operator $\{\underset{\sim}{I} | 0\} = \underset{\sim}{Q}_{o2}$. We have

$$\{\underset{\sim}{C}_2 | \hat{b}/2\}\hat{k}^b = \underset{\sim}{C}_2\hat{k}^b = -K_1\hat{b}_1 - K_2\hat{b}_2 + \hat{b}_3/2 = -\hat{k}^b + (\hat{K}_q = \hat{b}); \qquad \text{(b.7)}$$
$$\{\underset{\sim}{I} | 0\}\hat{k}^b = -\hat{k}^b;$$

and

$$X(\underset{\sim}{Q}_{o1}^{2}) = X[\underset{\sim}{T}(\hat{b})] = e^{i2\pi\hat{k}^b\cdot\hat{b}} = -1;$$
$$X(\underset{\sim}{Q}_{o2}^{2}) = X[\underset{\sim}{T}(0)] = 1; \qquad \text{(b.8)}$$
$$\sum_{Q_o} X(Q_o^{2}) = 0.$$

Q.E.D.

The above proof holds for any crystal system having a screw axis and an inversion operation.

c. Accidental Degeneracies

We designate the three basic primitive translations of the benzene orthorhombic crystal as

$$\begin{aligned} \hat{t}_1 &= \hat{c} = c\hat{e}_x = \{c,o,o\} ; \\ \hat{t}_2 &= \hat{a} = a\hat{e}_y = \{o,a,o\} ; \\ \hat{t}_3 &= \hat{b} = b\hat{e}_z = \{o,o,b\} ; \end{aligned} \tag{c.1}$$

and the three basic primitive translations in $\hat{k}$ space as

$$\hat{b}_1 = c^{-1}\hat{e}_x \; ; \; \hat{b}_2 = a^{-1}\hat{e}_y \; ; \; \hat{b}_3 = c^{-1}\hat{e}_z . \tag{c.2}$$

There are four molecular sites, I, II, III, IV, per unit cell at the positions o,o,o ; $c/2,a/2,o$; $c/2,o,b/2$; $o,a/2,b/2$, respectively. Let us assume only nearest neighbor interactions. The eigenstates, $|\hat{k}_\ell m>$, are given by equation 29. The corresponding energies, $\mathcal{E}_\ell$, are

$$\begin{aligned} \mathcal{E}_1 &= S + f_1(\hat{h}) + f_2(\hat{h}) + f_3(\hat{h}) ; \\ \mathcal{E}_2 &= S + f_1(\hat{h}) - f_2(\hat{h}) - f_3(\hat{h}) ; \\ \mathcal{E}_3 &= S - f_1(\hat{h}) - f_2(\hat{h}) + f_3(\hat{h}) ; \\ \mathcal{E}_4 &= S - f_1(\hat{h}) + f_2(\hat{h}) - f_3(\hat{h}) . \end{aligned} \tag{c.3}$$

S is a constant and the $f_1(\hat{h})$'s are defined as

$$\begin{aligned} f_1(\hat{h}) &= f_1 \cos \pi\hat{h}\cdot\hat{c} \cos \pi\hat{h}\cdot\hat{a} ; \\ f_2(\hat{h}) &= f_2 \cos \pi\hat{h}\cdot\hat{c} \cos \pi\hat{h}\cdot\hat{b} ; \\ f_3(\hat{h}) &= f_3 \cos \pi\hat{h}\cdot\hat{a} \cos \pi\hat{k}\cdot\hat{b} ; \end{aligned} \tag{c.4}$$

where

$$\begin{aligned} f_1 &= <o\,I\,m|\,\mathcal{H}_f\,|o\,II\,m> ; \\ f_2 &= <o\,I\,m|\,\mathcal{H}_f\,|o\,III\,m> ; \\ f_3 &= <o\,I\,m|\,\mathcal{H}_f\,|o\,IV\,m> . \end{aligned} \tag{c.5}$$

Let us assume for the sake of specificity that the ordering of the band energies at $\hat{k} = 0$ is $\mathcal{E}_1 < \mathcal{E}_4 < \mathcal{E}_2 < \mathcal{E}_3$. Consider the vector $\hat{k} = K_1 \hat{b}_1 + K_2 \hat{b}_2$ which lies in the xy symmetry plane. Set $K_2/K_1 = \delta$, a constant less than 1. Allow K_1 to take on all values between 0 and $\pm 1/2$. We thus proceed along a ray, i.e., a straight line that terminates on the boundary planes $K_1 = \pm 1/2$ where time-reversal symmetry requires a pairwise degeneracy of the bands. Using equations c.3, c.4, we see that

$$\begin{aligned} \mathcal{E}_1 (K_1 = \pm 1/2) &= \mathcal{E}_3 (K_1 = \pm 1/2) = S + f_3 \cos\left(\frac{\pi\delta}{2}\right); \\ \mathcal{E}_2 (K_1 = \pm 1/2) &= \mathcal{E}_4 (K_1 = \pm 1/2) = S - f_3 \cos\left(\frac{\pi\delta}{2}\right). \end{aligned} \tag{c.6}$$

Furthermore, the ordering at $\hat{k} = 0$ requires that $\mathcal{E}_1(1/2) < \mathcal{E}_2(1/2)$. We present below a schematic plot of energy vs. K_1 for an arbitrary ray in the xy plane.

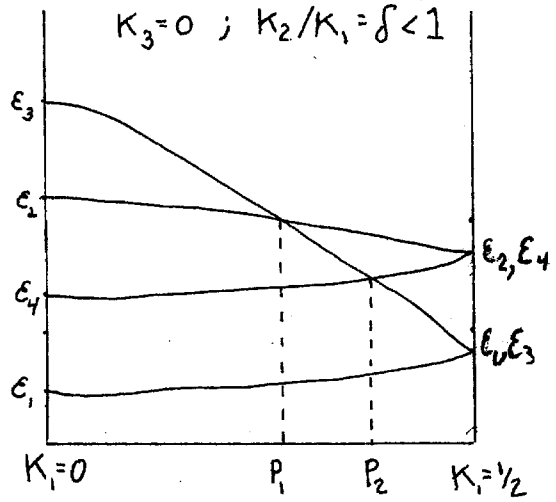

(c.7)

Accidental degeneracies occur at $K_1 = P_1, P_2$. If one considers other values of δ, other planes, and other points of the BZ one finds curves and surfaces of accidental degeneracies.

What happens when we take into account non-nearest neighbor interactions between sites? The eigenstates $|\hat{k}_\ell m>$, and eigenenergies $\mathcal{E}_\ell$, take on a more complicated form. Pairwise degeneracies still

occur at $K_1 = \pm 1/2$ where $\mathcal{E}_1 = \mathcal{E}_3$ and $\mathcal{E}_2 = \mathcal{E}_4$. Since one expects the nearest neighbor interactions to dominate over the non-nearest neighbor interactions, the ordering at $\hat{k} = 0$ is assumed unchanged. (If the ordering is changed our arguments below would have to be modified. This can be done in a straightforward manner.) There is now, however, no crossing of bands 2 and 3 (eq. c.7). This occurs because bands 2 and 3 have the same symmetry, and, consequently, by the well-known "non-crossing" rule (36) we cannot make them cross by varying only one parameter, namely, K_1*. Our new energy diagram becomes

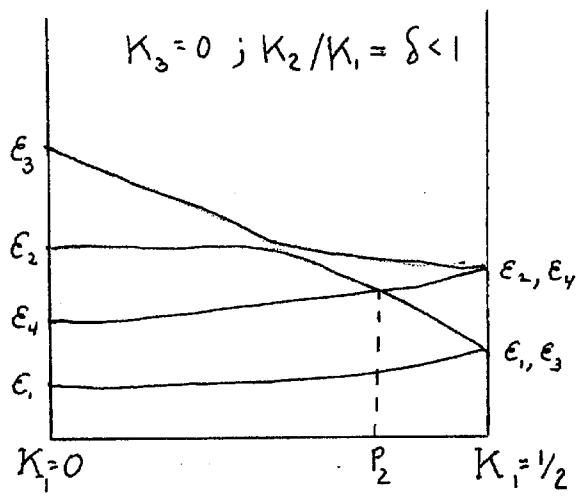

(c.8)

If one considers other energy orderings at $\hat{k} = 0$, other values of δ, other planes and points in the BZ, one can show by arguments analogous to the above that the overall effect of the nonneighbor interactions is to decrease the number of crossing points leaving only crossing points on

---

*The xy symmetry plane is left invariant by the C_s point group which consists of the identity operation and the reflection operation through the xy plane. The $|\hat{k}_\ell m>$'s serve as a basis for an irreducible representation of this group. We find that if (1) the lowest triplet is taken as a $^3B_{1u}$ state (i.e., changes sign upon inversion through the benzene molecule center of symmetry), and (2) the site functions are defined so that when $\hat{k} = 0$, $|o\ I\ m> \longleftrightarrow |o\ III\ m>$ and

axes of symmetry and crossing curves in planes of symmetry. However, if the magnitude of the non-nearest neighbor interactions is small compared with the spin-spin interactions, we have further curves and surfaces of "effective" degeneracies that extend through the BZ.

$|o\ II\ m> \longleftrightarrow |o\ IV\ m>$ upon a screw axis rotation $\{c_2(z) \mid \hat{b}/2\}$ parallel to $\hat{b}$, then $|\hat{k}_3 m>$, $|\hat{k}_2 m>$ go into $-|\hat{k}_3 m>$, $-|\hat{k}_2 m>$ respectively upon reflection through the xy plane. (The states $|\hat{k}_1 m>$, $|\hat{k}_4 m>$ are invariant to the reflection operation.)

d. Diffusing Excitons : Intermediate Field Case ($g_e|\beta|H_o = 3D$)

The oscillatory field, $H_1 \cos \omega t$, is applied in the x-direction. The rate of energy absorption by the sample is

$$P(\omega) = \frac{N}{V} \, 2H_1^{\,2} \omega \, g_e^2 \beta^{\,2} \, (KT)^{-1} \, \mathcal{K}(\omega). \tag{d.1}$$

$\mathcal{K}(\omega)$ is unitless and is plotted in Figures

$$\mathcal{K}(\omega) = \frac{\theta_4\theta_3 + \theta_2\theta_1}{(\theta_3)^2 + (\theta_1)^2} \, . \tag{d.2}$$

$$\theta_4 = \bar{\omega}_e \left[\begin{array}{l} 1.217 \times 10^4 \, \bar{\omega}^8 - (4.056 \times 10^4 \, \bar{\omega}_e^{\,2} + 1.391 \times 10^6) \bar{\omega}^6 \\ + (1.217 \times 10^4 \, \bar{\omega}_e^{\,4} + 1.793 \times 10^6 \bar{\omega}_e^{\,2} - 2.723 \times 10^8) \bar{\omega}^4 \\ - (5.475 \times 10^5 \, \bar{\omega}_e^{\,4} - 1.808 \times 10^8 \, \bar{\omega}_e^{\,2} - 2.262 \times 10^{10}) \bar{\omega}^2 \\ - (2.395 \times 10^7 \, \bar{\omega}_e^{\,4} + 6.849 \times 10^9 \, \bar{\omega}_e^{\,2}) \end{array} \right] .$$

$\bar{\omega}_e = 2\tau^{-1}$ (expressed in units of $\bar{D}\sqrt{2}/4$) (d.3)

$\bar{\omega} = \omega$ " " " " "

$$\theta_3 = \bar{\omega} \left[\begin{array}{l} - 1.69 \times 10^2 \, \bar{\omega}^{10} + (2.535 \times 10^3 \, \bar{\omega}_e^{\,2} + 4.462 \times 10^4) \bar{\omega}^8 \\ - (2.535 \times 10^3 \, \bar{\omega}_e^{\,4} + 3.870 \times 10^5 \, \bar{\omega}_e^{\,2} - 5.451 \times 10^6) \bar{\omega}^6 \\ + (1.69 \times 10^2 \, \bar{\omega}_e^{\,6} + 2.873 \times 10^5 \, \bar{\omega}_e^{\,4} - 1.245 \times 10^7 \, \bar{\omega}_e^{\,2} \\ \qquad - 1.284 \times 10^9) \bar{\omega}^4 \\ - (2.467 \times 10^4 \, \bar{\omega}_e^{\,6} - 1.109 \times 10^5 \, \bar{\omega}_e^{\,4} - 3.807 \times 10^9 \, \bar{\omega}_e^{\,2} \\ \qquad - 5.090 \times 10^{10}) \bar{\omega}^2 \\ + (8.761 \times 10^5 \, \bar{\omega}_e^{\,6} - 5.131 \times 10^8 \, \bar{\omega}_e^{\,4} - 1.313 \times 10^{11} \, \bar{\omega}_e^{\,2}) \end{array} \right] \tag{d.4}$$

$$\theta_2 = \bar{\omega} \left[\begin{array}{l} 2.028 \times 10^3 \, \bar{\omega}^8 - (3.042 \times 10^4 \, \bar{\omega}_e^{\,2} + 3.569 \times 10^5) \bar{\omega}^6 \\ + (3.042 \times 10^4 \, \bar{\omega}_e^{\,4} + 2.142 \times 10^6 \, \bar{\omega}_e^{\,2} - 9.141 \times 10^7) \bar{\omega}^4 \\ - (2.028 \times 10^3 \, \bar{\omega}_e^{\,6} + 1.087 \times 10^6 \, \bar{\omega}_e^{\,4} - 3.041 \times 10^8 \, \bar{\omega}_e^{\,2} \\ \qquad - 7.899 \times 10^9) \bar{\omega}^2 \\ + (1.460 \times 10^5 \, \bar{\omega}_e^{\,6} - 8.156 \times 10^7 \, \bar{\omega}_e^{\,4} - 2.157 \times 10^{10} \, \bar{\omega}_e^{\,2}) \end{array} \right] \tag{d.5}$$

$$\theta_1 = \bar{\omega}_e \left[\begin{array}{l} 1.014 \times 10^3 \bar{\omega}^{10} - (3.380 \times 10^3 \bar{\omega}_e^{\,2} + 2.021 \times 10^5)\bar{\omega}^8 \\ + (1.014 \times 10^3 \bar{\omega}_e^{\,4} + 4.191 \times 10^5 \bar{\omega}_e^{\,2} - 1.430 \times 10^7)\bar{\omega}^6 \\ - (1.224 \times 10^5 \bar{\omega}_e^{\,4} - 4.195 \times 10^6 \bar{\omega}_e^{\,2} - 3.712 \times 10^9)\bar{\omega}^4 \\ + (1.359 \times 10^6 \bar{\omega}_e^{\,4} - 1.748 \times 10^9 \bar{\omega}_e^{\,2} - 1.417 \times 10^{11})\bar{\omega}^2 \\ + (1.437 \times 10^8 \bar{\omega}_e^{\,4} + 4.055 \times 10^{10} \bar{\omega}_e^{\,2}) \end{array} \right] \quad \text{(d.6)}$$

In the limit of infinitely fast transfer we need keep only the highest power terms in $\bar{\omega}_e$ that appear in the θ_i expressions; in the limit of infinitesimally slow transfer, we keep only the lowest power terms. The resonance peak positions in the monomer and dimer limits are obtained by setting the dominant terms of θ_3 equal to zero and solving for $\bar{\omega}$.

PROPOSITION I

The lowest excited electronic states of many N-heterocyclic molecules are believed to be n, π^* states (1). These states are obtained by exciting one of the "lone-pair" electrons from a non-bonding (n) orbital centered on the nitrogen atom to the lowest unfilled anti-bonding orbital (π^*) of the polyatomic molecule. The n orbital is thought to be a sp^2 hybridized orbital, and is symmetric with respect to reflection in the molecular plane, while the π^* orbital is antisymmetric with respect to the reflection. The azines and diazines are examples of such compounds:

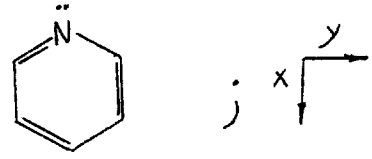

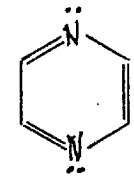

(1)

pyridine

pyrazine
(ortho-diazine)

Two somewhat different descriptions of the n, π^* states have been advanced. We refer to the first description, proposed by El-Sayed and Robinson after a detailed examination of the diazines spectra (2), as the "localized" model, and we refer to the second as the "delocalized" model (3, 4). In the "localized" model the excited electron is tightly bound to the positive hole it leaves behind. The π^* orbital is regarded primarily as a $2p_z$ orbital perpendicular to the molecular plane and

centered on the nitrogen atom. In the "delocalized" model, the excited electron is distributed over a number of atoms: the π^* orbital is made up of a linear combination of a number of carbon and nitrogen $2p_z$ orbitals. (These "delocalized" orbitals can be calculated by the method of Coulson and Longuet-Higgins (5).) The experimental data appear to favor the "delocalized" model (4).

We propose that electron spin resonance (ESR) studies of paramagnetic triplet states of the N-heterocyclic molecules would be particularly useful.† An analysis of the fine and hyperfine structure would give detailed information about the triplet state wave functions. The extent of delocalization of the excited electron, and the degree of hybridization of the n orbital could be determined. Experiments can be performed by "doping" a host crystal with an N-heterocyclic compound and exciting the guest molecules to the triplet state. A detectable concentration of triplets is expected for most of the mixed crystal systems.

In the diazines there are two nondegenerate n, π^* triplet states: the antisymmetric and symmetric states.* Theoretical calculations (2) suggest that the energy separation between the symmetric and antisymmetric triplets are ~ 25, 275, 5,500 cm^{-1} for the para-,

---

* An electron can be promoted to the π^* orbital from either one of the two nitrogen atoms, giving two degenerate n, π^* states. Electron-electron interactions, however, remove the degeneracies and give a symmetric and an antisymmetric state. In general, the number of low-lying n, π^* states is equal to the number of nitrogen atoms.

† Mr. A. Dubin of the California Institute of Technology has begun a number of preliminary experiments.

meta-, ortho-diazines, respectively. (The uncertainty in these values may be as large as a factor of two.) If a detectable concentration of triplets can be produced by illumination, both the symmetric and antisymmetric states of the para-, meta-diazines should be populated at room temperature. It is not generally possible to detect both these states by optical means. Optical transitions from the antisymmetric triplet state to the ground singlet state is expected to be weak because it is doubly "forbidden": it is "forbidden" spatially, and is "forbidden" because of spin multiplicity differences. In ESR different selection rules hold, and resonance absorptions are possible for both these triplet states. A study of spectra intensity as a function of temperature would give an estimate of the splitting between the symmetric and antisymmetric triplet states of the para-, meta-diazines.

If the "localized" model is correct, one can expect very large fine fields arising from the spin dipolar interaction of the two unpaired electrons centered mainly on the nitrogen atom (one in an n orbital; the other in a $2p_z$ orbital). If the "delocalization" model is correct, the fine fields are now expected to be somewhat smaller since one of the unpaired electrons is distributed over a number of atoms. Below we carry out an estimation of the fine field of pyrazine.

ILLUSTRATION

The triplet n,π* states can be approximated as

$$|{}^{(-)}_{+}\, M\rangle = \frac{|\underset{\sim}{A}\, n_a \pi^* M\rangle \pm |\underset{\sim}{A}\, n_b \pi^* M\rangle}{\sqrt{2}} \qquad (2)$$

$|{}^{(-)}_{+}\, M\rangle$ is a symmetric (antisymmetric) triplet state of spin component M = 1, 0, -1. $\underset{\sim}{A}$ is the antisymmetrization operator; $|\underset{\sim}{A}\, n_a \pi^* M\rangle$ denotes a triplet state of spin component M obtained by exciting an electron from an n orbital on nitrogen a into the π^* orbital. For specificity, consider the para-diazine, pyrazine. Its spin-spin interaction can be represented as $D(S_z^2 - S^2/3) + E(S_x^2 - S_y^2)$. (The cartesian axes are shown in equation 1.) As a first approximation to D and E we assume that the predominant spin-spin interaction comes from the unpaired electron in the n orbitals interacting with the unpaired spin density, $\rho/2$, centered on each of the two nitrogen atoms. This is a very good approximation for the "localized" model and is reasonably adequate for the "delocalized" model, provided $\rho > 0.2$. We obtain the following expressions (6) for D and E for both the symmetric and antisymmetric cases:

$$D_{(\text{in cm}^{-1})} = \frac{3 g_e^2 \beta^2 \rho}{4hc} \langle \psi | \frac{1}{r_{12}^3} \left(1 - \frac{3 z_{12}^2}{r_{12}^2}\right) | \psi \rangle;$$

$$E = -\frac{3 g_e^2 \beta^2 \rho}{4hc} \langle \psi | \frac{x_{12}^2 - y_{12}^2}{r_{12}^5} | \psi \rangle \quad . \qquad (3)$$

$$\Psi = \frac{n(1)\, p_z(2) - p_z(1)\, n(2)}{\sqrt{2}} \quad .$$

Both the n orbital and the $2p_z$ orbital are centered on the same nitrogen atom. $n(i)$ can be expressed as:

$$n(i) = a\, s(i) + b\, p_x(i) \quad . \qquad (4)$$

$$(b = \sqrt{1 - a^2})$$

$s(i)$ denotes a 2s orbital; $p_x(i)$; a $2p_x$ orbital.

(If sp^2 hybridization is assumed, a = 1/3. Equation 3 can be evaluated by the method of Hameka (7). We use Slater atomic orbitals. The calculation is fairly laborious, and we only quote our results.

$$D = \frac{-3g_e^3\beta^2\rho}{4hc} \frac{7Z^3}{1,920} \frac{1}{a_o^3} \left(a^2 + b^2/2\right) \quad cm^{-1};$$

$$E = \frac{-3g_e^2\beta^2\rho}{4hc} \frac{7Z^3}{1,920} \frac{1}{a_o^3} \left(b^2/2\right) \quad cm^{-1} . \qquad (5)$$

Z is the effective charge of the Slater 2s and 2p orbitals, and is approximately 3.9. a_o is the Bohr radius, 0.528×10^{-8} cm. We note that E is independent of the 2s orbital. (E is a measure of the asymmetry about the z axis. Clearly the 2s state does not contribute to this asymmetry.) The ratio $D/E = \frac{1 + a^2}{1 - a^2}$ determines the degree of hyrbidization of the n orbital.

For sp^2 hybridization we obtain the following values for D and E:

$$D = -1.275\ \rho\ cm^{-1}\ ;$$
$$E = D/2 = -0.6375\ \rho\ cm^{-1}\ . \qquad (6)$$

Figure I is a plot of energy vs. external field, $\hat{H}_o$. $\hat{H}_o$ is taken parallel to the z axis. We have set $\rho = 1$; i.e., we assumed tight bonding. Experiments are generally performed at X-band (~9,500 Mc). We note from Figure I that the tight bonding approximation gives only one resonance at ~7,800 gauss. These results contrast strongly with those from aromatic molecules like naphthalene. There D and E are approximately $0.1\ cm^{-1}$ and $-0.01\ cm^{-1}$, respectively; three resonances can be detected (8).

If the "localized" model is correct, we expect our values for D and E to be correct to within 1 or 2%.† The symmetric and antisymmetric states will have fine fields that differ also by a percent or two; consequently their spectra can be resolved. If the "delocalized" model is more appropriate, it may be necessary to modify our treatment in order to obtain greater accuracy. If the excited electron in the * orbital is more or less evenly distributed on all atoms of the ring, our estimate of D and E (eq. 5) are correct to within 10%.† Again the antisymmetric and symmetric triplet states will have fine fields that differ by the same amount.

†Our estimates of accuracy are somewhat optimistic. We have assumed that Slater orbitals can be used with little error, and that n (i) is accurately given by equation (4).

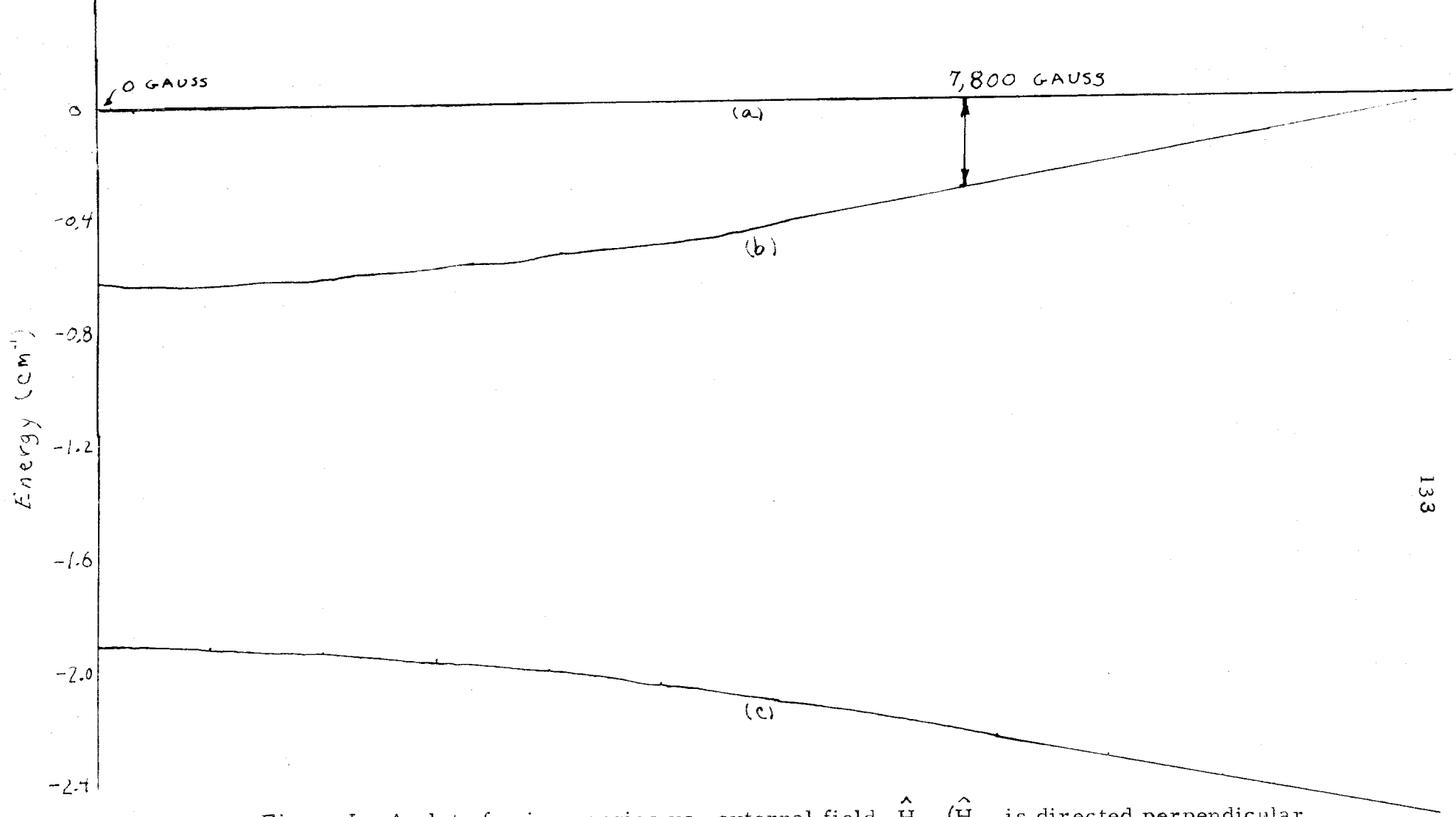

Figure I. A plot of spin energies vs. external field, $\hat{H}_o$ ($\hat{H}_o$ is directed perpendicular to the molecular plane). Curves (a), (b), (c) refer to the spin states $|0\rangle$, $\frac{|1\rangle - |\bar{1}\rangle}{\sqrt{2}}$ and $\frac{|1\rangle + |\bar{1}\rangle}{\sqrt{2}}$, respectively. ρ is set equal to 1. Only one allowed transition occurs at 9,500 Mc ($\sim 0.33\ cm^{-1}$).

REFERENCES

1. M. Kasha, Radiation Research, Supplement 2, 243 (1960).
2. M. A. El-Sayed and G. W. Robinson, J. Chem. Phys., 34, 1840(L) (1961); J. Chem. Phys., 35, 1896(L) (1961).
3. L. Goodman and R. W. Harrell, J. Chem. Phys., 30, 1131 (1959).
4. D. R. Kearns and M. A. El-Bayoumi, to be published.
5. C. A. Coulson and H. C. Longuet-Higgins, Proc. Roy. Soc. (London), A191, 39 (1947).
6. W. Moffitt and M. Gouterman, J. Chem. Phys., 30, 1107 (1959).
7. H. F. Hameka, J. Chem. Phys., 31, 315 (1959).
8. C. A. Hutchison, Jr., and B. W. Mangum, J. Chem. Phys., 34, 908 (1961).

PROPOSITION II

Numerous efforts, all unsuccessful, have been made to obtain phosphorescence spectra from pure molecular crystals. The phosphorescence spectra that have been obtained are generally due to impurities in their triplet state. We propose that triplet-triplet self annihilation is a significant non-radiative depopulation mechanism. The most plausible annihilation route being:*

$$2\,T_o \longrightarrow T_i + S_o \quad , \tag{1}$$

T_o denotes the lowest lying triplet state; T_i, an excited triplet; S_o, the ground singlet.

Fluorescence emission generally occurs with an exponential decay from the first excited singlet, S_1. The fluorescence lifetime is between 1×10^{-10} and 1×10^{-7} secs. Blake and McClure (1) have observed a nonexponential delayed fluorescence (emission occurs $\gtrsim 10^{-3}$ secs. from the time of excitation) in molecular crystals of naphthalene and phenanthrene. We propose that triplet annihilation may be responsible for the delayed fluorescence. The decay scheme being:

$$\begin{aligned} 2\,T_o &\longrightarrow T_i + S_o \ ; \\ \gamma\,T_i &\longrightarrow \gamma\,S_j \ ; \\ S_j &\longrightarrow S_1 \ ; \\ S_1 &\longrightarrow S_o \ . \end{aligned} \tag{2}$$

*We use the phrase annihilation somewhat loosely. It is perhaps more appropriate to regard the triplet-triplet quenching as a modified Auger process.

S_j is an excited singlet. γ is a constant less than one, and denotes the fraction of the T_i state that undergo a radiationless transition to S_j. The balance of the T_i states return to the lowest triplet, T_o, by a series of nonradiative transitions.

The arguments in support of this two part proposal briefly are as follows: The triplet state is believed to be populated indirectly by an intersystem radiationless crossing over from the singlet system to the triplet system (2). Experiments are generally conducted so that most of the radiationless transitions occur from the first excited singlet S_1 to the triplet system. Conceivably, this intersystem crossing may be reduced in the pure crystal to the extent that no significant triplet state population is built up. We know of no mechanism that could be responsible for such a situation. Arguments have been advanced that there may be a $\hat{k}$-selection rule because of crystal exciton bands (3). A closer examination of this suggestion fails, however, to reveal any such selection rule.

Although there is no unambiguous experimental evidence that rules out a reduced intersystem crossing in the pure crystal, we feel fairly confident that the explanation lies elsewhere. Recently excitation migration has been studied in $C_{10}D_8$ crystals doped with $C_{10}H_8$ (4), and C_6D_6 doped with C_6H_6 (5).* These experiments strongly suggest that (1) the intersystem crossings are relatively unaffected by the

* The undeuterated compound acts as an "impurity" trap.

crystalline state; (2) very rapid triplet excitation transfer occurs in the pure crystal (transfer times of the order of 10^{-10} or 10^{-11} secs.). Since the radiative lifetime for the $T_o \rightarrow S_o$ transition is of the order of 10 secs., a triplet transfer time of the order of 10^{-10} secs. provides ample opportunity for the triplet excitation to (1) fall into impurity or lattice defect traps; (2) "collide" with other triplet excitations if the trap depths or concentrations are sufficiently small. The decrease in phosphorescent yield with increasing crystal purity can be explained in two ways:

(1) When the impurity concentration is low relative to the defect concentration, the excitation migrates to defect sites. If the molecules at these defect sites are strongly coupled to the lattice, non-radiative transitions can occur directly from T_o to S_o. Since the non-radiative lifetime for triplet state aromatic molecules in the crystalline state (e.g., naphthalene in durene) are normally of the order of several seconds, these defect sites must give non-radiative $T_o \rightsquigarrow S_o$ lifetimes of the order of $\gtrsim 10^{-3}$ secs. to explain the virtual absence of any detectable phosphorescence or triplet state paramagnetism in pure aromatic crystals.* It is not clear why such strong coupling should occur. Recent experiments (5) indicate that the $T_o \rightsquigarrow S_o$ process at defect sites is most probably not the reason for the absence of phosphorescence (we discuss this further below). (If the defect site

---

* We assume radiative lifetimes of the order of 10 secs. or larger.

mechanism is important one would also expect it to be more important in polycrystalline or fractured crystals. The author is not aware of any significant differences in phosphorescence yields between single crystal and polycrystalline samples. If the defect mechanism is important, it may be possible to raise the temperature sufficiently so that the excitation escapes the trap. This would be possible to do for some aromatic crystals if the trap depth is not much greater than 200 cm^{-1}.)

(2) The reduced phosphorescence may be due to self-quenching; i.e., interactions between triplet state molecules may be responsible for an Auger-like annihilation. We indeed find this to be highly probable.

Consider a double excitation system consisting of two triplets, T_o. This system is degenerate with a large number of other vibronic states into which it can decay. In Figure I we illustrate two possible annihilation schemes. For the sake of specificity we have used the energy diagram of benzene.* All levels refer to the approximate position of the lowest vibrational level of the excited states relative to the lowest vibrational level of the ground singlet, S_o. The dotted levels correspond to states that have not been observed experimentally. We have used the theoretical values of Pariser (6). The positions of the

* The energy diagram does not include excited states obtained by promoting an electron from the σ system to the π system; nor does it include ionization states.

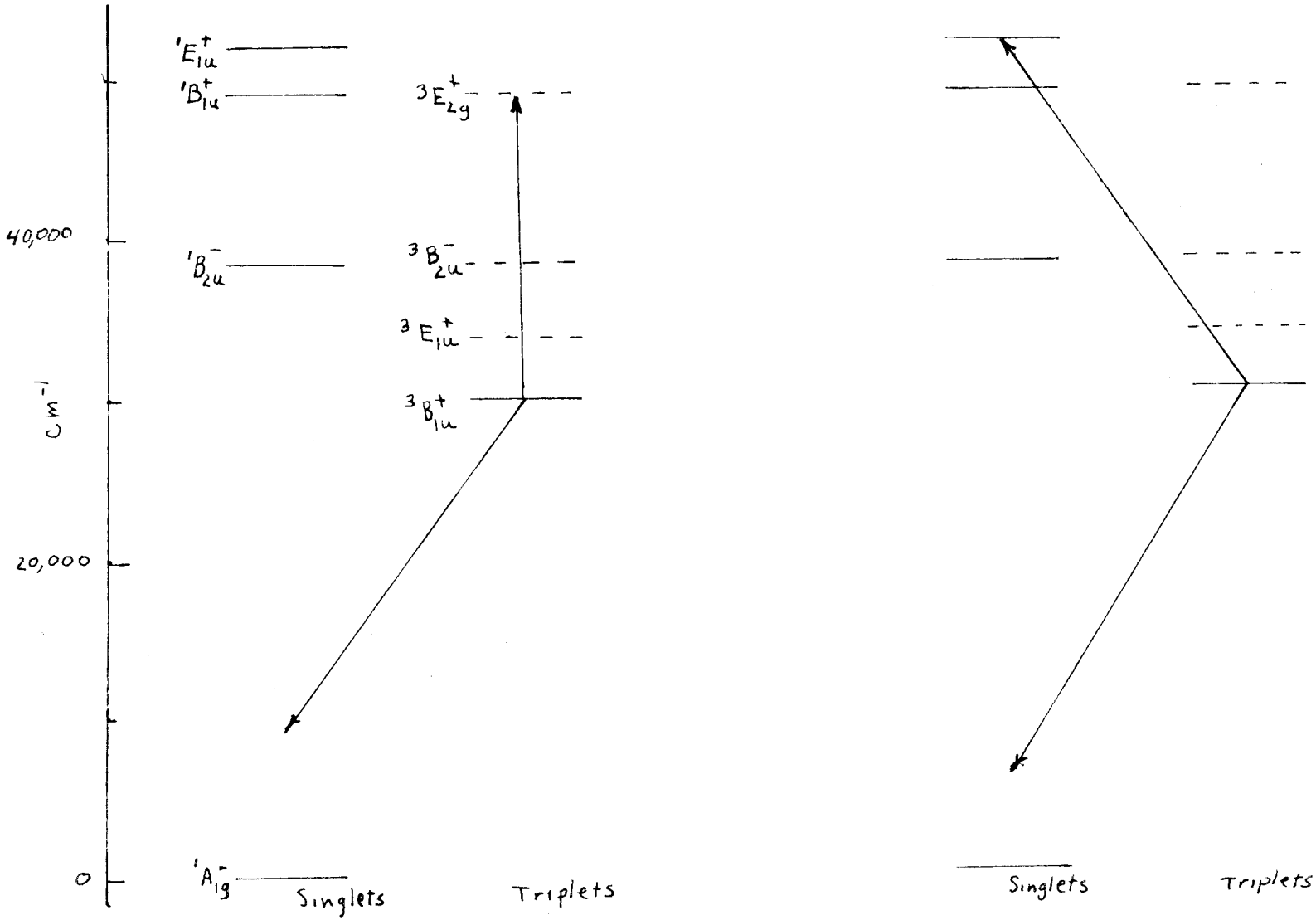

Figure I. The electronic levels of benzene.

excited triplets relative to T_o may well be underestimated by 5,000 cm^{-1}. The higher vibrational levels are not shown explicitly. At $\sim$ 4,000 cm^{-1} above the lowest vibrational level, we have essentially a continuum of excited vibrational levels.

The annihilation process conserves energy. We easily see from Figure I that there are a large number of other final vibronic levels into which our double excitation system could decay. Below we show that the $2\,T_o \longrightarrow T_i + S_o$ mode dominates the $2\,T_o \longrightarrow S_i + S_o$ mode.

Our initial double excitation state has an energy $2E(T_o)$. We denote this state as $|0\rangle$, and a possible final state as $|f\rangle$. The energy level of the final state is not well defined because of vibrational relaxation. It is broadened by an amount $\hbar/\tau_f$ where τ_f is a vibrational relaxation time; consequently we introduce the probability distribution function $g_f(E)$ such that $g_f(E)\,dE$ denotes the probability of finding the energy of the final state between E and E + dE. First order perturbation theory gives as the average transition rate, R_{of}:

$$R_{of} = \frac{2\pi}{\hbar} \int_o^\infty g_f(E)\, P_f(E)\, dE \,. \tag{3}$$

$P_f(E)$ is the spectral distribution function:

$$|V_{of}|^2 \int \left[E - 2E\,(T_o)\right] \,. \tag{4}$$

V denotes the interaction between the two triplet molecules; $\int$ is the delta function. The transition probability is

$$R_{of} = \frac{2\pi}{\hbar} \left| V_{of} \right|^2 g_f \left[2E(T_o) \right] \sim \frac{2\pi}{\hbar^2} \tau_f \left| V_{of} \right|^2 , \qquad (5)$$

The overall transition rate is

$$R_o = \frac{2\pi}{\hbar^2} \sum_f \tau_f \left| V_{of} \right|^2 . \qquad (6)$$

The sum is over all final vibronic states having energy $2E(T_o)$.

We give equations 3-5 the following physical justification: We imagine that at time $t = 0^-$ only one excitation exists at, say, position $\hat{R}_{n_1}$ in the crystal. At time $t = 0^+$ a second triplet excitation can now be found at position $\hat{R}_{n_2}$. This second excitation may have resulted from an intersystem singlet to triplet crossing from an excited singlet state molecule at $\hat{R}_{n_2}$. This double excitation system is now in a nonstationary state; the interaction, V, between the triplet excitations induces transitions to other vibronic states, f, whose energy levels are broadened by interactions with the lattice.

We apply the Born-Oppenheimer approximation and write our states as a product of electronic and nuclear wave functions.

$$\begin{aligned} |0\rangle &= |A\ T_{on_1}\ T_{on_2}\ X_o(T_{on_1})\, X_o(T_{on_2})\rangle ; \\ |f\rangle &= |A\ T_{in_1}\ S_{on_2}\ X_{j_1}(T_{in_1})\, X_{j_2}(S_{on_2})\rangle ; \qquad (7) \\ \text{or} \quad |f'\rangle &= |A\ S_{in_1}\ S_{on_2}\ X_{r_1}(S_{in_1})\, X_{r_2}(S_{on_2})\rangle . \end{aligned}$$

A is the antisymmetrization operator. T_{on_1} denotes the lowest triplet electronic wave function at lattice site position R_{n_1}; $X_o(T_{on_1})$ denotes the o'th (ground) nuclear wave function associated with T_{on_1}. The remaining symbols have analogous interpretations.

R_o can now be represented as:

$$R_o = \frac{2\pi}{\hbar^2}\,\tau_{ave}\left\{\sum_i \left|\langle A\, T_{on_1} T_{on_2} \left| V \right| A\, T_{in_1} S_{on_2}\rangle\right|^2 G(T_i) + \sum_i \left|\langle A\, T_{on_1} T_{on_2} \left| V \right| A\, S_{in_1} S_{on_2}\rangle\right|^2 G(S_i)\right\}. \tag{8}$$

We shall use an average vibrational relaxation time, τ_{ave}, of the order of 10^{-11} secs. $G(T_i)$, $G(S_i)$ are sums of nuclear overlap factors:

$$G(T_i) = \sum_{j,j_2} \left|\langle X_o(T_{on_1})\; X_{j_1}(T_{in_1})\rangle \langle X_o(T_{on_2})\; X_{j_2}(S_{on_2})\rangle\right|^2 ;$$

$$G(S_i) = \sum_{r_1,r_2} \left|\langle X_o(T_{on_1})\; X_{r_1}(S_{in_1})\rangle \langle X_o(T_{on_2})\; X_{r_2}(S_{on_2})\rangle\right|^2 . \tag{9}$$

Because of the nuclear overlap factors, transitions will occur mainly to those states T_{i_1} and S_{i_1} having <u>electronic</u> energies somewhat less than $2E(T_o)$ relative to S_o.* In the case of benzene (Fig. I),

* If the difference in electronic energy between an excited state and S_o is $2E(T_o) - \Delta$ where Δ is less than 4,000 cm^{-1}, we are in a region where the excited vibrational levels can no longer be regarded as giving a continuum. Under such conditions it may be difficult for a decay to this state to occur without phonon participation. The triplet quenching process is now a second order process requiring that a phonon

$T_{i_1} = {}^3E_{2g}^+$ and $S_{i_1} = {}^1E_{1u}^+$. We estimate that $G(T_{i_1}) \sim G(S_{i_1})$, and has a value between 10^{-3} and 10^{-6}. (These values are consistent with the rates of radiationless transitions for the $T_o \rightsquigarrow S_o$ process that have been observed for aromatic molecules in inert matrices.)

R_o has a value in $sec.^{-1}$ given by

$$R_o = 3\times10^{-2} G\left(\left|\langle AT_{on_1} T_{on_2}|V|AT_{in_1} S_{on_2}\rangle\right|^2 + \left|\langle AT_{on_1} T_{on_2}|V|AS_{in_1} S_{on_2}\rangle\right|^2\right). \tag{10}$$

(V is measured in cm^{-1}).

We now examine the $2T_o \longrightarrow S_{i_1} + S_o$ process. The spin angular momentum of the two triplet molecules can be added to form a state of total spin 0. We assume that $|AT_{on_1} T_{on_2}\rangle$ is such a state.

$|AT_{on_1} T_{on_2}\rangle = \frac{1}{\sqrt{3}} \sum_M (-1)^{M+1} |AT_{on_1}^{M} T_{on_2}^{-M}\rangle$; T^M denotes the spin component having the values 1, 0, -1. For the sake of simplicity we replace the many electron wave functions by two electron wave functions (i.e., we only consider the two optical electrons). $T_{on_1}^1$ is

---

be created or destroyed during the process in order to conserve energy. If T_{fn_1} is such a state, the assumption that only single phonons are involved requires that the final vibronic state, $|AT_{fn_1} S_{on_2} X_{j_1}(T_{fn_1}) X_{j_2}(S_{on_2})\rangle = |f\rangle$ have an energy that differs from the initial state $|0\rangle$ at most by an amount $h\nu_c$. ν_c is less than the Debye cutoff frequency. We have examined these second order processes, and find that if they can occur they give somewhat larger transition rates R_o than equation 7. In the balance of this proposal we explicitly exclude these second order transitions, although the reader should bear in mind that if they can occur they appear to be the most probable annihilation route.

approximated by $\left|u_{n_1}(1)\, u^{o}_{n_1}(2)\,\alpha(1)\,\alpha(2)\right|$ and S_{in_1} by $\left|u_{n_1}(1)\, u^{i}_{n_1}(2)\,\alpha(1)\,\beta(2)\right| - \left|u_{n_1}(1)\, u^{i}_{n_1}(2)\,\beta(1)\,\alpha(2)\right|$. $u^{o}_{n_1}$ and $u^{i}_{n_1}$ denote excited molecular orbitals; α and β are the usual spin functions. $\langle AT_{on_1} T_{on_2} | V | AS_{in_1} S_{on_2} \rangle$ reduces to an algebraic sum of terms like

$$\langle u^{o}_{n_1}(1) u_{n_2}(2) | V | u_{n_1}(1) u^{o}_{n_2}(2) \rangle \langle u_{n_1} | u_{n_2} \rangle \langle u^{i}_{n_1} | u_{n_2} \rangle .$$

$\langle u_{n_1} | u_{n_2} \rangle$, $\langle u^{i}_{n_1} | u_{n_2} \rangle$ are electronic overlap factors, and are expected to be quite small. When n_1 and n_2 correspond to neighboring sites, the overlap factors are estimated to be $\lesssim 1 \times 10^{-4}$.

$\langle u^{o}_{n_1} u_{n_2} | V | u_{n_1} u^{o}_{n_2} \rangle$ can be evaluated by the usual multipole expansion method. One expects values between 10 and 1,000 cm^{-1}.

$\left|\langle AT_{on_1} T_{on_2} | V | AS_{in_1} S_{on_2} \rangle\right|^2$ will be proportional to the electronic overlap integral to the fourth power.

Intramolecular spin-orbit coupling mixes singlet and triplet states.* The lowest triplet can be represented more appropriately as

$$T_o + \sum_{\ell} \lambda_{\ell} S_{\ell} .$$

λ_{ℓ} denotes the amount of singlet character. The $2T_o \longrightarrow S_i + S_o$ can proceed via the singlet contributions. We obtain transition rates proportional to λ^4; i.e.,

$$\left|\langle AT_{on_1} T_{on_2} | V | AS_{in_1} S_{on_2} \rangle\right|^2 \sim \left| \sum_{\ell, m} \lambda_{\ell} \lambda_{m} \langle S_{\ell n_1} S_{mn_2} | V | S_{in_1} S_{on_2} \rangle \right|^2 ,$$

*We ignore intermolecular spin-orbit coupling perturbations as these are expected to be small.

λ_ℓ can be evaluated from the work of Clementi (7), A. C. Albrecht (8), and the experimental oscillator strengths for the $T_o \longrightarrow S_o$, and $S_\ell \longrightarrow S_o$ radiative transitions. We find that the λ_ℓ's have values between 1×10^{-4} and 1×10^{-5} in the case of benzene.

The above treatment can be extended to the $2T_o \longrightarrow T_i + S_o$ process. We understand $|AT_{on_1} T_{on_2}\rangle$ to now be a state having a total spin angular momentum of 1. The net result of the calculation is to give results similar to the above except that $\left|\langle AT_{on_1} T_{on_2} | V | AT_{in_1} S_{on_2}\rangle\right|^2$ is proportional to λ^2, or to the electronic overlap factor to the second power. The contribution proportional to λ^2, for example, is approximately

$$\left| \sum_\ell \lambda_\ell \langle T_{on_1} S_{\ell n_2} | V | T_{in_1} S_{on_2}\rangle \right|^2 ,$$

Barring certain pathological cases where

$$\left|\langle T_{on_1} S_{\ell n_2} | V | T_{in_1} S_{on_2}\rangle\right| << \left|\langle S_{mn_1} S_{\ell n_2} | V | S_{in_1} S_{on_2}\rangle\right|$$

because of symmetry considerations, the above discussion suggests that the $2T_o \longrightarrow T_i + S_o$ mode will dominate the $2T_o \longrightarrow S_i + S_o$ mode. In the case of benzene we find that the annihilation via the singlet character present in the triplet wave function gives a transition rate, R_o, of the order of 1×10^7 G/sec.* If G has a value between 10^{-6} and 10^{-3}, we

*We have only considered interactions between neighboring triplet pairs (comparable rates are expected for other simple aromatic systems). If the annihilation occurs via electron overlap, approximately the same or possibly smaller rates, R_o, are obtained.

obtain a transition rate between 10 and 10^4 sec^{-1} per pair.

The above estimate has been made on the basis of a pair of excitations localized on single molecules. The experimental transition rate per pair, k_1, should be set equal to σR_o. σ is a constant taking into account the nature of the collision process, i.e., excitations distributed over large numbers of molecules will give transition rates different from that of a "gas" of diffusing narrow wave packet excitations. (Impurities in the crystal can also affect the transition processes.)

The delayed fluorescence that has been observed (1) may arise from a crossing over from T_{i_1}. Earlier we pointed out the crossing over rate from S_1 to T_o is of the order of 1×10^7 sec^{-1} for benzene. In the case of the T_{i_1} level, one expects non-radiative transitions from T_{i_1} back to T_o to occur at a rate, k_2, of the order of 1×10^{10} to 1×10^{11} sec^{-1}. The intersystem crossing from T_{i_1} to the singlets must be of the same order of magnitude, or approximately 1×10^3 faster than the S_1 to T_o. Recent work by M. F. O'Dwyer et al. (9) suggests that this may well be the case.

In the above we have ignored the effects of ionization states because of uncertainties as to their location. Possible significant effects can occur by decay to an ionization state. Photoconductivity in aromatics may be related to the triplet-triplet annihilation process.

Below we determine a lower bound on k_1 and σ. Our decay scheme

$$
\begin{aligned}
T_o &\xrightarrow{k_o} S_o \ ; \\
2T_o &\xrightarrow{k_1} T_i + S_o \ ; \\
T_i &\xrightarrow{k_2} T_o \ ; \\
T_i &\xrightarrow{\gamma k_2} S_j \ ,
\end{aligned}
\tag{11}
$$

leads to the following rate equations:

$$
\begin{aligned}
\frac{dT_o}{dt} &= -k_o T_o - 2k_1 (T_o)^2 + k_2 T_i + L \ ; \\
\frac{dT_i}{dt} &= -(1+\gamma) k_2 T_i + k_1 (T_o)^2 \ .
\end{aligned}
\tag{12}
$$

L denotes the rate at which triplets are produced by intense illumination. If we assume that the intersystem crossing from the singlets to the triplets is approximately the same in the crystal as in "inert" solvents, L has the approximate value of 1×10^{16} triplets sec^{-1} cm^{-3}. ESR experiments are generally conducted under conditions where a steady state triplet concentration of the order of 1×10^{12} to 1×10^{13} triplets cm^{-3} would be detectable. Assuming no potent spin-relaxation or other line broadening mechanisms, the failure to detect triplets in aromatic systems implies that the steady state concentration $(T_o)_s$ must be less than 1×10^{12} triplets/cm^3. From the above rate equations we conclude that $k_1 \lesssim 1 \times 10^{-8}$ sec^{-1}. This implies that σ has a value between 1×10^{-12} and 1×10^{-9} if $k_1 \sim 1 \times 10^{-8}$.

Recent experiments carried out by G. W. Robinson on mixed crystals of C_6D_6 and C_6H_6 (5) have been very illuminating. At low temperatures ($<70°K$) phosphorescence emission was observed only from the C_6H_6 isotope traps. As the C_6H_6 concentration increased from 2% to ~ 5%, the phosphorescence lifetime decreased at a rate approximately proportional to the concentration squared. In addition, a delayed fluorescence was observed with a lifetime related to the phosphorescence lifetime. Further experiments are being conducted to determine whether this is a linear relationship. k_1 from these experiments have a value less than 10^{-8}. The fact that the delayed fluorescence lifetime appears to be related to the phosphorescence lifetime and that the phosphorescence lifetime goes approximately as the concentration squared, strongly suggests that there may be no significant non-radiative transitions induced by lattice defect sites of the type discussed earlier.

We now briefly consider distributed excitations. We find that annihilations are particularly rapid from "bound" double excitation states. (The double excitation propagates as a pair.) In the limit of strong binding, a possible bound state would be:

$$\frac{1}{\sqrt{N}} \sum_n \exp\left(i2\pi \hat{K}_\ell \cdot \hat{R}_n\right) \quad \left|A\, T_{o,R_n}\, T_{o,R_n+R_a}\right\rangle \quad . \tag{13}$$

A double excitation exists at positions $\hat{R}_n$, and $\hat{R}_n + \hat{R}_a$. $N = N_1 N_2 N_3$ (cyclic boundary conditions are imposed along the three directions

parallel to the primitive lattice translations, $\hat{t}_1$, $\hat{t}_2$, $\hat{t}_3$). This bound state can undergo a transition to the state

$$|\Psi_f\rangle = \frac{1}{\sqrt{N}} \sum_n \exp\left(i2\pi \hat{K}_\ell \cdot \hat{R}_n\right) \; | A\, T_{i,R_n}\, S_{o,R_n+R_a} \rangle \quad . \tag{14}$$

(The nuclear wave functions are included in the above, although for simplicity purposes we have not shown this explicitly.)

If $\hat{R}_n$ and $\hat{R}_n + \hat{R}_a$ define nearest neighbors, we find that the transition rate is approximately R_o. Our kinetic scheme is now

$$2\, T_o \underset{k_{-f_1}}{\overset{k_{f_1}}{\rightleftharpoons}} (T_o)_2 \xrightarrow{k_{f_2}} T_i + S_o \quad . \tag{15}$$

$(T_o)_2$ denotes the "bound" dimer. If we assume equilibrium is reached between T_o and $(T_o)_2$, we obtain that $k_1 = k_{f_2} k_{f_1} / k_{-f_1}$ and can solve for the concentration of $(T_o)_2$. If k_1 is approximately 1×10^{-8}, then a steady state concentration for $T_o \sim 1 \times 10^{12}$ triplets/cm^3 implies a steady state concentration for $(T_o)_2$ between 1×10^{12} and 1×10^{15} (if R_o is between 1×10^4 and 10). The lower value for $(T_o)_2$ is more reasonable, and is consistent with our earlier estimate that G is near 10^{-3} rather than 10^{-6}.

We have examined the possibility of the existence of bound states using the methods of Merrifield (10), and find that such states may well exist. Blake and McClure (1) observed an activation energy of the order of 40 cm^{-1} in rate of delayed fluorescence emission. Conceivably

this may be associated with the above bound pairs.

If bound exciton pairs do not exist, we find that the transition rate per pair is approximately $B(\hat{K}_1,\hat{K}_2)\frac{R_o}{N}$. $0<B(\hat{K}_1,\hat{K}_2)\leq 1$ $\hat{K}_1,\hat{K}_2$ are wave vectors and cannot both be zero. We have assumed that transitions take place from the initial unbound state

$$\sum_{n_1,n_2>n_1} C(R_{n_1},R_{n_2})\,|A\,T_{o,R_{n_1}}\,T_{o,R_{n_2}}\rangle \quad , \qquad (16)$$

to $|\Psi_f\rangle$ above. The coefficients $C(R_{n_1},R_{n_2})$ can be obtained by the methods of Merrifield (10), and these determine $B(\hat{K}_1,\hat{K}_2)$. The unbound double excitation state has an "average" $\hat{K}$ value of $(\hat{K}_1+\hat{K}_2)/2$. We clearly see that if N is very large, negligible transitions will occur from the unbound states.

Acknowledgements

The author wishes to acknowledge a number of very helpful and stimulating discussions with Professor G. W. Robinson.

REFERENCES

1. N. W. Blake and D. S. McClure, J. Chem. Phys. 29, 722 (1958).
2. M. Kasha, Radiation Research, 2, 243 (1960).
3. D. Wood, California Institute of Technology, private communication.
4. M. A. El-Sayed, M. T. Wauk and G. W. Robinson, Mol. Phys., 5, 195 (1962).
5. G. W. Robinson, to be published.
6. R. Pariser, J. Chem. Phys., 24, 250 (1956).
7. E. Clementi, J. Mol. Spectroscopy, 6, 497 (1961).
8. A. C. Albrecht, J. Chem. Phys., 33, 937 (1960).
9. M. F. O'Dwyer, M. Ashraf El-Bayoumi, and S. J. Strickler, J. Chem. Phys. 36, 1395 (L) (1962).
10. R. E. Merrifield, J. Chem. Phys., 31, 522 (1959).

PROPOSITION III

A number of experiments have been conducted in recent years to determine the extent of spin correlation in biradical molecular compounds. Jarrett et al. (1), Reitz and Weissman (2) have used paramagnetic resonance to study biradicals of the form:

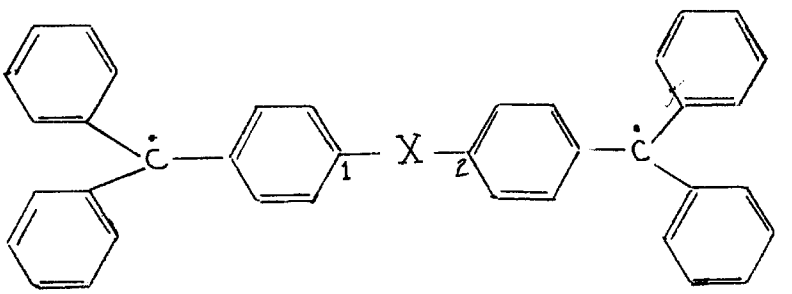

(1)

X is a group bridging the two triphenylmethyl monomer radicals. The X groups used were polymethylene $(-CH_2-)_n$, polyphenylene ( )$_n$, and ether $(-O-)_n$. Most of the electron spin density is on the central carbon atoms of the triphenylmethyls (TPM).

Bijl et al. (3), Matsunaga and McDowell (4) have used paramagnetic resonance to study charge transfer compounds in the solid state, The ground state of these compounds is presumed to be symbolically representable as $|D^+A^-\rangle$. An electron is "donated" by D and "accepted" by A. If A and D are molecules having completely filled electron shells, A^- and D^+ each have an odd electron. The charge transfer compounds investigated were chloranil, bromanil, iodanil, and tetrabromo o-quinone complexed with p-phenylene-diamine, and/or tetramethyl p-phenylene-diamine. The diamines are the electron

donors. The p-phenylene-diamine + chloranil complex, for example, has the following form:

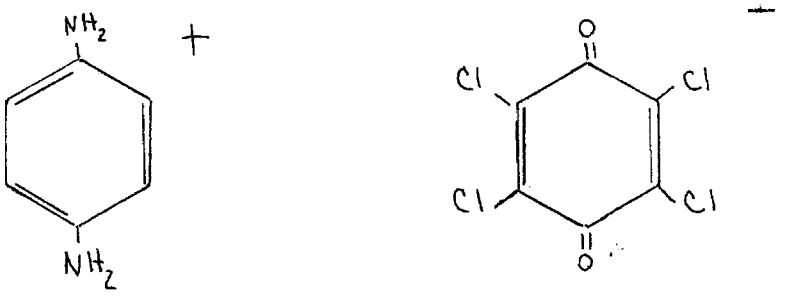

(2)

If the spin correlation, i.e., the exchange interaction term $\frac{1}{2} J \hat{S}_1 \cdot \hat{S}_2$, is sufficiently small, the biradical compounds will behave like two independent doublets. The magnetic susceptibility will show the usual $1/T$ dependence of a doublet. (T is the absolute temperature.) Any hyperfine structure present in the ESR spectra will correspond to a linear superposition of the hyperfine structure of two nearly independent doublet systems. If $|J|$ is sufficiently large, the ground state of the biradical will look like a diamagnetic singlet or a paramagnetic triplet. The magnetic susceptibility, χ, will now show a more complicated temperature dependence (3):

$$\chi \propto \frac{1}{T} \frac{1}{3 + \exp |J| /KT} \quad ; \quad \chi \propto \frac{1}{T} \frac{1}{3 + \exp -|J| /KT} \, . \qquad (3)$$

(ground singlet) (ground triplet)

All the above experiments indicate that the $|J|$'s are sufficiently small so that the biradical compounds can be considered as made up of two independent doublets. $|J|$ was estimated to be less than 4 cm^{-1} in the Bijl experiment, and to be less than 0.003 cm^{-1} in the Reitz experiment.

These small |J| values are perplexing. McConnell (5), for example, estimated theoretically the value of |J| for radicals made up of two TPM groups (eq. 1), and found them to be several orders of magnitude larger than the "experimental" values. No extensive theoretical work has been done on the J values of the diamine complexes because of the complexity of the problem and the lack of experimental data as to crystal structure; nevertheless, the small values of |J| reported appear to be at variance with other experimental facts (see below).

About a year and a half ago the author proposed a possible explanation for the small |J| values of the diamine complexes. A number of recent experiments (6, 7) lend support to his original proposal. The arguments are briefly repeated.

The orientation of the donor and acceptor molecules relative to each other is not known. Consider the following two cases:

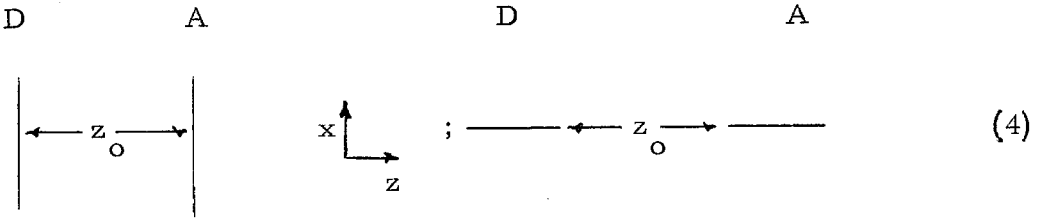

(4)

(a) (b)

One might expect structure (a) to be most probable because it maximizes overlap of the π orbitals (8). Virtually complete charge transfer from D to A is believed to occur; consequently, overlap is relatively unimportant for purposes of stabilizing the complex (the major source of bonding comes from the coulombic interaction between

the charged components of the complex). We consider (b) as an alternate structure.

The odd electrons of A and D can interact magnetically with each other, and anisotropic spectra should generally be obtained. This is true whether $|J|$ is small and the system can be regarded as doublets, or whether $|J|$ is relatively large and the paramagnetic species is a triplet state molecule. If a thermally accessible triplet exists, or if the ground state of the complex is a triplet, one expects a spin dipolar interaction term of the form (9, 10):

$$\bar{D}(S_z^2 - S^2/3) + E(S_x^2 - S_y^2) \; ;$$

$$\bar{D} = 3/4 \; \frac{g_e^2 \beta^2}{hc} \; \langle D^+A^- \left| \frac{1}{r_{12}^3} \left(1 - \frac{3 z_{12}^2}{r_{12}^2}\right) \right| D^+A^- \rangle, \qquad (5)$$

$$E = -3/4 \; \frac{g_e^2 \beta^2}{hc} \; \langle D^+A^- \left| \frac{x_{12}^2 - y_{12}^2}{r_{12}^5} \right| D^+A^- \rangle .$$

It is a relatively simple matter to estimated $\bar{D}$ and E. We assume that $z_o \sim 3$ Å, and that the odd electrons are in molecular orbitals made up of highly localized atomic orbitals. We take the charge distribution to be uniform over all carbon atoms. Structure (a) gives $\bar{D} \sim 0.04$ cm^{-1} or 400 gauss (E is negligible in comparison). Structure (b) gives $\bar{D} \sim 0.015$ cm^{-1} or 150 gauss. The assumption of highly localized atomic orbitals most likely overestimated $\bar{D}$. The true values may be 300 gauss and 100 gauss for structures (a)

and (b) respectively. (Similar conclusions as to the magnitude of the electron spin dipolar interaction hold if the complex can be regarded as two independent doublets.)

The experiments have been performed on polycrystalline samples; as a result, one might expect broad resonance lines ($\gtrsim 100$ gauss). The observed resonances are fairly narrow ($\lesssim 30$ gauss). p-Phenylenediamine + chloranil, for example, gives a resonance line having a width of ~ 10 gauss under low resolution (3). Under high resolution this line is observed to consist of two lines, approximately 2 to 5 gauss wide (4). Intermolecular spin exchange, possibly intramolecular spin exchange if the complex can be regarded as two nearly independent doublets, might be responsible for the fairly narrow, apparently isotropic lines.

Spin exchange narrowing would be expected if the concentration of paramagnetic species were large. This would be the case if a ground triplet exists or if $|J|$ is sufficiently small so that (1) one could regard the complex as two independent doublets, or (2) a thermally accessible triplet state exists. $|J|$ is estimated to be much less than $4\ cm^{-1}$, and spin exchange narrowing might well occur.

There are, however, a number of disturbing experimental points: (I) the resonance line shape depends somewhat on the method of preparation (4); (II) the radical concentration of the diamine complexes differs by as much as a factor of 200 (3). If $|J|$ is small compared with kT,

and if the ground state is a charge transfer state, it is indeed difficult to understand the reason for such large differences in radical concentration. One cannot attribute it to differences in electronegativity between the components of the complex since $|J|$ is supposed to be much less than 4 cm^{-1} for all complexes studied.

A possible explanation is the following: Let us assume that a thermally accessible triplet exists, and that $|J|$ is large compared with kT for some of the complexes. Assume $J \sim 0.1$ ev. or ~ 800 cm^{-1}. The concentration of triplets for that complex would be

$$\frac{3\, e^{-J/kT}}{1 + 3\, e^{-J/kT}} \times 100\% \sim 3\%.$$

A polycrystalline sample of the complex would give a resonance approximately 100-300 gauss wide, if we assume no significant spin exchange narrowing. Any impurity doublet of $\sim$ 0.3% concentration would dominate the spectra.* Organic doublets generally have a width of $\sim$ 30 gauss. Spin exchange of the impurity doublet with triplet neighbors may be responsible for the fairly narrow resonance observed.

E. E. Schneider (footnote reference (3)) is reported to have determined the radical concentration in p-phenylenediamine + chloranil (PPC) to be $\sim$ 0.4%. The tetramethyl p-phenylenediamine + tetrabromo o-quinone give a resonance that is 200 times more intense than

*Impurities would explain the dependence of line shape on the method of preparation (4).

PPC, implying a radical concentration of approximately 80% (3). Clearly, if Schneider's determination is correct, impurities cannot be responsible for the large radical concentration in the tetrabromo o-quinone complex. The $|J|$ value of this complex must be $< 4\ cm^{-1}$, or approximately 1000 times smaller than that of the PPC complex. This difference is surprising but may be due to differences in z_o, or differences in electronegativity between the components in the complex. Other possible explanations for this discrepancy between J's might be that the triplet lies lowest in the tetrabromo o-quinone complex, or that the basic unit of this complex is not $D^+ A^-$ but rather $D^+ A^- (D_m A_n)$, where m and n are integers. If the latter structure is correct, the odd electrons may be distributed over a number of D and A's resulting in a smaller J. Experiments performed on pure single crystals at various temperatures would verify or disprove the above explanations.

Chesnut and Phillips have recently examined the phosphonium and arsonium TCNQ charge transfer complexes (6) and found a thermally accessible triplet with $J \sim 0.06$ ev., and a zero field term, $\bar{D} \sim 100$ gauss. (These authors also raise the question of the possibility of impurities masking the resonance of any triplet molecules present in the phenylenediamine complexes.) Bell and McConnell have suggested that triplet excitons exist in TCNQ salts. Single crystal experiments on the above phenylenediamine complexes might also reveal triplet excitons. (In addition, other phenylelediamine complexes like

phenyleledіamine + halogen derivatives of naphthaquinone and anthraquinone could be synthesized and studied.)

The above analysis indicates the importance of working with pure single crystals. It is quite possible that the Jarrett and Reitz experiments performed on solution samples failed to reveal any significant singlet triplet separation because of spin dipolar interactions. If the TPM groups are directly linked, one can expect a spin dipolar interaction of the order of $\sim$ 65 gauss.* McConnell estimated that a thermally accessible triplet exists, with $J \sim 100\text{-}500\ cm^{-1}$ depending upon the planarity of the radical. Doublet impurities of the order of 1 or 2% would now dominate the spectra. (The above explanation may not be the complete answer, however. If X corresponds to $(\text{-}CH_2\text{-})_2$, the spin dipolar interactions are negligible. McConnell estimates J to now be 0.3 to 3 cm^{-1}, whereas the experimental J is less than 0.003 cm^{-1}. If McConnell's estimate is correct, and the experiment was done correctly, the explanation for the discrepancy between the experimental and theoretical values must be sought elsewhere for this particular biradical.)

---

*We assume that the spin density distribution in the TPM monomers are not perturbed significantly by the bonding. The spin density at positions 1 and 2 is 0.18 (5) $\bar{D}$ and E of the triplet state of ethylene are 0.2 and 0.23, respectively (10). The spin dipolar terms $\bar{D}$, E of the biradical are approximately $(0.18)^2 \times 0.2\ cm^{-1}$, or approximately 65 gauss.

REFERENCES

1. H. S. Jarrett, G. J. Sloan, and W. R. Vaughan, J. Chem. Phys., 25, 697 (1956).
2. D. C. Reitz and S. I. Weissman, J. Chem. Phys., 27, 968 (1957).
3. D. Bijl, H. Kainer, and A. C. Rose-Innes, J. Chem. Phys., 30, 765 (1959).
4. Y. Matsunaga, C. A. McDowell, Nature, 185, 916 (1960).
5. H. M. McConnell, J. Chem. Phys., 33, 115 (1960).
6. D. B. Chesnut and W. D. Phillips, J. Chem. Phys., 35, 1002 (1961).
7. D. B. Chesnut and P. Arthur, Jr., to be published.
8. S. P. McGlynn, Chem. Rev., 58, 113 (1958).
9. C. A. Hutchison, Jr., and B. W. Mangum, J. Chem. Phys., 34, 908 (1961).
10. W. Moffitt and M. Gouterman, J. Chem. Phys., 30, 1107 (1959).

PROPOSITION IV

Numerous investigators have sought to derive the vibrational frequency or electronic energy spectra of disordered lattices.* A solution of this problem would enable one to calculate the thermodynamic properties of alloys, isotopic systems, and glasslike substances. Particular attention has been given one dimensional chains. Dyson (1) and Schmidt (2) have obtained exact formal solutions for the frequency spectra of disordered linear chains. Their methods of solution, unfortunately, do not enable one to carry out calculations of the spectra. Other investigators (3) using less rigorous methods have obtained semiquantitative expressions for the frequency distributions. Numerical methods have also been devised by Dean (4) and Domb (5). Disordered two and three dimensional lattices are even less understood. The frequency spectra of these lattices have been approximately determined for low concentrations of impurities (3). There is at present, to the best of the author's knowledge, no adequate method for determining the energy spectra of a two or three dimensional lattice when the concentrations of A and B are both large and comparable. Below we explore a method that might be successfully applied to such cases. The arguments we give are nonrigorous. We desire only to point out future avenues of research. For simplicity purposes we only consider simple cubic lattices.

* The disorder is introduced by choosing fixed concentrations of two components, A and B, and distributing them randomly through the lattice. (Multicomponent systems are, of course, even more difficult to treat.)

The concept of the propagation vector, k, has been very useful for determining the frequency spectra of ordered lattices. If we denote a particular lattice position of an ordered monoatomic lattice by R_n, the x component of the displacement of the atom at that position is (3):

$$x_{R_n} \alpha \exp\left(i\omega t + \hat{k} \cdot \hat{R}_n\right),$$

$$\hat{k} = \frac{2\pi S_1}{Na}\,\hat{e}_x + \frac{2\pi S_2}{Na}\,\hat{e}_y + \frac{2\pi S_3}{Na}\,\hat{e}_z, \qquad (1)$$

$$S_i = 1, 2, \ldots N$$

ω is the frequency; N^3 is the total number of atoms in the crystal. Cyclic boundary conditions have been imposed; a denotes the interatomic spacing; e_i is a unit vector along the i axis.

If fixed boundary conditions are used, equation 1 becomes:

$$x_{R_n} \alpha - \exp i\omega t \sin \frac{\pi S_1 n_1}{N} \sin \frac{\pi S_2 n_2}{N} \sin \frac{\pi S_3 n_3}{N} \qquad (2)$$

We have set $\hat{R}_n = n_1 a\,\hat{e}_x + n_2 a\,\hat{e}_y + n_3 a\,\hat{e}_z$; $n_i = 0, 1, \ldots, N$; x_{R_n} is zero when n_1 or n_2 and/or n_3 are 0 or N. Equations analogous to equations 1 and 2 can be readily derived for ordered lattices having more than one kind of atom. The frequencies $\omega(S_1, S_2, S_3)$ and frequency distributions $G(\omega)$ can be determined (3, 6).

What happens when A and B are now distributed randomly through the lattice? Is it possible to talk about a "propagation vector"? If so, can it be used as a basis for calculating the frequencies and frequency

distributions? Rosenstock and McGill (7) have recently examined the vibrational modes of a disordered linear chain. The chains consist of two masses m_1 and m_2 distributed randomly. The displacement u_i of atom i satisfy Newton's equation of motion:

$$\underline{k}_i(u_{i-1} - u_i) + \underline{k}_{i+1}(u_{i+1} - u_i) = m_i \ddot{u}_i \quad . \qquad (3)$$

$$(i = 1, 2, \ldots N)$$

$\underline{k}_i$ is the restoring force constant between atoms i and i-1. Only nearest neighbor interactions are considered. $u_i(t) = u_i e^{i\omega t} = u_i e^{i\sqrt{\lambda}\, t}$. Figure I is a plot of u_i vs. i when N = 10, 16. Fixed boundary conditions are imposed: $u_o = 0$, $u_{N+1} = 0$. The k'th normal mode as exactly k-1 nodes. (This relationship is presumed to hold independent of the size of the chain.) We note a remarkable similarity to the modes, $\sin\left(\frac{\pi j S_1}{N}\right)$ of an ordered monoatomic linear chain. These results suggest that one might be able to talk about a pseudopropagation vector.

The optical spectra of pure molecular crystals often show Davydov splittings (8). The splittings are related to the resonance interaction between different site molecules of the unit cell. In pure crystals the electronic excitation is distributed coherently over large numbers of molecules. Optical absorption and emission only occur to and from eigenstates having k = 0; consequently sharp lines are obtained. Naphthalene crystals have two molecules per unit cell; the absorption to the first excited singlet shows a Davydov splitting of $\sim 150\ cm^{-1}$

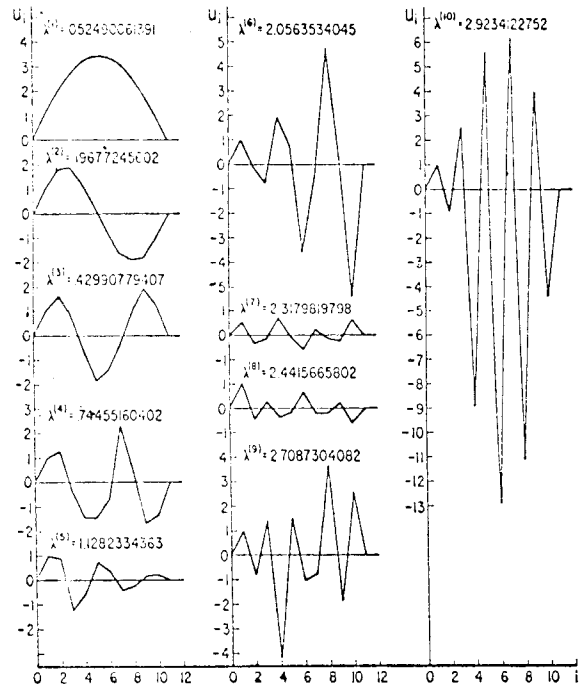

Normal modes of a disordered lattice [Eq. (3)]. N = 10, all $k_i = 1$, m_1 to m_{10} equal to 1, 2, 2, 1, 2, 1, 2, 1, 2, 1.

Normal modes of a disordered lattice [Eq. (4)]. N = 16, all $k_i = 1$, m_1 to m_{16} equal to 1, 1, 1, 1, 2, 1, 1, 2, 1, 1, 1, 2, 1, 2, 2, 1.

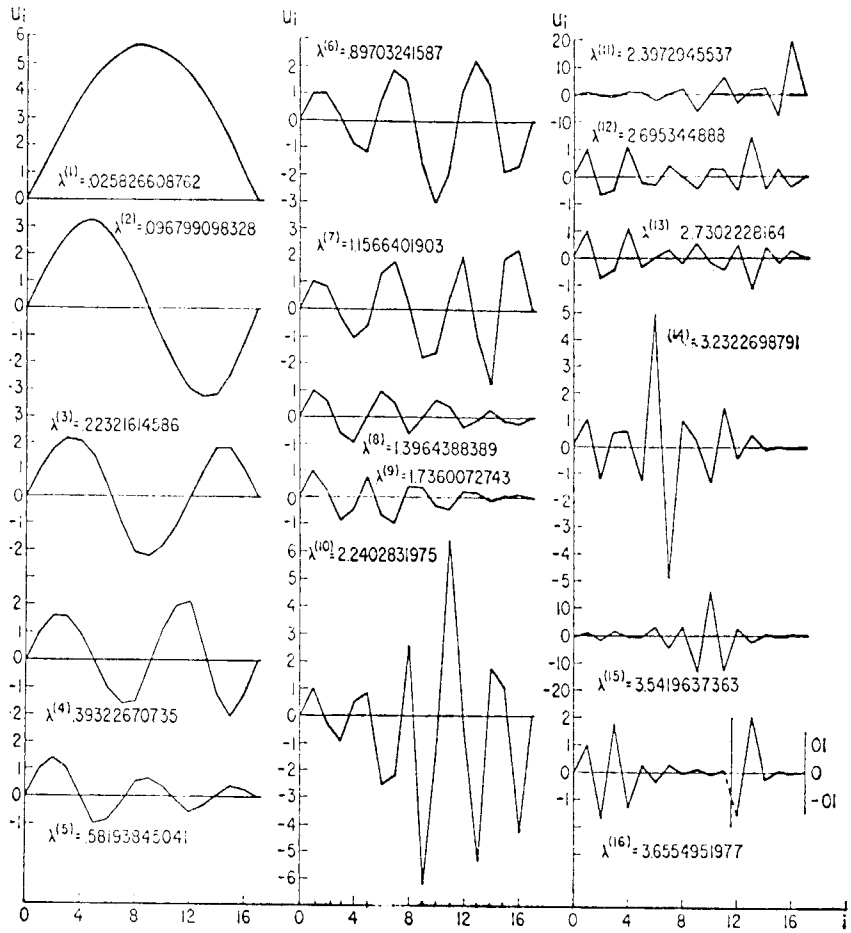

Figure I

located symmetrically about $\nu = 31,550\ cm^{-1}$.

Experiments have been recently performed on equimolecular mixtures of perdeutero ($C_{10}D_8$) and protonated naphthalene ($C_{10}H_8$) (9). These isotopic species are expected to be distributed randomly through the crystal lattice. The energy level of $C_{10}H_8$ is approximately 100 cm^{-1} lower than that of the $C_{10}D_8$. Fluorescence emission generally occurs from the lowest excited state, S_1, and also from higher states that are thermally accessible from S_1. The fluorescence spectra of the mixed crystal show a Davydov splitting of $\sim 35\ cm^{-1}$ located symmetrically about $\nu = 31,545\ cm^{-1}$. The lower line is sharp, whereas the upper line is uncertainty broadened. The splittings increase continuously as the concentration of naphthalene is increased continuously (10). These results strongly suggest (1) that exciton-like band structure exists in the mixed crystal; (2) that a pseudopropagation vector "$\hat{k}$" exists and that a "$\hat{k}$" = 0 selection rule is operative.*

Let us consider the following problem: We desire the energy spectra of an electron distributed over N^3 atoms A and B arranged randomly in a three dimensional array. (If this problem can be solved, analogous problems like the vibrational spectra of the lattice can also be solved.) We assume only nearest neighbor interactions and make the tight bonding approximation.

---

* The above experiment may not be a good example of the validity of the pseudopropagation vector for three-dimensional crystals. Experiments are required to determine whether the "$\hat{k}$" = 0 states are really crystal states in the sense that the excitation is distributed over large numbers of $C_{10}H_8$ and $C_{10}D_8$ molecules, or whether the exicitation is confined mainly to chainlike clusters of $C_{10}H_8$. The fact that

Eigenfunctions can be designated as

$$\psi = \sum_{n_1,n_2,n_3} C(n_1,n_2,n_3)\ u_{n_1n_2n_3} \quad . \tag{4}$$

$u_{n_1n_2n_3}$ may either be an orbital of A or of B. We impose the boundary conditions $C(n_1,n_2,n_3) = 0$ whenever n_1,n_2,n_3 defines a boundary plane. Decompose the three dimensional lattice into a set of planes of atoms, the planes into linear chains. The system is now a collection of parallel chains. Ignore the interaction between chains. The eigenenergies of the truncated Hamiltonian $\mathcal{H}_o$ are $\epsilon_{n_2,n_3}(S_i)$; the eigenstates are

$$\varphi_{n_2,n_3}(S_i) = \sum_{n_1}^{N} D(n_1;n_2,n_3,s_i)\ u_{n_1n_2n_3}\ ;\ s_i = 1,2,\ldots N\ . \tag{5}$$

We know from the work of Rosenstock and McGill that each eigenenergy and eigenvector can be associated with a particular S_i, where S_i is the number of modes obtained by plotting D vs. n_1. Unfortunately, the eigenenergies and eigenvectors must be obtained numerically. The formal solutions that do exist (1, 2) are not readily accessible. The energies, the energy distributions, and the eigenvectors can be obtained numerically using the methods of references (4) and (7) from an NXN Jacobian secular determinant.

We now turn on the interaction, V, between the chains in the

---

the splittings are displaced about the 0-0 line of the $C_{10}H_8$ crystal suggests the latter.

plane. The eigenfunctions, equations 4 and 5, define a complete set. The eigenfunctions are

$$\varphi_{n_3} = \sum_{n_2, S_i}^{N} F(n_2, S_i; n_3)\, \varphi_{n_2, n_3}(S_i) \quad . \tag{6}$$

The eigenenergies of $H_o + V$ can be obtained from the $N^2 X N^2$ secular determinant obtained from equation 6. This is a formidable task and does not appear practical to do. Instead we approximate equation 6 by

$$\bar{\varphi}_{n_3}(S_i, S_j) = \sum_{n_2}^{N} f(n_2; n_3, S_i, S_j)\, \varphi_{n_2, n_3}(S_i) \tag{7}$$

and obtain the energies $\epsilon_{n_3}(S_1, S_2)$ numerically from the corresponding NXN Jacobian secular determinant (4, 7).

We now turn on the interaction between the planes and approximate the "eigenstates" of the lattice Hamiltonian, $\mathcal{H}$, as

$$\bar{\Psi}(S_i, S_j, S_\ell) = \sum_{n_3}^{N} r(n_3; S_i, S_j S_\ell)\, \bar{\varphi}_{n_3}(S_i, S_j) \quad . \tag{8}$$

Again an NXN Jacobian determinant is solved to give the "eigenenergies."

Since the above procedure (equations 7 and 8) are not really correct, we must carry out a transformation of the $\epsilon(S_1, S_2, S_3)$'s. Let $\sigma_i = S_i/N$. We rewrite $\epsilon(S_1, S_2, S_3)$ as $\epsilon(\sigma_1, \sigma_2, \sigma_3)$. The actual eigenvalues of the lattice, $E(\sigma_1, \sigma_2, \sigma_3)$ are given by

$$E(\sigma_1,\sigma_2,\sigma_3) = \int_0^1 \int_0^1 \int_0^1 T(\sigma_1,\sigma_2,\sigma_3,\sigma_1',\sigma_2',\sigma_3')\,\epsilon(\sigma_1',\sigma_2',\sigma_3')\,d\sigma_1'\,d\sigma_2'\,d\sigma_3' \quad . \tag{9}$$

A 1 to 1 correspondence between E and ϵ is expected. If we denote the energy distribution function derived from the $\epsilon(\sigma_1, \sigma_2, \sigma_3)$'s by $g(\epsilon)$, the true distribution function is given by

$$G(E) = \int_{-\infty}^{\infty} R[E,\epsilon]\,g(\epsilon)\,d\epsilon \quad . \tag{10}$$

When N^3 is large, a numerical determination of $g(\epsilon)$ is more practical than a numerical determination of the $\epsilon(\sigma_1, \sigma_2, \sigma_3)$'s. Dean's method (4) permits one to determine the distribution functions, $g_1(\epsilon_{n_2, n_3})$, $g_2(\epsilon_{n_3})$ and $g(\epsilon)$. A computer program can be readily devised to obtain these distribution functions. Values of the order of 1×10^9 for N^3 can be handled (11).

If the lattice was ordered so that atoms A and B were in alternate positions, the above procedure (eqs. 4-8) would give the exact eigenfunctions and eigenenergies. The matrix elements $(\mathcal{H}_o + V)_{i,i'} = \langle \varphi_{n_2, n_3}(S_i) | \mathcal{H}_o + V | \varphi_{n_2 \pm 1, n_3}(S_i') \rangle$, $\langle \bar{\varphi}_{n_3}(S_i, S_j) | \mathcal{H} | \bar{\varphi}_{n_3 \pm 1}(S_i', S_j') \rangle = (\mathcal{H})_{i,i',j,j'}$ are zero because of the translatory symmetry of the lattice whenever $S_i \neq S_i'$, $S_j \neq S_j'$. The functions T and R of equations 9 and 10 are given by:

$$T = \prod_{i=1}^{3} \delta(\sigma_i - \sigma_i') \; ; \; R = \delta(E-\epsilon) \, . \tag{11}$$

δ is the delta function. In the case of a disordered lattice T and R are no longer delta functions since the above matrix elements no longer are zero. We do expect that $(V+\lambda)_{o\,i,i'}$, $(\lambda)_{i,i',j,j'} << |$ when $|S_i - S_i'|$ or $|S_j - S_{j'}| >> |$ because of destructive interference between the eigenvectors; consequently, T and R are expected to be decreasing functions of $|S_i - S_i'|$, $|E-\epsilon|$, respectively. We do not know the functional form of T and R.

If the concept of the pseudo-propagation vector is meaningful, it is plausible to assume that T and R are gaussian and peaked about the σ_i's and ϵ, respectively:

$$T = (2/\pi)^{3/2} \prod_{i=1}^{3} \frac{1}{\gamma_i} \exp\left[-2(\sigma_i - \sigma_i')^2/\gamma_i^2\right];$$

$$R = (2/\pi)^{1/2} \frac{1}{\bar{\gamma}} \exp\left[-2(E-\epsilon)^2/\bar{\gamma}^2\right] .* \tag{12}$$

The above discussion can be easily modified to handle the vibrational spectra of a disordered cubic lattice. It would be of some interest

---

* The terms $\bar{\gamma}$, γ_i most likely are not constants. We note from the work of Rosenstock and McGill (7) that the sinusoidal character of the modes of the random chain is lost with increasing σ_i. This implies that departures from the propagation vector concept probably arise predominantly because of these modes; consequently $\bar{\gamma}$ and the γ_i's may be (slowly?) increasing functions of E, ϵ and σ_i, σ_i' respectively. Equation 12 in that case would have to be modified to take these points into account.

to carry out a calculation using the above ideas and compare it with experiment. One system that might be studied is a mixed crystal of H_2 and D_2. The crystal structure is cubic, the force constants of the mixed crystal are expected to be essentially the same as that of the pure crystals, and the masses are sufficiently different.

REFERENCES

1. F. J. Dyson, Phys. Rev., 92, 1331 (1953).
2. H. Schmidt, Phys. Rev., 105, 425 (1957).
3. A. A. Maradudin, P. Mazur, E. W. Montroll, and G. H. Weiss, Rev. of Mod. Phys., 30, 175 (1958).
4. P. Dean, Proc. Roy. Soc. (London) A254, 507 (1960); Proc. Phys. Soc., 73, 413 (1959).
5. C. Domb, A. A. Maradudin, E. W. Montroll, and G. H. Weiss, J. Phys. Chem. Solids, 8, 419 (1959).
6. C. Kittel, "Introduction to Solid State Physics," (John Wiley & Sons, Inc., New York, 1956).
7. H. B. Rosenstock and R. E. McGill, J. Math. Phys., 3, 200 (1962).
8. D. McClure, "Solid State Physics" (Academic Press Inc., New York, 1959), Vol. 8, p. 1.
9. D. P. Craig, L. E. Lyons, and J. R. Walsh, Mol. Phys., 4, 98 (1961).
10. G. W. Robinson, California Institute of Technology, private communication.
11. J. Sharpe, Burroughs Corporation, Pasadena, private communication.

PROPOSITION V

Within the past few years considerable progress has been made in determining the structure of DNA (deoxyribonuclic acid). It is believed to be a double helix resembling a twisted ladder. The sides of the ladder are alternating sugar (deoxyribose) and phosphate units. The rungs of the ladder are paired nitrogenous bases of four types: adenine (A), guanine (G), cytosine (C), and thymine (T). Adenine is paired only with thymine, and cytosine only with guanine (1). In this proposition we show how, under suitable conditions, one can determine the degree of pairing between bases* along the axis of the double helix by means of NMR. This is of interest because the genetic code is determined by the sequence of bases along the axis of the double helix.

Our method can be used as an analytical tool. It can also be used in structural problems. Fibrous crystals of DNA salts can be prepared showing a high degree of orientation (2). These fibers give several distinct types of x-ray diffraction patterns because of several possible configurations of the nucleic acid (3, 4). The relative concentration of a particular configuration is determined by the water content of the fiber, which, in turn, is a function of the relative humidity of the atmosphere surrounding the crystals. Presumably

---

* We shall refer to such pairs as axial neighbors.

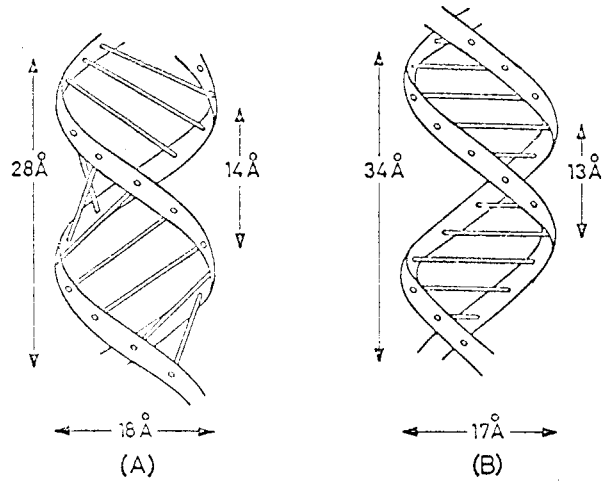

Diagram to show the main differences between the proposed models of the A and B forms of sodium deoxypentose nucleate
(G. B. B. M. Sutherland and M. Tsuboi: *Proc. Roy. Soc. A* 1957, 239, p. 459)

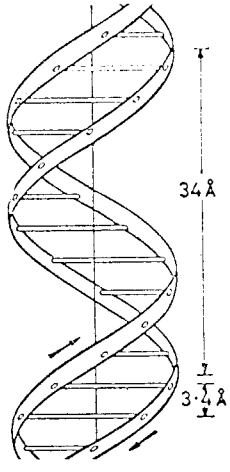

The helical structure of sodium deoxypentose nucleate as proposed by Watson and Crick
(J. D. Watson and F. H. C. Crick: *Nature, Lond.* 1953, **171**, p. 737)

Figure I

changes in the hydrogen bonding between neighboring chains are responsible for the different configurations. In Figure I we display two possible configurations, A and B. One cannot be sure as to which of the configurations, if either, corresponds most closely to the DNA molecule in the living cell. Configuration B conforms very well to the Watson and Crick model (1). In the case of the sodium salt (2) the A configuration is obtained at 75 percent relative humidity; the B configuration at high humidities (~ 90%). The A configuration apparently results in fibers showing a high degree of crystallinity; the B configuration leads to a somewhat reduced crystallinity. A and B are believed to interconvert reversibly; the B configuration persists over a wide range of humidity. We propose that the interconversion process can be studied by means of NMR.

The degree of axial pairing between bases can be inferred from solid state samples by measuring the nuclear dipolar interactions. We find that the interactions between axial neighbors can be most readily determined if one works with isotopic samples. It is desirable to have the DNA sample virtually completely deuterated so as to reduce background dipolar contributions. If one wishes to study a synthetic DNA this poses no problem; if one wishes to study the DNA from a living organism that organism must be capable of thriving on a deuterium diet. We find that the relative orientation of the axial molecules favors the use of H^3 (tritium) isotopes. This

necessitates replacing one of the protons by H^3 in one of the base pairs. No difficulty is anticipated in obtaining the tritiated base.

As an example,* we consider the problem of determining the percent axial pairing of adenine with thymine in a polycrystalline sample. We assume configuration B.

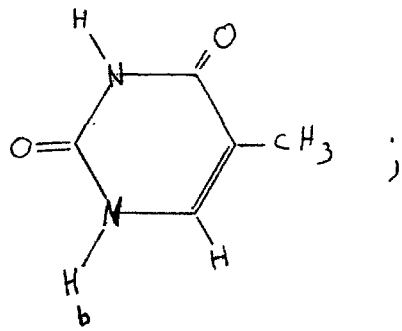

thymine

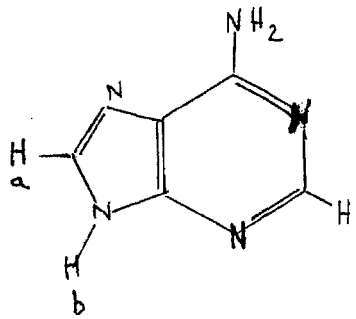

adenine (1)

An examination of the DNA structure reveals that there are four distinct ways that the pairing can occur. Both helices are right (?) handed helices,† but differ in the sequence of atoms in the sugar phosphate chain. Helix I may have the following sequence down the axis, starting with the sugar:

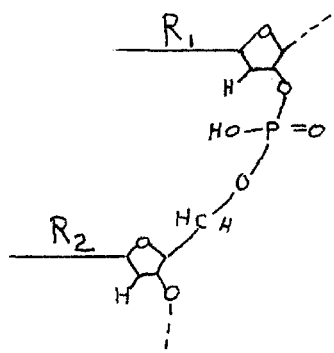

*All base pairs can be handled by the same method.

†For convenience we assume the helices are right-handed as suggested by Watson and Crick. This does not affect

Helix II has the reverse sequence:

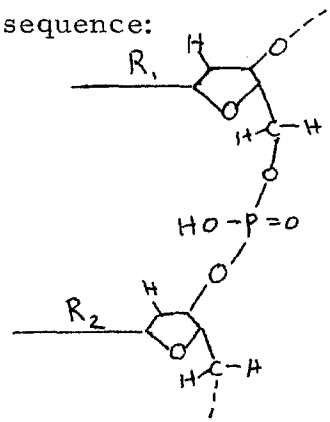

(3)

The nitrogenous bases are parallel to each other. Let R_1 be base A; R_2 be base T for helix I (eq. 2). We find that proton (a) (eq. 1) is above the methyl group and about 4 Å away from the center of gravity of the methyl protons. We replace this proton with tritium; i.e., we either synthesize the DNA from adenine bases having tritium in position (a) or we feed the organism such bases. (Proton (b) is lost when the base is joined to the sugar.) If R_1 were T and R_2 were A, we find the methyl group and the tritium atom too far apart to result in any measurable dipolar contribution. We now examine helix II. If R_1 were T and R_2 were A, the tritium and the center of gravity or the methyl protons are again 4 Å away. If T and A are interchanged, again the tritium and methyl group are too far apart to interact appreciably.

Our isotopic DNA has all the hydrogens of the sugar-phosphate units along the helices replaced by deuterium. All the hydrogens of all the bases other than T and A are replaced by deuterium. Proton

(a) of A is replaced by tritium. (It would be desirable to deuterate the amino group, but this is not absolutely essential.) The T's are left undeuterated. (Some exchange of the ring protons might occur in D_2O. This does not affect our treatment. We are mainly interested in having hydrogens on the methyl carbon.)

We now do an NMR experiment on tritium. Van Vleck (5) has derived the following expression for the second moment of the resonance line for a polycrystalline sample:

$$(\Delta H)^2 = \frac{4}{15} \beta^2 \sum_f I_f (I_f + 1) g_f^2 r_f^{-6} \qquad (4)$$

β is the Bohr nuclear magneton; g_f is the g factor of nucleus f; I_f is the corresponding spin in units of $\hbar$; r_f denotes the distance of nucleus f from the tritium atom; $(\Delta H)^2$ is the second moment in units of $(\text{gauss})^2$. Using equation 4 we find a second moment of the order of 0.25 gauss^2. The contribution of the methyl group is between 20-40%.

The observed spectra will be a superposition of two resonances: one from the tritiums of the AT pairs, and one from the tritiums of the unpaired A's. The latter will be somewhat sharper. In the case of polycrystalline samples one expects that the two resonances will merge making resolution of the two resonances difficult. It we assume that the second moment can be measured with an accuracy of 5%, the

concentration C_A of the unpaired A cannot be much larger than the concentration, C_{AG}, of the AG pairs:

$$\frac{C_A}{C_{AG}} < 4. \tag{5}$$

The above inequality restricts the kind of DNA polycrystalline samples that can be studied by the above technique. One expects the ratio to increase with increasing crystallinity. By studying the absorption intensity and determining the 2^{nd} moment, the percent pairing can be ascertained.

The DNA molecules are very large; consequently we encounter a concentration problem. We estimate that the minimum concentration at room temperature of TA pairs relative to the total base concentration that can be detected by highly sensitive laboratory instruments is between 1 and 10%. Significant improvement in the sensitivity is expected with decreasing temperature provided the spin lattice relaxation rate does not significantly decrease causing saturation broadening.

We now return to the problem of studying the interconversion between the A and B configuration in fibrous crystals. Poly AT, prepared with the above isotopic requirements, can be used as a probe. Poly AT is a synthetic DNA that consists of A and T in alternating sequence. We schematically sketch poly AT below for configuration B.

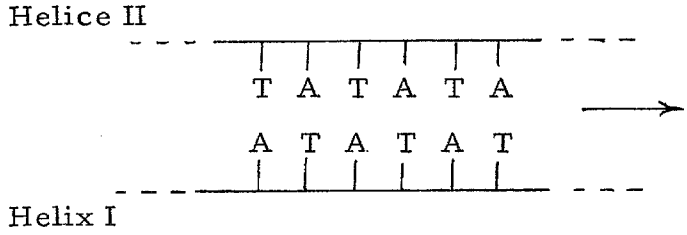

(6)

Dipolar interaction need only be considered between AT axial neighbors for helix I; dipolar interactions need only be considered between TA pairs in helix II. (The helices "advance" in the direction indicated.) Dipolar interactions between paired bases of the rung can be neglected. If configuration B fibers can be regarded to be almost crystalline, which they appear to be, then the structural aspects of the interconversion between A and B can be studied at room temperature using the above sensitive instruments, otherwise less precise information can be obtained. Bundles of reasonably parallel fibers can be prepared. Direct $\hat{H}_o$, the external field, along the chain axis of the configuration B fibers. The second moment of crystalline samples is given by (5):

$$(\Delta H)^2 = \tfrac{1}{5} \beta^2 \sum_f I_f (I_f + 1)\, g_f^2\, r_f^{-6} (3\cos^2\theta_f - 1)^2 \qquad (7)$$

θ_f is the angle between $\hat{r}_f$ and the external field, $\hat{H}_o$. We estimate that the second moment is ~ 0.4 gauss^2, and that the interaction of the methyl group contributes at least 40% in the case of configuration B.

The second moment for configuration A is more difficult to obtain. It is expected to be measurably different. By determining the second moment as a function of humidity, one can follow the interconversion process and study it in detail.*

REFERENCES

1. J. D. Watson and F. H. C. Crick, Proc. Roy. Soc. 223A, 80 (1954).

2. D. O. Jordan, "The Chemistry of Nucleic Acids" (Butterworth & Co., London, 1960).

3. G. B. B. M. Sutherland and M. Tsuboi, Proc. Roy. Soc. 239A, 459 (1957).

4. Wilkens et al., J. Mol. Biol., 2, 38 (1960).

5. E. R. Andrew, "Nuclear Magnetic Resonance" (Cambridge Press, London, 1956), 158 ff.

* The objection could be raised that our Poly AT sample is highly radioactive. The curie content of 0.1 grams of Poly AT is ~10 curies, however only low energy beta rays are emitted (~10 KeV). Shielding would be easy. Experiments have been done on tritium samples having approximately the above curie content. [D. Pooley, C.I.T., private communication].
We have also ascertained that our H^3 concentration is compatible with biological synthesis.